FABRICATION AND MULTI-RESPONSE OPTIMIZATION OF PROCESS PARAMETERS OF ALUMINIUM METAL MATRIX COMPOSITE AND ITS MACHINABILITY

Biranu Kumsa Gonfa

A Thesis Submitted to the Department of Mechanical Engineering,

School of Mechanical, Chemical, and Materials Engineering

Presented in Partial Fulfillment of the Requirement for the Degree of Master's in Manufacturing Engineering

Office of Graduate Studies

Adama Science and Technology University

June-2022

Adama, Ethiopia

FABRICATION AND MULTI-RESPONSE OPTIMIZATION OF PROCESS PARAMETERS OF ALUMINIUM METAL MATRIX COMPOSITE AND ITS MACHINABILITY

Biranu Kumsa Gonfa

Advisor:

Dr. Devendra Kumar Sinha

A Thesis Submitted to the Department of Mechanical Engineering

School of Mechanical, Chemical, and Materials Engineering

Presented in Partial Fulfillment of the Requirement for the Degree of Master's in Manufacturing Engineering

Office of Graduate Studies

Adama Science and Technology University

June-2022

Adama, Ethiopia

Declaration

I hereby declare that this Master Thesis entitled "**Fabrication and Multi-Response Optimization of Process Parameters of Aluminium Metal Matrix Composite and Its Machinability**" is my original work. That is, it has not been submitted for the award of any academic degree, diploma or certificate in any other university. All sources of materials that are used for this thesis have been duly acknowledged through citation.

Biranu Kumsa Gonfa ______________________ _______________

Name of the student Signature Date

Recommendation

I, the advisor of this thesis, hereby certify that I have read the revised version of the thesis entitled "**Fabrication and Multi-Response Optimization of Process Parameters of Aluminium Metal Matrix Composite and Its Machinability**" prepared under my guidance by **Biranu Kumsa Gonfa** submitted in partial fulfillment of the requirements for the degree of Mater's of Science in Manufacturing Engineering.

Therefore, I recommend the submission of a revised version of the thesis to the department following the applicable procedures.

Dr. Devendra Kumar Sinha ________________________ ________________

Major Advisor Signature Date

Approval Page

I, the advisor of the thesis entitled "**Fabrication and Multi-Response Optimization of Process Parameters of Aluminium Metal Matrix Composite and Its Machinability**" and developed by **Biranu Kumsa Gonfa**, hereby certify that the recommendation and suggestions made by the board of examiners are appropriately incorporated into the final version of the thesis.

Dr. Devendra Kumar Sinha	______________________	_______________
Major Advisor	Signature	Date

We, the undersigned, members of the Board of Examiners of the thesis by **Biranu Kumsa Gonfa** have read and evaluated the thesis entitled "**Fabrication and Multi-Response Optimization of Process Parameters of Aluminium Metal Matrix Composite and Its Machinability**" and examined the candidate during an open defense. This is, therefore, to certify that the thesis is accepted for partial fulfillment of the requirement of the degree of Master of Science in Manufacturing Engineering.

____________________________	____________________	__________________
Chairperson	Signature	Date
____________________________	____________________	__________________
Internal Examiner	Signature	Date
____________________________	____________________	__________________
Eternal Examiner	Signature	Date

Finally, approval and acceptance of the thesis is contingent upon the submission of its final copy to the Office of Postgraduate Studies (OPGS) through the Department Graduate Council (DGC) and School Graduate Committee (SGC).

____________________________	____________________	__________________
Department Head	Signature	Date
____________________________	____________________	__________________
School Dean	Signature	Date
____________________________	____________________	__________________
Office of Postgraduate Studies, Dean	Signature	Date

ACKNOWLEDGEMENT

My first and big appreciation goes to the almighty **God** for all the mercy, blessing, protection, and patience he gives me to complete this thesis work.

I am extremely thankful to my advisor, Dr.Devendra Kumar Sinha, Assistant Professor in the Department of Mechanical Engineering, Adama Science and Technology University, for his supervision, guidance, and encouragement.

I would like to acknowledge the head of the Mechanical Engineering Department (Mr. Girmachew Ashagre) for his availability, suggestions, and cooperation in writing a request letter to get support from a different organization, and for creating a pleasant atmosphere for the success of my thesis work.

I also would like to thank my respected teacher Dr. Moera Gutu, Dr. Guteta kabeta, Dr. Mellese Workneh, Dr. Dinsefa, Dr. Devendra Kumar and Dr. P.J. Ramulu in the department of Mechanical Engineering for their knowledge and life experience sharing and to all the others member of departments.

I am grateful for my parents whose constant love and support keep me motivated and confident. Deepest thanks to Betelihem, who is my love. I am forever thankful for her unconditional love and support throughout the entire thesis process and every day.

Finally, I gratefully recognize the help of Adama Science and Technology for their education and support and for funding the thesis. I also wish to acknowledge the help provided by Addis Ababa Science and Technology University, Manufacturing Technology department of Ethiopian Technical University, Manufacturing Technology department of Adama Poly Technic College for their help in providing facilities to conduct the experiments and testing during my thesis work.

TABLE OF CONTENTS

LIST OF TABLES

TABLE PAGE

LIST OF FIGURES

FIGURE PAGE

List of Acronyms and Abbreviations

Abbreviation	Description
A	Stirring speed indication in analysis
AMMCs	Aluminium metal matrix composites
ANOVA	Analysis of Variance
ASTM	American Society for Testing and Materials
B	Stirring time indication in analysis
C	Wt.% of SiC indication in analysis
CNC	Computer Numerical Control
CMCs	Ceramic matrix composites
DOE	Design of experiment
DoF	Degree of freedom
D	Wt.% of MoS2 indication in analysis
d	Depth of Cut
f	Feed Rate
GRA	Grey relational Analysis
GRC	Grey Relational Coefficient
GRG	Grey Relational Grade
HAMMC	Hybrid Aluminium metal matrix composite
HMMC	Hybrid metal matrix composite
HV	Vickers hardness
mm	Millimeter
MMC	Metal Matrix Composite
mm/rev	Millimeter per revolution
MoS2	Molybdium disulphide
MPa	Mega Pascal
MRR	Material removal rate
MSS	Mean Sum of Square
N	Spindle Speed
OA	Orthogonal Array
OM	Optical microscopy
p-value	Probability

Ra	Average Surface roughness
rpm	Revolution per Minute
S1, S2, ….., S9	Sample (one, two,………., nine)
S/N	Signal to Noise
SiC	Silicon Carbide
SS	Sum of Square
UTM	Universal Testing Machine
UTS	Ultimate Tensile Strength
VHN	Vickers Hardness Number
V_T	Total volume of material required
Wa	Weight sample after wear
Wb	Weight of sample before wear
Wc	Weight of Composite
W_L	Weight (or mass) loss of sample
Wm	Weight of Matrix
µm	Micro meter
ρ	Density
Wt,%	Weight percentage

Abstract

Aluminium Metal Matrix Composites are potential materials for aerospace and automobile industrial applications due to its enhanced mechanical and tribological properties. Aluminium reinforced with Silicon Carbide particles have been developed with enhanced mechanical and tribological behavior but, it lacks wettability between matrix and reinforcement and cause weak bonding which reduce the degree of enhancement. The objectives of this study were to fabricate Aluminium based metal matrix composite with enhanced wettability at varying stirring speed (350, 450, 550rpm), stirring time (5, 10, 15min), wt. % of SiC (0, 5, 10 wt.%), and wt.% of MoS2 (0, 2, 4 wt.%). Nine samples were fabricated using stir casting based on Taguchi L9 orthogonal array. Hardness, tensile strength, tensile toughness and wear resistance of developed composite were investigated and analyzed as a single response characteristics using Taguchi's S/N ratio and as multi-response characteristic using Hybrid Taguchi Grey Relational Analysis (HTGRA). Results revealed that, addition of SiC in composite showed better hardness, tensile strength, tensile toughness and wear resistance. Addition of MoS2 in composite showed better hardness, tensile strength and tensile toughness only upto 2 wt.% of MoS2 and in case of wear rate addition of MoS2 in composite up to 4% showed better wear resistance. Al-SiC-MoS2 hybrid composite shows better enhancements in hardness, tensile strength, toughness and wear resistance than Al-SiC composite. Therefore, the enhancement of wettability has been achieved due to the addition of MoS2 in Al-SiC composite. From HTGRA, the optimum condition for multi-response characteristics has been obtained at A3B2C3D2. The machinability of the optimum composite also studied at varying spindle speed (500, 750, 1000rpm), feed rate (0.1, 0.2, 0.3mm/rev) and depth of cut (0.2, 0.3, 0.4mm) on CNC lathe using tungsten carbide tool. Surface roughness and material removal rate of machined composite were measured and analyzed as single response characteristics using Taguchi's S/N ratio and as multi-response characteristic using Hybrid Taguchi Grey Relational Analysis (HTGRA). The results revealed that, Surface roughness decreases with increasing the spindle speed and increased with increasing feed rate and depth of cut. Material removal rate increases with increasing feed rate, depth of cut and spindle speed increases. Feed rate is the highly influential parameter which influences the surface roughness and MRR in machining of hybrid composites. From HTGRA, the optimum prediction condition for multi-response characteristics has been obtained at N1f3d3.

Keywords: Metal matrix composites, GRA, Al/SiC/MoS2, Al 6061, SiC, Stirring speed.

CHAPTER ONE

INTRODUCTION

1.1. Background of the Study

Nowadays, engineering applications require materials that are stronger, lighter, and less expensive, and conventional engineering materials are replaced by composite materials. Composite materials are produced by two dissimilar materials into a new material that may be better suited for a particular application than either of the original materials alone. Many composite materials are composed of just two phases, one is termed the matrix which is continuous and surrounds the other phase often called the dispersed phase. Particularly, Metal Matrix Composites (MMC) are widely used in many industrial applications such as Automotive, Aerospace Applications (Campbell, J. (2015)). There is increasing attention towards Metal Matrix Composites (MMCs) due to their properties like high specific strength, high stiffness, better wear resistance, and improved thermal resistance compared to base metals (Rajasekar et al. (2018)). MMCs are combinations of two or more different materials with at least one being metal and another being a ceramic or organic compound. A new system of materials containing hard particulates embedded in a metal matrix has exhibited superior operating performance and improved tribological behaviors.

In MMCs, the characteristics of base alloys have to be ductility, conductivity, and toughness) and ceramic properties of reinforcements have to be superior strength, high wear resistance, high thermal stability, and high modulus (Yadav et al. (2016)). Therefore, Metal Matrix Composites can be Aluminium alloy-based composites (Madeva et al. (2017)), Magnesium alloys based composites (Karthick et al. (2017)), and Titanium alloys based composites (Imayev et al. (2018). The materials used as reinforcement in the production of MMC are Aluminium oxide (Al_2O_3), Silicon carbide (SiC), Titanium bromide (TiB_2), Titanium carbide (TiC), Molybdenum disulfide (MoS_2), Titanium nitride (TiN), Boron carbide (B_4C) (Parswajinan et al. (2018)). Among MMCs, aluminium alloy-based composites have shown significant improvement in the mechanical, thermal, and wear properties to provide to the demand of the industries.

There are several series of Aluminum alloys (e.g. 1xxx, 2xxx, 5xxx, 6xxx, 7xxx, and others) used in the production of composites. Among Aluminum alloys, the 6xxx and 7xxx series of aluminum alloys have good machinability and extrude-ability and are mostly used as a matrix material in the production of AMMC aerospace industry, architectural construction, marine industries, and the automotive applications (Halil et al. (2019)).

Aluminum hybrid matrix composites have become better substitutes for conventional aluminum alloys and single composites because of their characteristics like improved strength-to-weight ratio, energy saving, and better wear resistance. In Aluminum hybrid matrix composites, the matrix is Aluminum alloy only and Reinforced can be any materials but, it must be two and more than two and Aluminum hybrid matrix composites a composite for the use of the aerospace, the automotive industry has been increased because of the tribological, physical and mechanical properties it possesses (Poovazhagan et al. (2013)). AMMC materials can be produced by many different techniques. The focus of the selection of suitable process engineering is the desired kind, quantity, and distribution of the reinforcement components (particles and fibers), the matrix alloy, and the application. Different fabrication techniques are used for the preparation of aluminum MMCs such as liquid state processing and Solid state processing (Vijaya Ramnath et al. (2014)).

The main challenge of AMMC material is its machining characteristics. The machining performance is defined in terms of tool life, material removal rate, or surface quality of the machined part. The presence of ceramic reinforcement particles in aluminium metal matrix composites makes the composite difficult to machine due to the presence of hard abrasive ceramic reinforcing. Ceramic reinforcements build them stronger and stiffer than the base matrix and they lead to rapid tool wear and thereby short tool life and high tooling cost and also poor surface finish (Duong et al. (2016)). The machinability of composites becomes vital for manufacturing industries. Therefore, it needs to study the influence of process parameters on its machinability in a dry environment. The parameters of an AMMC material influencing the machining performance are the particle size, wt.%, temperature, hardness, the tool, its type, and grade (Jain et al. (2014)). The majority of investigations into MMC machinability have been performed using cemented carbide or polycrystalline (PCD). Carbide tools are effective for short-run machining operations but, PCD tools are widely used because diamond offers excellent abrasion resistance, low friction coefficient, and low thermal expansion than carbide tools and others.

1.2. Problem Statement

Now a day, the Aerospace and automobile industries are highly in need of materials that are stronger, harder, lighter, wear resistant and low cost. Therefore, metal matrix composites material is replacing the conventional materials due to their properties like high specific strength, high stiffness, better wear resistance, and improved thermal resistance compared to base metals (Halil et al. (2019)). Among MMC, aluminium alloy-based composites have shown a significant improvement in mechanical and tribological properties to provide the demand of aerospace and automobile industries (Kumar Sharma et al. (2020)). But, the abiding problem of Aluminium based composite is that the fabricated composite shows heterogeneous and low improvement of mechanical and tribological behavior due to poor wettability between matrix and reinforcement and as well as due to Particle segregation because of the difference of densities between matrix and reinforcement in metal matrix composite (Elango and Annamalai (2020)) and (Ajith et. al (2020)). Therefore, the wettability between matrix and reinforcement (bonding between matrix and reinforcement) has to be improved to enhance the mechanical and tribological behavior of the composite.

After the fabrication of AMMC materials, the main challenge of AMMC material is its machining characteristics. AMMC materials are very difficult to machine due to the presence of hard abrasive ceramic reinforcing particles that build them stronger and stiffer than the base matrix. Therefore, AMMC materials lead to rapid tool wear and poor surface finish on machined parts (Duong et al. (2016)). The measure of machinability performance includes MRR, specific energy consumption, surface finish, tool life, and chip flow pattern.

1.3. Objectives of the Study

1.3.1. General Objectives

The general objective of the study is to fabricate and optimize process parameters for the mechanical and tribological behavior of developed composites and its machinability.

1.3.2. Specific Objectives

The specific objectives of the study are:

- To fabricate Aluminium based composites and identify particle distribution in Al matrix.
- To investigate mechanical and tribological behavior of developed composite and optimize its process parameters using single and multi-response characteristics.
- To study the machinability for the optimum composite and optimize its cutting parameters using single and multi-response characteristics.

1.4. Significance of the Study

Now a day's, manufacturing industries such as automotive industries, and aerospace industries are highly in need of lightweight, harder, stronger components using cost-effective composite materials instead of steel and aluminum alloys. It has crucial benefits for individuals and stakeholders at the national and international levels. Investigation of mechanical and tribological behavior of developed composite and optimization of process parameters for better mechanical and tribological behavior of developed composite as a single and multi-response which identified the best material suitable for the case of lightweight, harder, stronger and also wear resistance is so important and which highly benefits any industry too rather than aerospace and automobile. One of the significances of studying the machinability and optimizing cutting parameters for minimum surface roughness and higher MRR by increasing the quality of final product and productivity are highly significant for metal manufacturing industries. It is also used to grasp theoretical and practical knowledge of any reader on this research area and for students, who are studying this research area, for the future researcher as literature, and also for aerospace and automobile manufacturing industries that require this composite material.

1.5. Scope of the Study

The scope of this research was delimited to fabrication of composites at varying weight composition of SiC and MoS2, investigation of mechanical behavior and tribological behavior characterization of the particle distribution in developed composite via optical microscope was also performed. Optimization of process parameters to enhance mechanical and tribological behavior of developed composite as single and multi-response characteristics have been done. Experimental investigation of CNC dry turning for optimized composite and measurement of surface roughness and determination of material removal rate was performed. Optimizations of cutting parameters as single and multi-response characteristics to lower surface roughness and improve MRR have been done.

1.6. Research Motivation

A lot of researchers have been working on the development and characterization of aluminum reinforced metal matrix composite mainly due to the increasing usage of aluminum alloys in different industries. But, the abiding problem of Aluminium based composite is that the fabricated composite has shown low improvement of mechanical and tribological behavior due to poor wettability between matrix and reinforcement which weakens the bonding. Therefore, this study focus to control the wettability and enhancing the mechanical and tribological behavior of fabricated composite. Machining characteristics of the fabricated composite are also difficult due to the presence of hard abrasive ceramic reinforcing particles that build them stronger and stiffer than the base matrix. Therefore, they lead to rapid tool wear and poor surface finish on machined parts.

1.7. Thesis Organization

This research paper consists of five chapters. The 1st chapter is about the introduction and background of the study, problem statement, objectives of the study, significance of the study, the scope of the study, and thesis organization. The 2nd chapter is about the theoretical and empirical review of Al alloy-based reinforced MMC, literature summary, and gap. The 3rd chapter is about materials and methodologies like Al-matrix and wt.% of SiC and MoS2 reinforcements and fabrication method and investigation. The 4th chapter is about detailed discussion and analysis based on the experimental result of mechanical and tribological properties, the microstructure of developed materials, and also machining characteristics. Finally, the 5th chapter presents the conclusion and recommendations for future works.

CHAPTER TWO

LITERATURE REVIEW

2.1. Theoretical Review

A composite material can be defined as a combination of two or more materials that results in better properties than those of the individual components used alone. There are matrix and reinforcement constituents. The matrix material surrounds and supports the reinforcement materials by maintaining their relative positions. The reinforcements impart special physical, mechanical, and electrical properties to enhance the matrix properties. The two constituents are reinforcement and a matrix (Mohamadigangaraj et al. (2020)). The main categories of composite materials can be classified; Based on the chemical nature of the matrix phase or Material, Based on the dispersed phase (geometry of reinforcements) Material. Based on the chemical nature of the matrix phase measurement, composite materials are classified as the metal matrix (MMC), polymer matrix (PMC), and ceramic matrix composites (CMC), composite materials are also classified as particle reinforced composite, fiber reinforced composite and structural composites are based on the geometry of the reinforcements (Kalaa et al. (2014)).

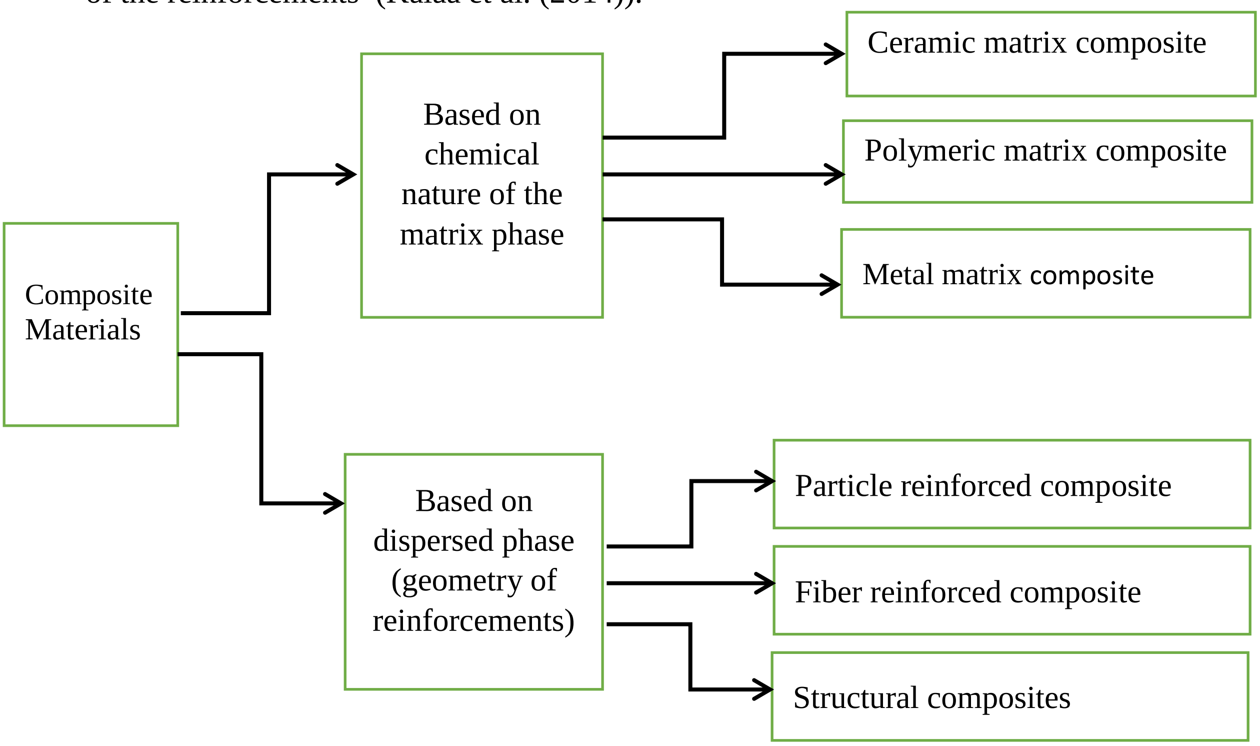

Figure 2.1: Classification of composite (Kalaa et al. (2014)).

2.1.1. Ceramic-Matrix Composites

Ceramic-matrix composites are the third major type and examples include silicon carbide fibers fixed in a matrix made from borosilicate glass. The ceramic matrix makes them particularly suitable for use in lightweight, high-temperature components, such as parts for airplane jet engines. The principal advantages of ceramic materials over other materials are their resilience to oxidation and deterioration at elevated temperatures, their high melting points, and high compressive strengths. Unfortunately, ceramics suffer from susceptibility to brittle fracture and therefore have relatively low values of fracture toughness. One method of increasing the fracture toughness of ceramic is to reinforce it with fibers, whiskers, or particles.

2.1.2. Polymer Matrix Composites

Polymer matrix composites commonly used matrix materials are polymeric. The reason for this is twofold. In general, the mechanical properties of polymers are insufficient for structural purposes. In particular, their strength and stiffness are low compared to metals and ceramics. These difficulties are overcome by reinforcing other materials with polymers. Secondly, the processing of PMC need not involve high pressure and doesn't require high temperature. Also, the equipment required for manufacturing PMC is simpler. The most commonly adopted polymer composites in more industries are thermosetting and thermoplastic polymer matrix composites (Kumar Sharma et al. (2020)).

2.1.3. Metal Matrix Composite

Metal Matrix Composites (MMCs) are materials produced by adding reinforcement in the form of particles (ceramic or metal), fibers, whiskers, or even a sheet metal to a metal or alloy matrix. High strength, fracture toughness, and stiffness are offered by metal matrices more than those offered by their polymer counterparts. Most metals and alloys could be used as matrices and they require reinforcement materials that need to be stable over a range of temperatures and non-reactive too. However, the guiding aspect for the choice depends essentially on the matrix material (Kumar Sharma et al. (2020)). Most metals and alloys make good matrices. Only light metals are responsive, with their low density proving an advantage. Titanium, Aluminium, and magnesium are the popular matrix metals currently in vogue, which are particularly useful for aircraft applications. The main reinforcements employed are silicon carbide and alumina. Metal matrix composites can be classed as having either continuous or discontinuous fiber reinforcement (Kala et al. (2014)).

2.1.4. Particle Reinforced Composite:

A composite that strengthens is a particle of all the dimensions more or less equal is called particulate reinforced composites. Particulate fillers are working to improve high-temperature performance, reduce friction, increase wear resistance, and reduce shrinkage. The particle will also donate the load with the matrix, but to a smaller extent than a fiber. A particulate reinforcement will therefore get better stiffness but will not normally strengthen (Kumar Sharma et al. (2020)).

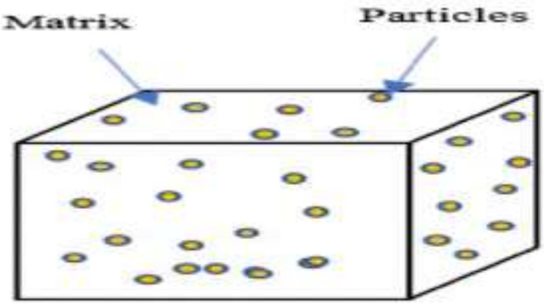

Figure 2.2: Particle reinforced composite (Kumar Sharma et al. (2020)).

2.1.5. Fiber-Reinforced Composite

Fiber reinforced composites enclose reinforcements having lengths higher than cross-sectional dimensions. Fibrous reinforcement represents physical rather than chemical means of changing material to leave well with various engineering applications. These can be usually classified as follow. Composites consist of fibers in the matrix structure and can be classified according to fiber length. Composites with long fiber reinforcements are termed continuous fiber reinforcement composites, while composites with short fiber reinforcements are termed discontinuous fiber-reinforcement composites (Kumar Sharma et al. (2020)).

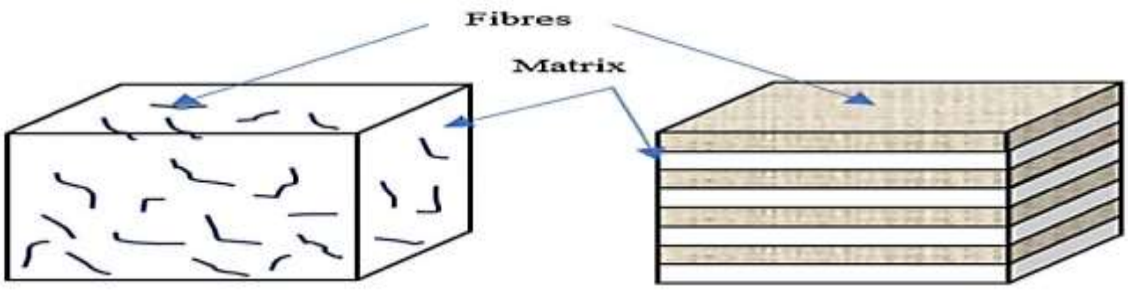

Figure 2.3: Fiber reinforced composite (Kumar Sharma et al. (2020)).

2.1.6. Aluminum Alloy-Based Matrix Composite

Aluminum metal matrix composites are a class of materials that have proven successful in meeting most of the rigorous specifications in applications where light-weight, high stiffness, and moderate strength are the requisite properties. Aluminum material is used as a matrix phase with a variety of reinforcement materials and flexibility in their primary processing; AlMMCs offers a great potential for the development of composites with the desired properties for certain applications (Kumar Sharma et al. (2020)). The addition of reinforcement particles to pure aluminum metal is to enhance the mechanical properties of tensile strength, hardness, and wear resistance of the composites. Silicon carbide particles have become one of the popular reinforcing phases for many aluminum alloy-based metal matrix composites (Kala et al. (2014)).

2.1.7. Reinforcement Used In Metal Matrix Composite

Reinforcements: A strong, inert woven and nonwoven fibrous material incorporated into the matrix to improve its metal glass and physical properties. Typical reinforcements are asbestos, boron, carbon, metal glass and ceramic fibers, flock, graphite, jute, sisal, and whiskers, as well as chopped paper, macerated fabrics, and synthetic fibers. The primary difference between reinforcement and filler is that reinforcement markedly improves tensile and flexural strength, whereas filler usually does not. Also to be effective, reinforcement must form a strong adhesive bond with the resin. The role of the reinforcement in a composite material is fundamentally one of increasing the mechanical properties of the neat resin system (Poovazhagan et al. (2012)).

Reinforcements for the composites can be fibers, fabric particles, or whiskers. Fibers are essentially characterized by one very long axis with other two axes either often circular or near circular. Particles have no preferred orientation and so does their shape. Whiskers have a preferred shape but are small both in diameter and length as compared to fibers. Based on the physical factors of reinforcement (fiber or granular particle) like type, size and weight fraction give the better properties to the MMCs, and the reinforcement's chemical nature reacted with a matrix material to influence their physical properties like microstructure (Poovazhagan et al. (2012)).

In the MMCs fabrication process, the creation of well-built chemical bonds between matrix and reinforcement is good for the reinforcement wetting in the matrix molten pool. The wettability is minimum it creates the oxide films on the reinforcement surface in the metal pool. It affects the composite properties because of reinforcement adsorbed contaminant. Reinforcement's metallic coverings, like calcium, titanium, and magnesium to the metal pool, and before the addition of particles, it needs to do the heat treatment. It improves reinforcement– Matrix wettability (Kala et al. (2014)). Reinforcements based on ceramics are used normally carbides or oxides or borides such as Al2O3, TiB2, TiO2, SiC, TiC, B4C, etc are used in the Aluminum matrix composites (Kala et al. (2014)).

2.1.8. Silicon Carbide Particle Reinforcement

It is a very hard dark crystalline compound SiC of silicon and carbon that is used as an abrasive as a refractory and in electric resistors. Silicon carbide particles have become one of the popular reinforcing phases for many aluminum alloy-based metal matrix composites. They are hard and brittle ceramic particles with high strength, high modulus of elasticity, and high thermal and electrical resistance. Silicon carbide (SiC) is one of the most important advanced ceramics in contemporary usage. With an exceptional hardness of 25 GPa, and a low density of 3.21 g cm^{-3}. Other ceramic uses include specialized aerospace and automotive components, the nuclear industry, and electronics, particularly as a thin film semiconductor (Parswajinan et al. (2018)).

Moreover, SiC is very important in the abrasives and refractories industries. Silicon carbide (SiC) is a hard covalently bonded material. SiC compound consists of a silicon (Si) atom and four carbon (C) atoms which are covalently bonded between two of them. Silicon carbide (SiC) is a non-oxide ceramic engineering material that has gathered a considerable amount of interest. Silicon carbide particles have become one of the popular reinforcing phases for many aluminum alloy-based metal matrix composites. They are hard and brittle ceramic particles with high strength, high modulus of elasticity, and high thermal and electrical resistance. The SiC particle retains its elastic resistance even up to a temperature of 1650°C, which leads it to a wide range of industrial applications at elevated temperatures. When these SiC particles are embedded in MMCs, it certainly improves the overall strength of the composite along with corrosion and wear resistance (Parswajinan et al. (2018)).

2.1.9. Effect of Reinforcement on Metal Matrix Composite

The addition of the reinforcement enhances the mechanical properties of aluminum-based composites when compared to the matrix alloy. However, the addition of any hard reinforcement to aluminum reduces the corrosion resistance, electrical conductivity and surface finish, etc (Reddy et al. (2017)). The inclusion of reinforcement into the metal matrix enhances the strength, hardness, and stiffness and reduces the wear and density of the materials. Ling et al. (2010) fabricated an Aluminium matrix composite reinforced with aluminum reinforced with silicon carbide. They observed that the ultimate tensile strength and the yield strength of the composites increased with an increase in the volume fraction of reinforcement. While the elongation fracture first increased and then decreased with an increase in reinforcement.

Kalaiselvan et al. (2011) produced Al (6061-T6)/B4C composite and investigated its mechanical properties. They observed that the hardness and the tensile strength of the composite are linearly increasing with the increasing weight percentage of the B4C particulate. Kumar et al. (2013) fabricated A359/ Al2O3 composite via the electromagnetic stir casting method. The author revealed that the hardness values increased to 72.8 HRC compared to pure alloy (46HRC). Also, the tensile strength of the composite increased to 148.7N/mm^2 as compared to pure alloy at 103.7N/mm^2.

The mechanical and wear properties of the MMCs have been extensively investigated by various researchers (Toptan et al. (2012)). The results have shown that the wear performance of MMCs is higher than that of unreinforced matrices. The wear of metals depends on many variables; it is not an intrinsic material property but characteristics of the engineering system which depend on load, speed, temperature, hardness, presence of foreign material, and the environmental condition (Dwivedi et al. (2010)) statistically studied the dry reciprocating wear behavior of Al-Si-SiCp composite and observed that composite with high silicon content showed lower wear loses compared to that of low silicon content composite. Sliding distance is the main factor that affects the wear behavior of the composite followed by load, reciprocating velocity, and weight percentage of silicon. The interaction between load and sliding distance also had a pronounced effect on wear behavior.

2.1.10. Effect of Reinforcement on Machinability of Metal Matrix Composite

The machining performance or machinability is defined in terms of tool life, material removal rate, or surface quality of the machined part. The presence of Silicon carbide (SiC) particles in aluminum metal matrix composites makes the composite difficult to machine and they lead to rapid tool wear and thereby short tool life and high tooling cost. Also, poor surface finish is seen after machining the composite. Tool wear is low if a PCD diamond tool is used, but the cost of the diamond tool is very high. The surface roughness of the aluminum metal matrix composite is highly influenced by the feed rate, cutting speed, and volume fraction of SiC. Carbide tools are effective in short-run machining operations but, the Poly Crystalline Diamond (PCD) tool is used because diamond offers excellent abrasion resistance, low friction coefficient, and low thermal expansion than carbide tools and others. Diamond tools give a good surface finish and dimensional accuracy (Duong et al. (2016)).

The machinability of hybrid composites becomes vital for manufacturing industries. Therefore, the need to study the influence of process parameters on the cutting forces in turning such hybrid composite in a dry environment is essentially required. MMCs are difficult to machine due to the presence of hard abrasive ceramic reinforcing medium set within a more ductile matrix material. Machining MMCs is difficult as the ceramic reinforcements build them stronger and stiffer than the base matrix. The parameters of a hybrid MMC material influencing the machining performance are the particle size, wt.%, temperature, hardness, the tool, its type, and grade (Jain et al. (2014)).

2.1.11. Fabrication Techniques of Metal Matrix Composite

Metal matrix composite materials can be produced by many different techniques. The focus of the selection of suitable process engineering is the desired kind, quantity, and distribution of the reinforcement components (particles and fibers), the matrix alloy, and the application. By altering the manufacturing method, the processing, and the finishing, as well as by the form of the reinforcement components it is possible to obtain different characteristic profiles, although the same composition and amounts of the components are involved. Different fabrications techniques are used for the preparation of aluminum MMCs, e.g., stir casting, powder metallurgy, and squeeze casting, in-situ process, deposition technique, and electroplating (Vijaya Ramnath et al. (2014)).

The common processing methods are categorized as follows: Liquid state fabrication process and Solid state fabrication process. In the case of the liquid state fabrication process, the molten matrix and reinforcements are formed together by a solidification mechanism and which includes stir casting, squeeze casting, and centrifugal casting). In the case of the solid state fabrication process, bonding is induced between the matrix material and dispersed phase because of communal diffusion taking place between them in the solid phase and it includes powder metallurgy, High Energy Ball Milling, and Diffusion Bonding (Soltani et al. (2015)). The widely used processes are stir casting and squeeze casting (Shukla et al. (2018)). Stir casting (vortex techniques) is generally considered the most economical one among all the available methods of Al MMC production, and it allows the fabrication of very large components. Its advantages lie in simplicity, cost, flexibility, and applicability to large-volume production (Soltani et al. (2015)). In this process, the matrix material is superheated above its melting temperature. The particles are also preheated at approximately 1000–1200^{o}C to oxidize the surface. The melted matrix is then stirred at an average stirring speed of 300–600 rpm as the vortex is formed during stirring (Sidhu et al. (2013)). The major problem with stir casting is the segregation or dusting of reinforced particles (Shukla et al. (2018)).

2.1.12. Liquid State Process Fabrication Techniques

Liquid state fabrication of MMCs involves the integration of dispersed ceramic phase into molten metal, followed by its solidification process. Stir casting is a type of casting process in which a mechanical stirrer is introduced to form a vortex to mix reinforcement in the matrix material. It is a suitable process for the production of metal matrix composites due to its cost effectiveness, applicability to mass production, simplicity, almost net shaping, and easier control of the composite structure. The stir casting setup consists of a furnace, reinforcement feeder, and mechanical stirrer. The furnace is used to heat and melting of the materials. The bottom pouring furnace is more suitable for the stir casting as after stirring the mixed slurry instant poring is required to avoid the settling of the solid particles in the bottom of the crucible. The mechanical stirrer is used to form the vortex which leads to the mixing of the reinforcement material which is introduced in the melt. This stirrer is connected to the variable speed motors; the rotation speed of the stirrer is controlled by the regulator attached to the motor. Further, the feeder is attached to the furnace and used to feed the reinforcement powder in the melt. A permanent mold, sand mold, or lost-wax mold can be used for pouring the mixed slurry (Saikrupa et al. (2021)).

2.1.12.1. Stir Casting Process Parameter

Stirring speed: The stirring speed is openly controlled by the molten metal flow pattern and its range are between 300 and 600 rpm for better fabrication. As the wettability percentage increase, the solidifying rate also increases directly (Singh & Kumar (2019)).

Stirring temperature: It is very important chemical reaction acceleration among the matrixes and reinforcements due to its viscosity condition. When observed most of the research work was carried out by maintaining the Stirring temperature in the fabrication keeps at 630˚C for Al (6061) condition (Singh & Kumar (2019)).

The pre-heat temperature of Reinforcement: One of the research works describes the reinforcement materials are preheated at 900-1100C temperature for 30-90 minutes to clean the unwanted moisture or surrounding gases present over them (Singh & Kumar (2019)).

Stirring time: The Stirring time is a very significant impact on the homogeneous circulation of the reinforcement particle in the MMCs (Gowri Shankar et al. (2018)).

Pouring temperature range: The pour temperature plays the most important role in the solidification process. To make sure a suitable metal flow temperature avoids the coarse structure formation, the pouring temperature should be adequately high (Gowri Shankar et al. (2018)).

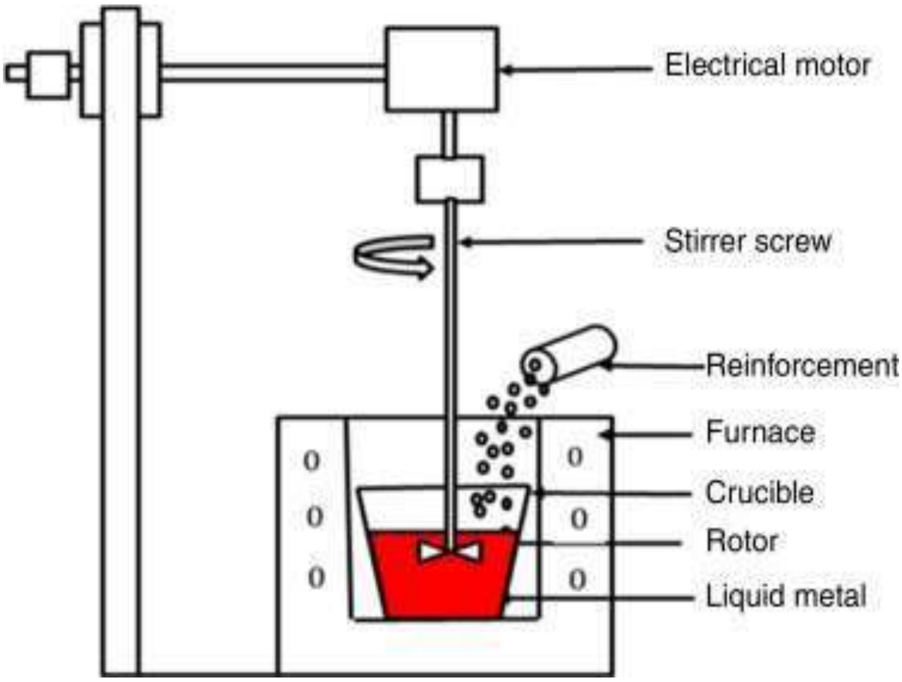

Figure 2.4: Schematic diagram of the stir casting setup (Ajagol et al. (2018)).

2.1.13. Taguchi Methods Optimization Techniques

Taguchi Methods is a technique for designing and performing experiments to investigate processes where the output depends on many factors (variables; inputs) without having to tediously and uneconomically run the process using all possible combinations of values of those variables. Taguchi Method" was developed by Japanese Scientist Genichi Taguchi in the 1950s, using statistics; he aimed to improve the quality of manufactured goods. This method is based on the principle of performing the minimum number of experiments to minimize costs (Sirvanc et al. (2011)). The Taguchi method is a tool for improving the most useful product performance, process, design, and system with a significant reduction in experimental time and cost (Wiley and Sons (2008)). By systematically choosing certain combinations of variables it is possible to separate their individual effects and used them to design the experiment combination of parameters like used in the fabrication of composite and for machining combination of process parameters. The design of experiments (DOE) is the design of any task that aims to describe and explain the variation of information under conditions that are hypothesized to reflect the variation.

2.1.13.1. Signal-Noise Ratio Analysis

According to the Taguchi method, to find the optimal machining parameters, the signal-to-noise ratio (S/N) of each machining parameter level must be assessed for each output function. The highest S/N of the considered best parameter levels indicates an optimal level. Taguchi uses the S/N ratio to measure the quality characteristics deviating from the desired value with three categories of signal-to-noise ratios as follows (Upinder et al. (2012));

Nominal is the best characteristics,

$$\frac{S}{N} = 10\log[\frac{\mathrm{Y}^2}{S^2}] \quad (2.1)$$

Smaller is the better characteristic,

$$\frac{S}{N} = -10\log[\frac{1}{n}\sum_{i=1}^{n} \mathrm{Yi}^2] \quad (2.2)$$

Larger is the better characteristics,

$$\frac{S}{N} = -10\log[\frac{1}{n}\sum_{i=1}^{n} \frac{1}{\mathrm{Yi}^2}] \quad (2.3)$$

Here Y = observation n = total number of observations, $\bar{Y}$ = the average of observed data, $S2$ = the variation of Y and Yi = ith response.

2.1.13.2. Analysis of Variance (ANOVA)

The purpose of the analysis of variance (ANOVA) is to find which parameters significantly affect the quality characteristic. ANOVA is the statistical technique used to find the influence of all control parameters. In the analysis of variance, the percentage contributions of each control factor are used to measure the corresponding effects on the performance characteristics. The significance level of 5 %, i.e. for a 95 % level of confidence was considered in this analysis. ANOVA results indicate whether there is a statistical significance in difference or not in output characteristics. ANOVA analysis involves when α values are below 0.05 is significant and above 0.05 is not significant. Percent contribution measures the percentage contribution of each model term relative to the total sum of squares. The percentage contribution is often a rough but effective guide to the relative importance of each model term. From the analysis of variance percentage contribution of each influential parameter was calculated by the following formula (Debnath (2016)):

$$P = \frac{SS}{SST} * 100 \qquad (2.4)$$

Where, P: Percentage contribution of individual factor,

SS: Sum of squares or treatment sum of squares,

SST: Total sum of squares.

2.1.14. Grey Relational Analysis Optimization Techniques

Grey relational analysis is widely used for measuring the degree of relationship between sequences by grey relational grade. Grey relational analysis has been applied by several researchers to optimize the control parameters having multi-responses through grey relational grade (Kuo et al. (2008)). In this approach, a grey relational grade is obtained for analyzing the relational degree of the multiple responses. Lin et al. (2002) have attempted a grey relational-based approach to solve multi-response problems in the Taguchi methods. The Grey relational analysis is widely used to combine all the considered performance characteristics into a single value that can be used as the single characteristic in optimization problems.

2.1.14.1. Optimization Steps Used In Grey Relational Analysis

Step 1: Transform the original response data into S/N ratio (*Yij*) using the appropriate formula depending on the type of quality characteristic using Eq.2.1, Eq.2.2, and Eq. 2.3.

Step 2: Normalize *Yij* as *Zij* (0 _ *Zij* _ 1) by the following formula to avoid the effect of using different units and to reduce variability. Normalization is a transformation performed on a single input to distribute the data evenly and scale into an acceptable range.

Zij = Normalized value for *i*th experiment/trial for *j*th dependent variable/response

$$Zij = \frac{Yij - \min(Yij, i=1,2,3,....n)}{max(Yij, i=1,2,3,....n) - \min(Yij, i=1,2,3,....n)} \quad (2.5)$$

(To be used for S/N ratio with larger—the better case)

$$Zij = \frac{\min(Yij, i=1,2,3,....n) - Yij}{max(Yij, i=1,2,3,....n) - \min(Yij, i=1,2,3,....n)} \quad (2.6)$$

(To be used for S/N ratio with smaller—the better case)

$$Zij = \frac{Yij - T - \min(Yij - T, i=1,2,3,....n)}{max(Yij - T, i=1,2,3,....n) - \min(Yij - T, i=1,2,3,....n)} \quad (2.7)$$

(To be used for S/N ratio with nominal—the best case)

Step 3: Compute the grey relational coefficient (GRC) for the normalized S/N ratio values.

$$GRCij = \frac{\Delta\min + \partial\Delta\max}{(\Delta ij + \partial\Delta\max)} \quad (2.8)$$

Where, i== 1, 2, ...,n-experiments and j== 1, 2, ...,m-responses

GRC*ij* = GRC for the *i*th experiment/trial and Δ= absolute difference between *Yoj* and *Yij*

Yoj = optimum performance value or the ideal normalized value of *j*th response

Yij = the *i*th normalized value of the *j*th response/dependant variable

Δmin = minimum value of Δ and Δmax = maximum value of Δ

∂ is the distinguishing coefficient which is defined in the range $0 \leq \partial \leq 1$

Step 4: Compute the grey relational grade (*GRGi*).

$$GRGi = \frac{1}{m} \sum GRCi \quad (2.9)$$

Where *m* is the number of responses

Step 5: Use the response graph method or ANOVA and select optimal levels for the factors based on the maximum average GR*Gi* value.

2.2. Empirical Review

There are several Aluminum based composites with single-reinforced aluminum (Al6061) alloy matrix composite and hybrid-reinforced aluminum (Al6061) alloy matrix composite that are studied for the enhancement of mechanical properties and tribological behavior at different wt. % of various reinforcements.

2.2.1. Mechanical and Tribological Properties of Single-Reinforced AMMC

R. Karthigeyan et al. (2012) successfully and effectively developed Al 7075 alloy and Short Basalt Fibre composite through liquid metallurgy technique. They have performed an experimental characterization by changing weight percentage composition at three levels 2%, 4%, and 6% wt of short basalt fiber. The composite containing 6% wt of short basalt fiber signifies a higher hardness value of 97.1HV when compare to the base matrix hardness of 92HV. The distribution of reinforcements in the metal matrix is genuinely uniform. Meena et al. (2013) investigated SiC reinforced aluminum with different weight fractions (5, 10, 15, and 20%) and particle sizes (220, 300, and 400 mesh) by using the stir casting technique. They determined the hardness, tensile strength, and impact strength of the fabricated composite. The result revealed that hardness, tensile strength, and impact strength were increased by increasing the reinforced weight fraction but impact strength was decreased by increasing the reinforced weight fraction

Dwivedi et al. (2014) successfully fabricated and investigated the effect of the amount of SiC particle as well as two different stirring methods (mechanical and electromagnetic) on mechanical properties. They used a direct melt reaction for each stirring method and the same percentage of SiC particles: 0, 5, 10, and 15%. The conclusions show that mechanical properties such as hardness, toughness, and fatigue life increase with increasing the addition of SiC and they concluded that the best mechanical properties and homogeneity can be obtained by using the electromagnetic stirring method. Rahman et.al (2014) successfully fabricated silicon carbide (SiC) reinforced aluminum matrix composites (AMCs) via a stir casting process by varying SiC content (0, 5, 10, and 20 wt. %). The results showed that introducing SiC reinforcements in the aluminum (Al) matrix increased hardness, wear resistance, and tensile strength and 20 wt. % SiC reinforced AMC showed maximum hardness and tensile strength. Microstructural observation revealed clustering and non-homogeneous distribution of SiC particles in the Al matrix and porosities were found in microstructures.

Jegan et al. (2014) fabricated aluminum metal matrix composites reinforced by SiC and B4C using stir casting with a percentage composition of 2.5%, 5%, and 7.5% for both reinforced. They have investigated hardness and tensile strength. The hardness and the tensile strength of AMCs were found to be maximum for the higher weight percentage of reinforcement. It is noticed that there was a significant increase in mechanical properties of B4C reinforced AMC compared to SiC reinforced AMC. Radha and Vijaya Kumar (2015) prepared Aluminium(Al 6061) is reinforced with SiC (28 μ size) particles by Stir Casting Technique by weight fraction from 0%, 5%, 10%, and 15% of SiC. The result revealed that Hardness and Ultimate Tensile Strength (MPa) result on graphs increases with the increase in reinforced particulate weight fraction of SiC particles. Maximum Vickers Hardness (VH) = 75 has been obtained at 15 % wt of SiC particles. Impact Strength (N-m) of composite increases with increasing weight fraction (5% and 10%) decreases at 15 wt% of SiC. Optical micrographs showed a reasonably uniform distribution of SiC particles in the Al matrix.

Vijay et al. (2016) developed an Aluminum metal matrix composite workpiece having different weight composition of silicon carbide with constant Al2O3 and has investigated the hardness of composite with increasing reinforcement SiC (5, 10, 15%). From the above research paper, the percentage weight of Sic and Al2O3 influences the hardness of Al/SiC/Al2O3 metal matrix composites. As the percentage weight of SiCp increases hardness increases. Karvanis et al. (2016) investigated the effect of SiC particles on the mechanical properties of aluminum metal matrix composites by using a centrifugal casting machine. They observed that the compressive and tensile strength and the hardness increase with increasing the percentage of SiC particles. Rayjadhay et al. (2016) developed Al 6061 reinforced with SiCp composite by stir casting and studied the effect of weight % of Silicon carbide powder, pouring temperature, and stirring time on the hardness. The L9 orthogonal array of SiC Wt.% (0, 5, 10%), pouring temperature (660, 710, 760C), stirring time (20, 30, 40sec). Silicon Carbide (SiC) is the most significant effective parameter for hardness and followed by pouring temperature and stirring time. Composite has higher hardness when it is fabricated weight % of silicon carbide powder, pouring temperature, and stirring time (10%, 760C, 30sec) respectively.

Subramanya Reddy et al. (2017) successfully fabricated the aluminum alloy Al2024 with different proportions of composites reinforced SiC particles of 35 μm as size in the ratios of 0%, 5%, 10%, and 15% using the stir casting technique. The result revealed that the ultimate tensile strength increases as the weight of SiC increases s to decreases when the % SiC increases. The impact strength of the composite is increased up to 10% and decreases at 15%.

Miss. Laxmi et al. (2017) fabricated and investigated the mechanical properties of SiC reinforced with Aluminum 6061 metal matrix composites at 10%, 15%, and 20% of SiC formed by stir casting. The test outcomes demonstrate that with improves in rate from 10% to 15%, the hardness of the composites is improved. To further increment of sic particles up to 20%, result as declination of hardness. The hardness is more for 15% SiC. Scanning Electron Microscopy was used to investigate the microstructure of the composite and heterogeneous particle distribution was observed. Shukla et al. (2018) fabricated and investigated the mechanical properties of SiC reinforced with Aluminum 6061 metal matrix composites. The varying SiC content in AMCs (0, 5, 10, 20 Wt. %) were fabricated by the stir casting process. These composites show that the reinforcement of silicon carbide into the Al matrix increased tensile strength and hardness, and maximum tensile strength was shown at 20 Wt. % SiC reinforced in AMCs. Increasing the percentage of SiC in composites increase the porosity of the composites and also decreases the ductility.

Ajagol et al. (2018) fabricated aluminum with silicon carbide (average particle size 30-45μm) reinforced in varying weight percentages of 5%, 10%, and 15 wt% using stir casting techniques. Ultimate tensile strength, microhardness, and porosity of the fabricated composites were investigated as a function of varying SiC wt%. Microstructure analysis was carried out on casted composites using optical microscopy and scanning electron microscopy. Tensile strength and hardness were significantly increased with an increase in SiC content in the Aluminium matrix. Ajith et al. (2020) successfully fabricated the hybrid metal matrix composites through a stir casting process by reinforcing different sizes of SiC (10,20&40 μm) with aluminum at different weight fractions (5 %,10% &15%). The tensile strength and hardness increase with increasing SiC reinforcement particles and increase with small particle sizes than larger. The impact energy of composite material increases as the content of SiC particles increases. Also, small particle size exhibits better hardness than coarse particles due to the higher surface area and it fills the small pores in the matrix than coarse particles.

Siddharthan et al. (2020) successfully fabricated an Aluminium alloy-based Silicon Carbide Metal Matrix Composite by die casting at three different weight compositions of the silicon carbide (10%, 20% 30%) and investigate tensile strength, hardness, and wear test of the sample. The result of hardness was analyzed qualitatively and it has shown that the addition of reinforcement increases the hardness of the composite. From the above research paper, the addition of silicon carbide particles to the pure metal enhances the mechanical properties of tensile strength, hardness, and wears resistance of the composites. S et al. (2021) developed an Al6061/SiC metal matrix composite that has 7.5% silicon carbide by stir casting and has studied the effect of sliding speed, load, and sliding distance process parameters on the wear rate and friction. Sliding speed is (2, 3, 4 m/s), the load is applied at (10, 20, 30N), and sliding distance (500, 1000, 1500m). The composite material shows a low wear rate at 4m/s, 10N, and 1500m. From the above research paper, increasing sliding distance will strictly increase the wear rate of Al6061/Sic metal matrix composite and vice versa. Increasing load increases slightly the wear rate of Al6061/Sic metal matrix composite and the third is sliding speed.

2.2.2. Mechanical and Tribological Properties of Hybrid-Reinforced AMMC

Rajeswari et al. (2014) successfully fabricated Aluminium(Al7075) alloy fixed at 90%Al weight reinforced with SiC and Al2O3 having various weight fractions of particulates by Stir Casting. They investigate on Pure Al 7075 alloy and three samples with their weight proportion of (90% Al + 5% SiC + 5% Al2O3), (90% Al + 7.5% SiC + 2.5% Al2O3), (90% A l + 2.5% SiC+7.5% Al2O3) to know the effect of silicon carbide and alumina particles in matrix material regarding to hardness and microstructural properties. The OM shows that the addition of SiC and alumina was found to be floating on the surface and increase porosity. Therefore, SiC has a great effect on the hardness of composite than Al2O3. Velavan and Palanikumar (2015) successfully fabricated aluminum alloy composite material reinforced by individual Silicon Carbide with aluminum and combined influence of Silicon Carbide with graphite reinforcements Aluminium Metal Matrix Composites and Silicon Carbide with graphite reinforcement Aluminum. From the research paper, with an increase in the composition of Sic, an improved (hardness, tensile strength,) and wear resistance of composite materials are seen. Al-Sic-Gr hybrid composites with combined equal % reinforcement of Sic and Gr particulates can be chosen for tribological applications.

Elango and Annamalai (2020) developed aluminum hybrid composites using stir casting with 5% SiC and 2.5 % Gr, 5 % Gr, and 7.5 % Gr and studied the effect of graphite addition on hardness and cutting process parameter on surface roughness of machined part using tungsten carbide insert. Then, the result revealed that the addition of graphite in Al/SiC/Gr composite increases the surface roughness, which leads to easier machining, due to the lubricant property of graphite particles. The higher percentage of graphite results in decreased hardness of Al/SiC/Gr hybrid composite. The major influencing factors of surface roughness are feed rate and, cutting speed while the depth of cut has a minor effect on surface roughness. Sesharao et al. (2021) developed aluminum reinforced metal matrix composite using stir casting with a combination of 90%Al+6% high-speed steel and 4% of copper alloy and studied the effect of cutting parameter on the tool wear, surface roughness, and thrust force with turning operation done on a lathe with the CBN insert tool. The L9 orthogonal array method is used. Tool wear has cutting depth and feed as the most and least priority parameters, respectively. Surface roughness has cutting depth and cutting fluid pressure as the greatest and smallest priority parameters correspondingly. The thrust force, cutting fluid pressure, and cutting depth are the highest and lowest priority parameters.

2.2.3. Machinability of Hybrid-Reinforced AMMC

Palanikumar and Karthikeyan (2014) investigate the factors affecting the surface toughness of the machining of Al/SiC particulate MMCs. Process parameters like cutting speed, feed rate, and percentage volume fraction of SiC were optimized to achieve minimum surface roughness. Surface roughness is greater influenced by feed rate than cutting speed and percentage fraction of SiC. The recommended machining conditions are high cutting speed and low feed rate to produce a better surface finish by using coated carbide cutting tool. Vijay et al. (2016) developed an Aluminum metal matrix composite workpiece having different weight composition of silicon carbide with constant Al2O3 and has investigated the effect of process parameters: cutting speed (2000, 2400, 2800rev/min), feed rate (50, 60, 70mm/min), and depth of cut (0.2, 0.3, 0.4mm) and SiC (5, 10, 15%) on the surface roughness of machined workpiece. spindle speed has more effect on surface roughness compared to the depth of cut and percentage variation. Feed rate has very less effect on surface roughness. An increase in percentage variation and spindle speed of SiC particle surface roughness is decreased. An increase in feed rate and depth of cut surface roughness increases.

Rayjadhay et al. (2016) developed Al 6061 reinforced with SiCp composite by stir casting and studied the effect of weight % of Silicon carbide powder, pouring temperature, and stirring time on surface roughness. The L9 orthogonal array of SiC Wt.% (0, 5, 10%), pouring temperature (660, 710, 760C), stirring time (20, 30, 40sec). Pouring temperature is the most significant effective parameter for surface roughness, followed by stirring time and silicon carbide weight percentage. Surface roughness is highly dependent on the pouring temperature, followed by stirring time and silicon carbide. The lower surface roughness happened on weight % of silicon carbide powder, pouring temperature, and stirring time (0%, 760C, 40sec) respectively. Umamaheswarrao et al. (2020) developed Al 6061 reinforced with SiCp particles at various weight fractions of 4%, 8%, 12%, 16%, and 20% added to molten metal and studied the effect of process parameters in end milling to minimize cutting force and surface roughness on the specimen in the dimensions 110x90x45 mm. Four different input parameters varied at five levels considered are cutting Speed (500, 1000, 1500, 2000, 2500rpm), feed (10, 20, 30, 40, 50mm/rev), depth of cut (0.2, 0.4, 0.6, 0.8, 1mm), % wt fraction (4, 8, 12, 16, 20%). Feed is was the most significant parameter followed by the depth of cut, weight fraction, and speed.

Ramanathan et al. (2019), the turning of the composite on 6% SiC + 6% Al_2O_3 + Al6061 aluminum alloy was performed at three different cutting speeds ranging from 20 m/min to 60 m/min. The feed rates were 0.20, 0.40 and 0.60 mm/rev. The depth of cut used for machining was 0.5, 0.75, and 1 mm. The surface roughness of the machined component was measured using a surface roughness tester Mitutoyo Surftest 301. The average surface roughness of the tested hybrid MMC specimen is minimum when the cutting speed is high (60m/min). The result indicates that the increase in cutting speed reduces the surface roughness and vice versa. Feed rate is the highly influential parameter that influences the surface roughness in the machining of hybrid composites and the increase of feed rate increases the surface roughness. The minimum surface roughness is achieved at a cutting speed of 60 m/min, feed rate of 0.20 mm/rev, and a depth of cut of 0.50 mm. To obtain reduced average surface roughness it is recommended to use medium cutting speed, minimum feed rate, and lower depth of cut.

2.3. Summary of Literature Review

Numbers of researches have been carried out on the fabrication and characterization of aluminum matrix composites with different types of reinforcement, various particle sizes of reinforcement, different fabrication techniques, and also various testing conditions. The above literature review clearly shows that various fabrication methods mainly liquid state processing techniques and the effect of processing conditions, and the effect of reinforcement have been widely studied. The primary advantages of the AMMCs materials are their improved mechanical properties, particularly in the areas of hardness, tensile and impact strength, and tribological properties (wear resistance). AMMCs are reinforced with varied particulate ceramic reinforcements and the influence of weight composition and particle size of reinforcement on the mechanical and tribological behavior of developed composite has been studied. Ceramic particles were widely employed as reinforcements in the production of aluminum matrix composites. From the above literature, it is shown that the mechanical and tribological properties of aluminum alloy matrix are significantly improved by the addition of different particulate reinforcements.

2.4. Research Gaps

AMMCs are widely used in Aerospace and Automobile industrial applications and many studies have been done in this area. Almost all research papers have developed a composite material having air gaps between reinforcement and final solidified matrix due to poor wettability between two phases which reduces ultimate strength, a composite material having high particle segregation at the bottom and floats over the surface of liquid metal which results in high porosity as well as heterogeneous mechanical and tribological properties. Most research has lack testing material properties such as; the toughness of composite to control its ductility because a very high weight percentage of ceramic reinforcement will increase properties of brittleness which leads to a decrease in the toughness (impact strength) and fracture toughness. The machinability of composite is also one of the challenges because of the presence of hard abrasive ceramic reinforcing particles in the base matrix.

CHAPTER THREE

MATERIALS AND METHODOLOGY

3.1. Materials

The required properties of composite used for the aerospace and automobile application have been known regarding mechanical properties, microstructural and tribological properties. Al 6061 alloy used as matrix and reinforcement SiC and MoS2 was used for self-lubrication properties are selected based on cost, properties, and availability.

3.1.1. Aluminium Alloy (Al6061) Matrix materials

The aluminum has superior to magnesium and titanium in the greater flexibility, resistance the corrosion, low density, wettability, and strong bonding at the interface. Among several series of aluminum alloys, heat treatable Al6xxx and Al7xxx are much revealed. Al6xxx alloy is extremely corrosion resistant, extricable, and exhibits moderate strength. It finds enormous applications in industrial applications.

Table 3.1: Chemical Composition of Al6061 by Weight Composition

Elements of Al 6061	Si	Mn	Mg	Cr	Zn	Cu	Fe	Ti	Al
wt%	0.7	0.05	0.9	0.3	0.2	0.30	0.6	0.1	96.85

Source: Radha and Vijaya Kumar (2015)

Table 3.2: Properties Aluminum Al6061 alloy

Property	Value
Formula	Al6061
Density	2.71 g/cm^3
Melting point	605 °C
Modulus of elasticity	70GPa
Tensile strength (σt)	115 MPa
Hardness	30Kg/mm^2
Elongation (ε) at break	12-25
Poisson's ratio (ν)	0.33
Form	Rod

Source: Radha and Vijaya Kumar (2015)

3.1.2. Silicon Carbide (SiC) Reinforcement Materials

Silicon carbide is used as reinforcement in the form of particulates to develop the properties of the composite. Silicon carbide particles have become one of the popular reinforcing phases for many aluminum alloy-based metal matrix composites. They are hard and brittle ceramic particles with high strength, high modulus of elasticity, and high thermal and electrical resistance. Owing to its high hardness SiC has several applications such as in cutting tools, aerospace parts, automobile parts, etc.

Table 3.3: Properties of Silicon Carbide (SiC)

Property	Value
Formula	SiC
Density	3.21 g.cm-3
Melting point	2730°C
Modulus of elasticity	410GPa
Tensile strength (σt)	3900MPa
Poisson's ratio (ν)	0.14
Form	Powder
Particle size	270mesh
Hardness	2800 Kg/mm^2

Source: Subba and Ramanaiah, (2017).

3.1.3. Molybdenum Disulfide (MoS2) Reinforcement Materials

Molybdenum disulfide (moly) is an inorganic compound made from molybdenum and sulfur atom. The Chemical formula for this compound is MoS2. It is a silvery black solid that occurs as the mineral Molybdenite, which is the principal ore for molybdenum. MoS2 is relatively unreactive. It is widely used as a dry or solid lubricant because of its low coefficient of friction.

Table 3.4: Typical properties molybdenum disulfide

Property	Value
Formula	MoS2
Color	black
Density	5.06g.cm-3
Size	2.5μm
Melting point	1185°C
Purity	98.8%
Form	Powder

Source: Subba and Ramanaiah, (2017).

3.2. Experimental Procedure

3.2.1. Flow Chart of Experimental Procedure

The research work methodology can be expressed as follow by using a flow chart.

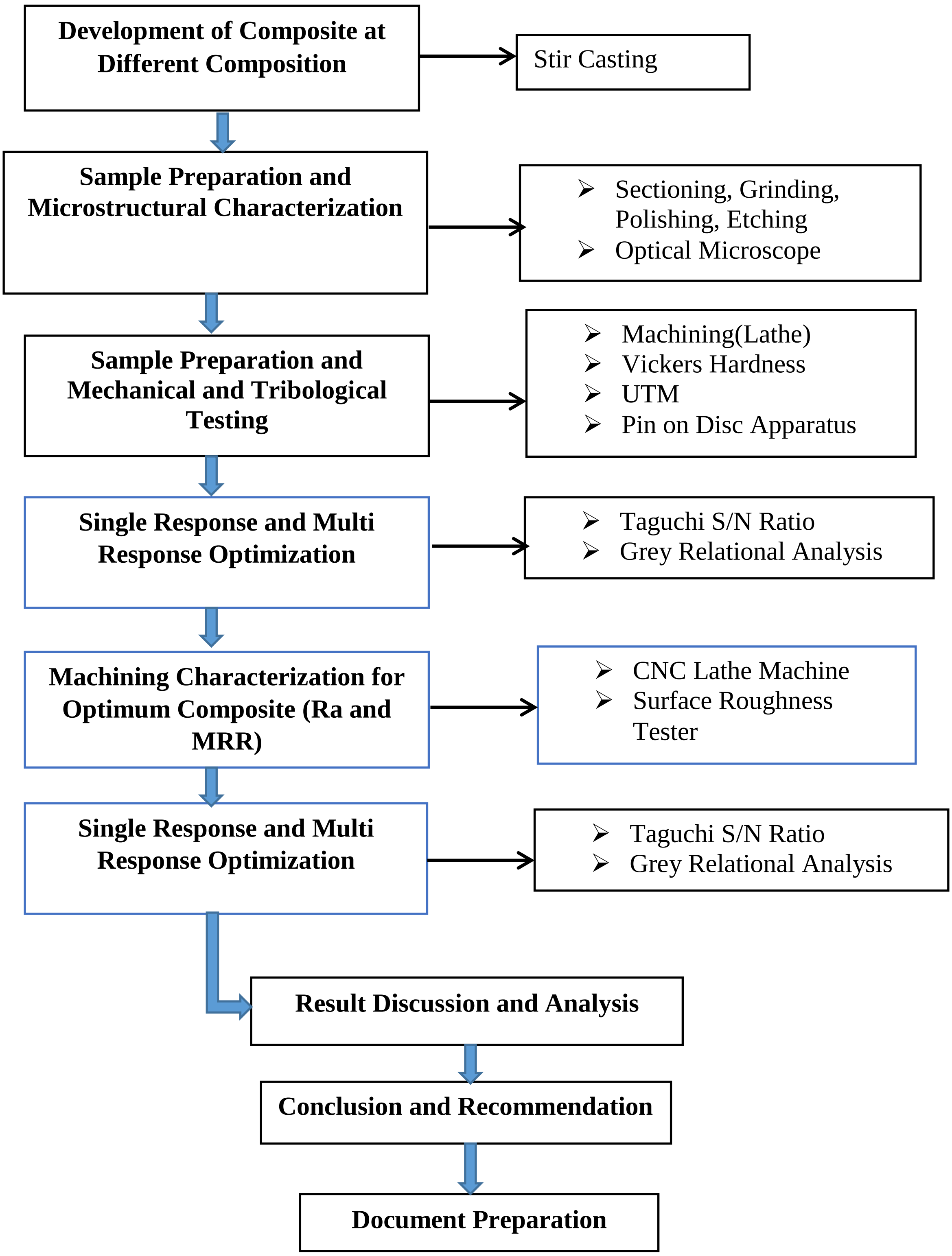

Figure 3.1: Flow chart of the experimental procedure

3.2.2. Design of Experiment for Composite Fabrication

The fabrication of composite was achieved by stir casting machine with Taguchi experimental design prepared based on basic input variables of process parameters (stirring speed, Stirring time, the weight percentage of reinforcement) at the same pouring temperature 730°C for each fabrication and Taguchi L9 orthogonal array experimental design at three different levels are used.

Table 3.5: Experimental Parameters and Their Level.

S. No	Process parameters	Levels			Units
1	Stirring speed (A)	350	450	550	rpm
2	Stirring time (B)	5	10	15	min
3	Wt% of SiC (C)	0	5	10	%
4	Wt% of MoS2 (D)	0	2	4	%

Table 3.6: Experimental Design for Fabrication.

S. No	A (rpm)	B (min)	C (%)	D (%)	Designation
1	350	5	0	0	S_1
2	350	10	5	2	S_2
3	350	15	10	4	S_3
4	450	5	5	4	S_4
5	450	10	10	0	S_5
6	450	15	0	2	S_6
7	550	5	10	2	S_7
8	550	10	0	4	S_8
9	550	15	5	0	S_9

3.2.3. Determination of Requirement Matrix and Reinforcement Materials

The total weight amount of matrix and reinforcement required for Al, SiC, and MoS2 composite samples production, is found from the total specimens required for hardness, microstructure, tensile strength, impact strength, and wear tests. Therefore, the shape, dimension, and volume of each sample are calculated as follows to estimate the total required materials of matrix and reinforcement.

The mechanical and tribological properties of the developed composite materials are highly dependent on the weight percentage (wt%) of the reinforcements. Therefore, the weight percent composition of SiC and MoS2 used in this research work have been taken based on the literature review, and the following researchers' studies are considered for taking the wt% composition of reinforcement in each of the samples. The wt% composition of any reinforcement addition should not exceed 30% to minimize the porosity formation in the composite, for better uniformly distribution of reinforcement and good densification of the composite fabricated (Ramanathan et al. (2019)), therefore, the maximum reinforcement for this research study was 14 wt% (10%SiC and 4MoS2).

The required volume of material for a cylindrical sample is calculated using Eq (3.1);

$$\mathbf{V}= \frac{\pi}{4} D^2 * L \qquad (3.1)$$

Where

V= volume of sample in mm3,

L=length of sample in mm, and

D=diameter sample in mm

V_T= the total volume of material required for each sample in mm3

For the hardness and microstructure test, the sample size required was L=15mm, D=20mm, for the tensile test, depending on the ASTM E-8 standard the sample size required was L=80mm, D=10mm, for the wear test, depending on the ASTM G99-05 standard the sample size required was L=12mm, D=6mm the calculation to get the required material for fabrication used are within the consideration sample preparation. Then, the total length and diameter of the composite are the summation of all tests.

Length = 15 (hardness) + 80 (tensile) + 12 (wear) + 20 (sample preparation) = 127mm

D = 24mm

V_T= the total volume of material required for each sample in mm3

$V= \frac{\pi}{4} D^2 * L$= $V= \frac{\pi}{4} 24^2 * 127$= 5745.44$mm^3$ = 5.745cm^3

V_T = 51.705cm^3 (for nine sample fabrication)

The total volume of material required for sample fabrication includes both matrix and reinforcement materials and for nine (9) sample fabrications V_T = 51.705cm^3 amount of material is required and the weight percentage of each material is varied depending on the Taguchi orthogonal array.

Table 3.7: Total required volume of materials.

Fabricated sample based on L9 Taguchi orthogonal array	**V_T = 51.705cm^3**		
	Al (cm^3)	SiC (cm^3)	MoS2 (cm^3)
Sample 1	5.745	-	-
Sample 2	5.343	0.2872	0.115
Sample 3	4.941	0.5745	0.23
Sample 4	5.228	0.2872	0.23
Sample 5	5.1705	0.5745	-
Sample 6	5.63	-	0.115
Sample 7	5.0556	0.5745	0.115
Sample 8	5.400	-	0.23
Sample 9	5.458	0.2872	-
The total required volume	48 cm^3	2.585 cm^3	1.035 cm^3

The density of matrix (Al6061) and the reinforcements (SiC, and MoS2) are:

Density of Aluminum alloy (Al6061) = 2.71 gr/cm^3

Density of Silicon carbide (SiC) = 3.21 gr/cm^3

Density of Molybdenum disulfide (MoS2) = 5.06 gr/cm^3

The weight of matrix material (Al6061) and the reinforcement material (SiC, and MoS2) in each specimen for the given compositions are estimated as follows.

Mass (weight) of material is the product of the volume of material with the density of material (m=V*ρ). Therefore,

Total weight of (Al6061) = Total volume of (Al6061) * density of (Al6061)

=48 cm^3*2.7 gr/cm^3 =129.6gram

Total weight of Silicon carbide (SiC) = Total volume of (SiC) * density of (SiC)

=2.585cm^3*3.21 gr/cm^3=8.3gram

Total weight of (MoS2) = Total volume of (MoS2) * density of (MoS2)

=1.035 cm^3*5.06 gr/cm^3 =5.24gram

3.2.4. Tools and Equipment

Table 3.8: Shows a list of equipment used in the study.

S.NO	Tools	Function/task
1	Stir casting machine	To fabricate the composite materials.
2	Lathe machine	To prepare the specimen for tests as per ASTM standards.
3	Grinder/Polisher	To obtain a flat mirror-like surface free from excessive deformation.
4	Abrasive Cutter	Abrasive cutting is the most commonly used method for sectioning materials during sample preparation for testing.
5	Chemical (Keller’s etchant) solution.	To keep away from any particles, dust, debris…. etc, from the fabricated specimen for micro structural characterization
6	Optical Microscope	For microstructural analysis of the developed composite.
7	Universal testing machine (UTM)	To determine the composite material's tensile strength or capacity to endure loads that causes it to enlarge in size.
8	Vickery hardness machine	To determine the composite's hardness
9	Pin on disc Apparatus	To determine the materials' wear resistance performance, they are subjected to a wear test.
10	Electronic weighting machine	To determine how much weight loss of the sample during the wear test.
11	DMTG CNC Lathe Machine	To perform turning for study machining characteristics
12	Surface-Roughness Tester	To measure the surface roughness of machined work piece
13	ImageJ software	ImageJ is an image analysis program extensively used for microstructural analysis
14	Minitab 17 software	Minitab is a software package used for the analysis of data and optimization using tools in it Taguchi (S/N ratio, ANOVA)

3.2.5. Fabrication Composite Procedure

To achieve the optimum properties of metal matrix composites, the distribution of reinforcement material in the matrix alloy must be uniform and the wettability or bonding between these substances should be optimized and porosity levels need to be minimized.
Steps involved in the fabrication of Aluminum metal matrix composites are as follows: The experimental arrangement consists of the main furnace and components along with four mild steel stirrer blades. In this work for preparing metal–matrix composite, aluminum alloy (Al6061) circular rod form is used as base material, and SiC particles and MoS2 in powder form are used as the reinforcements The first process in the experiment is preheating the reinforcement powders in a graphite crucible and, namely, silicon carbide powder is preheated in the furnace at 1100^{o}C for 1 to 3 hours to make their surfaces oxidized. The melting of the aluminum alloy circular rod at different (%) is carried out in the graphite crucible inside the furnace.

Then, the crucible with aluminum alloy is heated to 730^{o}C while the preheated powders of SiC with MoS2 are mechanically mixed below their melting points. This metal–matrix is then kept in the furnace at the same temperature. The vigorous automatic stirring of the material takes place for 5-15 minutes with a 350-550rpm stirring rate, thereby uniformly dispersing the additive powders in the aluminum alloy matrix. The temperature rate of the furnace was controlled at 730^{o}C in the final mixing process. Pouring of the composite slurry has been carried out in the sand mold prepared. This experiment is repeatedly done by varying the compositions of the materials used in composite fabrication.

Figure 3.2: Cylindrical fabricated (casted) sample

3.2.6. Sample Preparation for Characterization

After successful fabrication of composite material using the stir casting method, the composite was then prepared for mechanical testing, physical testing, microstructural characterization, and tribological testing. For physical, mechanical, and tribological tests, the specimen was prepared to the required shape and size according to ASTM standards by machining on a lathe.

3.2.6.1. Machining and Cutting

The surfaces of the fabricated composite were very rough and have unwonted parts on them. To reduce surface roughness and avoid unwanted parts, and also to get the required shape and size as per ASTM standards, machining on a lathe was done.

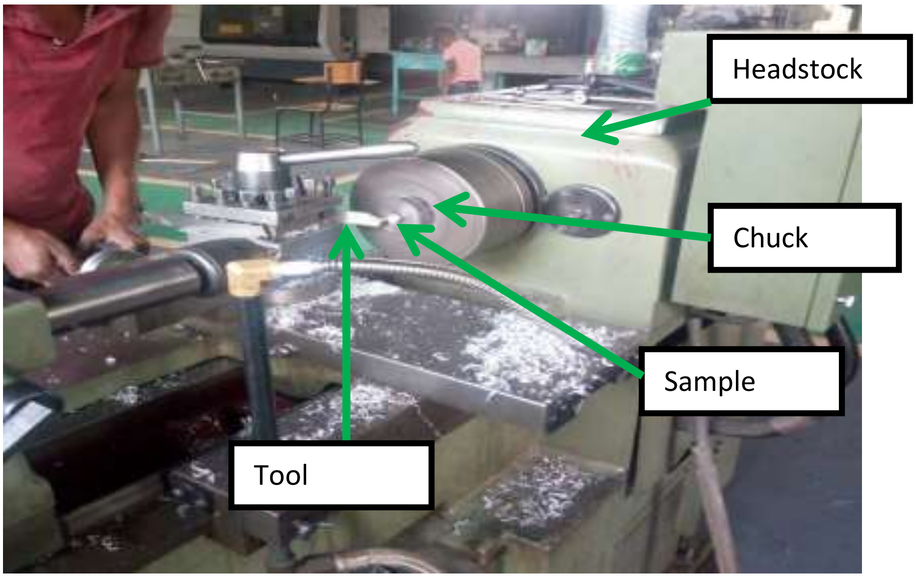

Figure 3.3: Machining of casted sample on a lathe machine.

3.2.7. Density and Porosity Measurement

Density and porosity are the physical property of the material. Theoretically, the density of the material generally can be defined as mass over unit volume. The existence of "porosity, its size, and distribution in composites play an important role in controlling the mechanical properties and it has to be minimum to achieve desired high performance in service applications. Porosity in composites results primarily from air bubbles entering the slurry during the stirring period or as air envelopes to the reinforcing particles".

The theoretical density (ρ_{theo}) of hybrid aluminum matrix composite was calculated using the rule of mixtures as shown in Eq. (3.2) (Rajesh et al., (2018)). Consider that the produced Hybrid aluminum matrix composite is the mixture of aluminum alloy (Al6061), silicon carbide (SiC), and Molybdenum disulfide (MoS2).

Where Vmat and Vrein1 represent a fraction of the volume, ρmat is the matrix density, and ρrein1 is the reinforcement density, respectively

$$\rho_{theo} = V_{Al6061} * \rho_{Al6061} + V_{SiC} * \rho_{SiC} + V_{MoS2} * \rho_{MoS2} \quad (3.2)$$

Where: ρtheo= theoretic density of composite; V_{Al6061}= fraction of the volume of aluminum alloy in the composite specimen; V_{SiC} = fraction of the volume of silicon carbide in the composite specimen; V_{MoS2}= fraction of the volume of Molybdenum disulfide in the composite specimen; ρAl6061= density of aluminum alloy; ρSiC = density of silicon carbide and ρMoS2= Molybdenum disulfide

Experimentally, the Density hybrid aluminum matrix composite can be formulated as follows: the actual density of the composite can be calculated using the Archimedes principle. The cylindrical specimen was weighted in the air (mair) and weighted again in distilled water (water). The actual/experimental density (ρ_{actual}) was calculated according to Eq. (3.3) (Wang et al., 2004).

$$\rho_{actual} = \frac{m_{air}}{m_{air} - m_{water}} * \rho_{water} \quad (3.3)$$

Where, mair = mass of composite in air and mwater = mass of composite in distilled water, and ρwater = density of distilled water at 25°C = 997.044 kg/m3. The porosity of each hybrid composite material can be determined based on Eq. (3.5) (Aatthisugan, (2017)).

$$P = 1 - \frac{\rho_{actual}}{\rho_{theo}} \quad (3.4)$$

Where P = the porosity of composite material, ρ_{actual} = the actual density of composite material, and ρ_{theo} = the theoretic density of composite material.

Table 3.9: Theoretical density and Actual density of composite

Sample	The theoretical density of composite	The actual density of composite (gr/cm^3)
S1	2.71 gr/cm^3	2.668
S2	2.782 gr/cm^3	2.702
S3	2.854 gr/cm^3	2.764
S4	2.829 gr/cm^3	2.747
S5	2.76 gr/cm^3	2.675
S6	2.757 gr/cm^3	2.712
S7	2.807 gr/cm^3	2.715
S8	2.804 gr/cm^3	2.753
S9	2.735 gr/cm^3	2.670

Where, Density of (Al6061) = 2.71 gr/cm^3, Density of (SiC) = 3.21 gr/cm^3, Density of (MoS2) = 5.06 gr/cm^3

3.2.8. Microstructural Characterization of Composite

The microstructural analysis is performed on each combination of fabricated composite and hybrid composites using an optical microscope to know the fair distribution of reinforcement and to determine the volume fraction of grain particle size.

3.2.8.1. Sample Preparation for Microstructural Characterization

Specimen preparation for microstructure characterization includes; sectioning, grinding, polishing, etching, and then microscopic examination.

3.2.8.2. Sectioning of Sample

Sectioning serves two purposes: generating a cross-section of the sample to be examined and reducing the size of a sample to be placed on a stage of a light microscope. Abrasive cutting is the most commonly used method for sectioning materials. Samples are sectioned by a thin rotating disc in which abrasive particles are supported by suitable media which is shown in figure 3.4A.

3.2.8.3. Grinding of Sample

Grinding is the process of making Al/SiC/MoS2 composite sample clear surface from scratches using the sand paper of gradually increasing scale 400, 800, 1200, and 2000 grits, that is shown in figure 3.4B in steps are; rough grinding, fine grinding, and polishing.

3.2.8.4. Polishing of Sample

Polishing is the process of creating a smooth and shiny surface by rubbing the sample using a diamond suspension with a gradual reduction of the pressure to keep the specimen from plastic deformations and the sand wheel rotation speed using the RB 204 Metpol-II Model polishing process was used as shown in figure 3.4C.

3.2.8.5. Etching of Sample

Etching is the process of making microstructural features through selective chemical attacks to present the grains and grain boundaries. The polished samples Al/SiC/MoS2 composite were etched with recommended mixed etchants solution (25ml-methanol, 25ml-hydrochloric acid, 25ml-nitric acid, and 1-drop of hydrofluoric acid) and simply performed by immersion of the samples into the prepared etchant solution for 15 seconds and washed with distilled water before the microstructural characterization as shown on figure 3.4D.

A. Sectioning B. Grinding

C. Polishing D. Etching

Figure 3.4: Sample preparation A. Sectioning, B. Grinding, C. Polishing, D. Etching.

3.2.9. Mechanical Characterization of Composite

Investigations of the hardness, tensile strength, and impact strength of the fabricated composite have been achieved based on their ASTM standard. This means the size and shape of the composite and apparatus of testing depend on the ASTM standard.

3.2.9.1. Hardness Testing

The hardness of material usually implies resistance to deformation. The Vickers hardness tester was used and uses a square-base diamond pyramid as the indenter. This included angle between opposite faces of the pyramid is 136°. The diamond-pyramid hardness number (DPH), or Vickers hardness number (VHN, or VPH), is defined as the load divided by the surface area of the indentation. The Vickers hardness test is comprised of a diamond indenter and a light load to produce an indentation on the subject under testing. The depth of indentation is converted into the hardness value of the object. Therefore, the harness of composite testing was done with the help of a Vickers hardness machine shown in below figure 3.5, and the sample having 10mm length and 20mm dia are shown in figure 3.6.

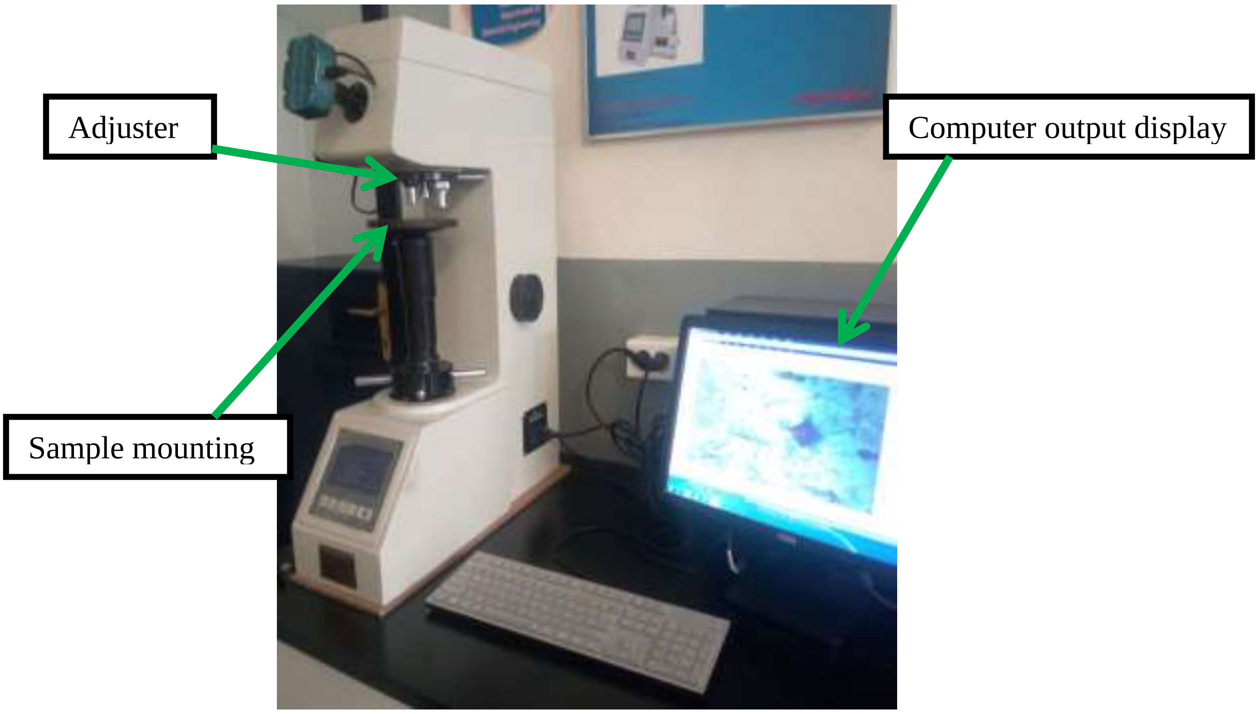

Figure 3.5: Vickers hardness tester machine and its parts

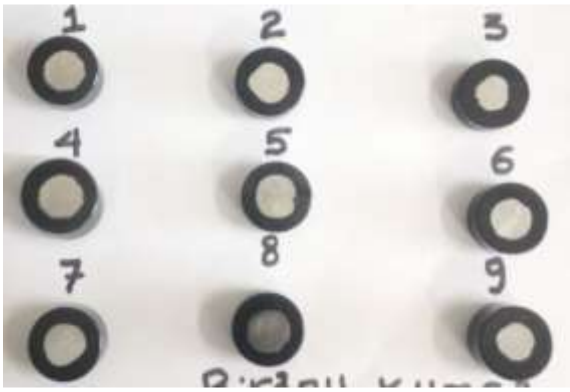

Figure 3.6: Sample for hardness test

3.2.9.2. Tensile Strength Testing

The ability of a material to withstand a static load can be determined by testing the material in tension or compression. The tensile specimen was prepared by machining as per the ASTM E-8 standards. The test was conducted using Shimadzu AG-X plus TM 50kN, a universal testing machine as shown in figure 3.7 and the dimensions of the tensile specimens are as shown in figure 3.8, and tensile properties like ultimate tensile strength, percentage elongation of the tensile tested samples were also analyzed. The sample size has gauge length (G=43.75mm), R=6.25mm, overall length (L=82.5mm), parallel length (A=50mm), and grip width (C=14mm).

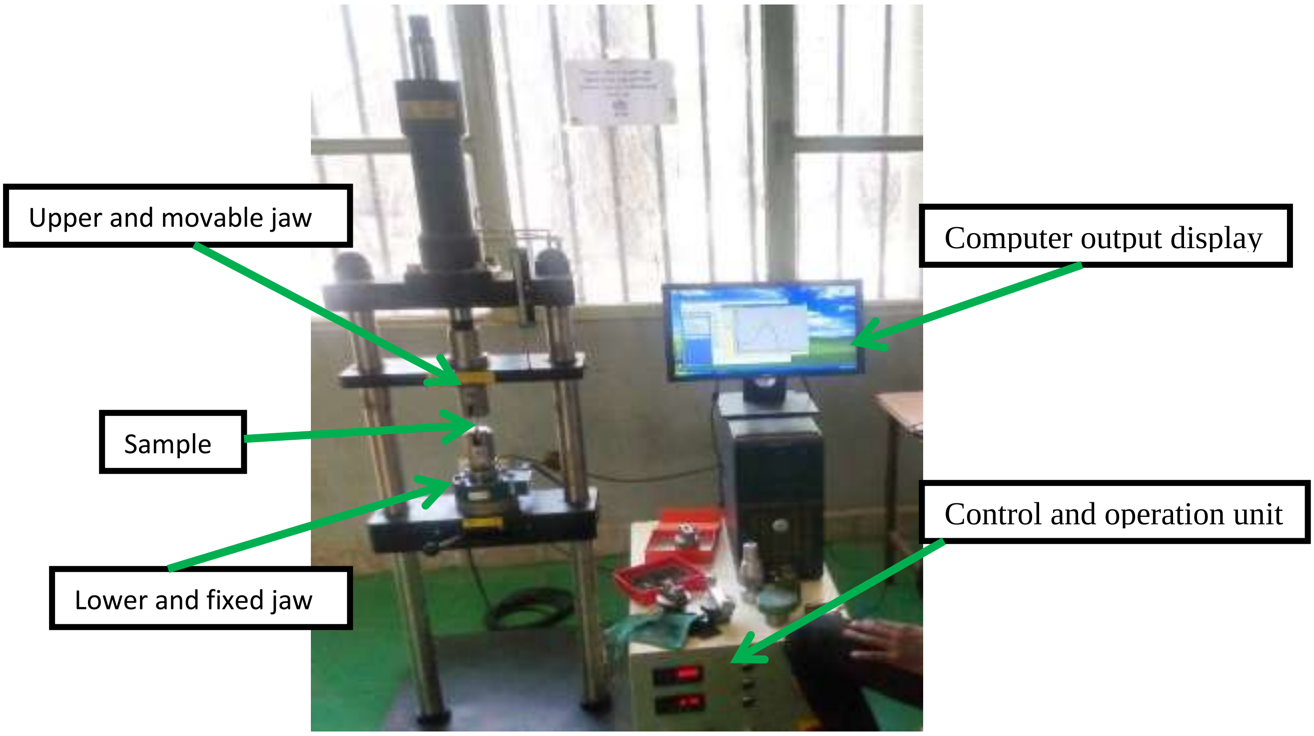

Figure 3.7: Universal testing machine (UTM) and its parts

Figure 3.8: Sample before and after tensile testing and sample size

3.2.9.3. Impact Strength (Tensile Toughness) of Composite

Impact energy is the energy that the specimen absorbs once a sudden load is applied. Another definition is the ability to absorb mechanical energy up to the point of failure. The area under the stress-strain curve is called toughness. Toughness can be determined by integrating the stress-strain curve. It is the energy of mechanical deformation per unit volume before fracture. The explicit mathematical description is:

$$\text{Toughness} = \int_0^{\varepsilon f} \sigma d\varepsilon$$

Where: ε is strain and εf is strain up to failure, σ is stress

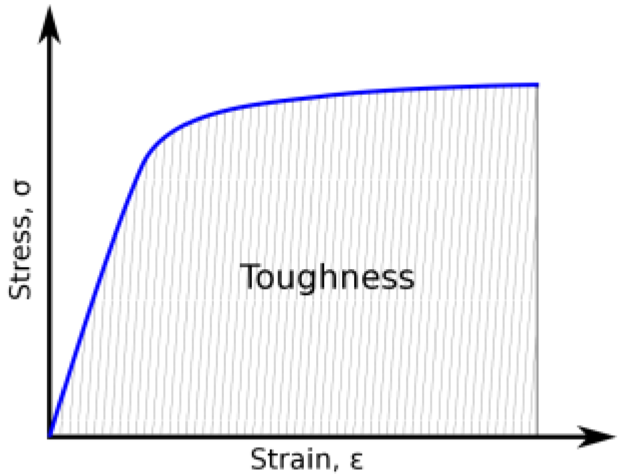

Figure 3.9: Trapezoidal principle to determine tensile toughness

3.2.10. Tribological Characterization of Composite

The wear performance of the fabricated composite has been achieved based on the ASTM G99-05 standard. This means the size and shape of the composite depend on it. Wear is the progressive loss of material from a contact surface during relative motion between a surface and the contacting substance or substances. In this paper, the dry sliding wear behavior the was investigated using pin-on-disc (DUCOM TR-20 MICRO) equipment as shown in figure 3.10 and the sample size of 6mm diameter and 12mm height pins dimension and then polished metallographically for the wear test based on the ASTM G99-05 standard, as shown in figure 3.11. The test was conducted at room temperature (25°C) under the applied load of 40N with a sliding speed of 600 rpm on a wear track diameter of 25mm. The friction coefficient and wear rate are considered the main response functions for evaluating the wear performance of the composites. The wear mass loss of each sample was calculated by measuring the weight difference between the samples before and after conducting the test.

The weight or mass loss of each sample was used to calculate the wear rate (W.R). The wear rate (W.R) of the specimen by weight technique is calculated using Eq (3.5). This way can be giving the result of wear more accurate from weight techniques (Rao et al. (2009)).

$$W.R = \frac{Wear\ volume\ loss}{sliding\ distance} = \frac{WL}{\pi x d x n x t} \quad (3.5)$$

Where, W.R is wear rate, d is the diameter of the wear track of the disc (25mm), n is revolution per minute (600rpm), t is time (6 minutes), and WL is the weight (or mass) loss (Weight before wear (Wb) – weight after wear (Wa)).

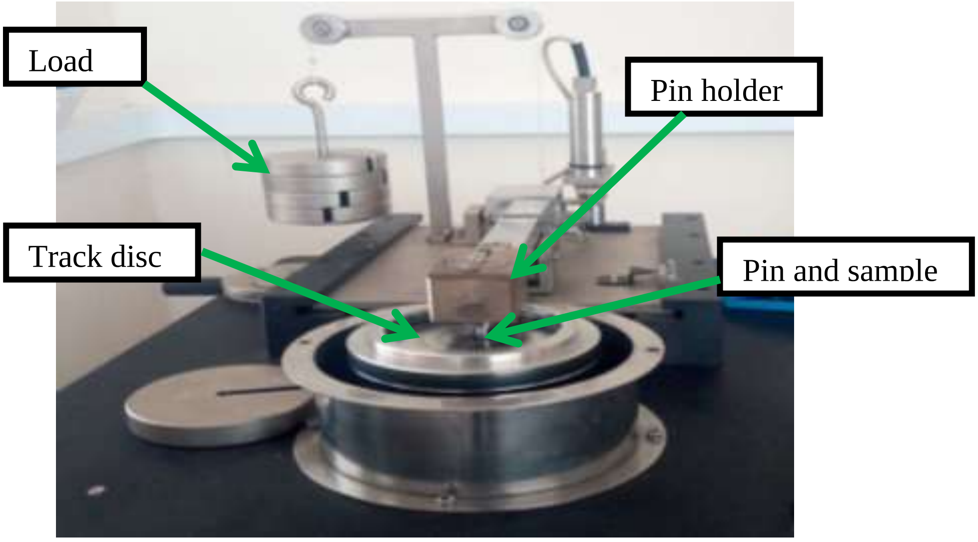

Figure 3.10: Pin-on-disc (DUCOM TR-20 MICRO) equipment and its part

Figure 3.11: Sample for the wear test

3.2.11. Taguchi Analysis for Single Response Optimization

3.2.11.1. Analysis of variance

ANOVA is conventionally used to investigate whether the experimental design parameters have a significant effect on the responses and identify their percentage contribution. Generally, the F-test was employed as a measure to evaluate the extent of factors controlling the test results. For a 95% confidence level, if the value of 'Prob > F', commonly known as 'p-value', was less than 0.05, the factors and interactions were considered significant (Şahin, (2015)). In ANOVA, the adjusted correlation coefficient, $Radj2$ was used to evaluate the validity of the fitted model. $Radj2$ measures the percentage of variation explained exclusively by those independent factors and interactions which predominantly affect the response variables. Further, to conclude that the created models fit the performed experiments well, it desired that the values of $R2$ and $Radj2$should be high and close to each other (Şahin, (2015)).

3.2.11.2. S/N Ratios in the Taguchi Method

The Taguchi method employs orthogonal arrays to reduce variance and optimize process parameters. In the Taguchi method, the signal-to-noise ratio (S/N) is used as a performance characteristic to measure process robustness and to evaluate deviation from desired values (Sylajakumari & Ramakrishnasamy, (2018)). The S/N ratio a logarithmic function was computed by assessing the proportion of signal (mean) to the noise (standard deviation). To diminish noise and the effects of uncontrollable factors, higher values of S/N ratios are preferred (Navaneethakrishnan & Athijayamani, (2015)). High S/N ratios indicate the improved quality of the product.

3.2.12. Grey Relational Analysis for Multi-response Optimization

Grey Relational Analysis is a tool that is used for solving complicated interrelationships between the multiple response characteristics problems. The multi-objective problem of getting higher Hardness, tensile strength, impact strength and wear performance is changed into a single-objective optimization problem using grey relational analysis. This grey relational analysis was completed in three steps: Data Preprocessing, Grey relational coefficient, and Grey relational grade. Since the response characteristics are multiple responses for the same input process parameters, GRA was used for optimization purposes.

3.2.13. Machining Characterization of the Optimum Composite

The term hybrid refers to a composite that has more than one type of matrix or reinforcement in its construction. The use of hybrid composites can expand the range of achievable properties when using composite materials and can be more cost-effective than conventional or advanced composites. One of the main attractions when using hybrids is their synergy effect also called as ‘hybrid effect’. The most common effect is to obtain a composite property, like tensile strength, hardness, and wear performance whose value is higher than would be predicted from a simple application of the rule of mixtures. This would be a positive hybrid effect. In some cases, a negative effect may also occur like machining performance. The main challenge of aluminum metal matrix hybrid composites material is its machining characteristics. The machining performance is defined in terms of tool life, material removal rate, or surface quality of the machined part. The presence of ceramic reinforcement particles in aluminum metal matrix composites makes the composite difficult to machine due to the presence of hard abrasive ceramic reinforcing.

3.2.13.1. Selection of Turning Process Parameter

For this CNC dry turning process, the selection cutting parameters for aluminum metal matrix composites was selected depending on knowledge found in the literature, according to the recommendations of the previous researcher because, since these aluminum metal matrix composites were developed by the researcher and it has no standard range. The selected cutting parameters were shown in table 3.10.

Table 3.10: Machining process parameters and its level

S. No	**Process parameters**	**Levels**			**Units**
1	Spindle speed (N)	500	750	1000	(rev/min)
2	Feed rate (f)	0.1	0.2	0.3	mm/rev
3	Depth of cut (d)	0.2	0.3	0.4	mm

3.2.13.2. Design of Experiment for Machining

The experimental design for machining was prepared based on basic input variables of process parameters (cutting speed, feed rate, and depth of cut), and an L9 orthogonal array experimental design at three different levels was used for machining. Based on Taguchi L9 orthogonal array experimental design, the cylindrical rod of hybrid composite with 150mm long and 20mm diameter for machining experiment on CNC dry turning operation was performed and then the surface roughness and material removal rate are recorded.

Table 3.11: L9 Orthogonal array of experimental design for machining

S.NO	Parameters		
	Spindle speed N (rev/min)	Feed rate f (mm/rev)	Depth of cut (d)(mm)
1	500	0.1	0.2
2	500	0.2	0.3
3	500	0.3	0.4
4	750	0.1	0.3
5	750	0.2	0.4
6	750	0.3	0.2
7	1000	0.1	0.4
8	1000	0.2	0.2
9	1000	0.3	0.3

3.2.13.3. Design of Machining Section Based on Design of Experiment

The work piece material used for this study was the optimum developed composite material having150mm in length and 20mm diameter was prepared. TNMG 220408 tungsten carbide cutting tool was selected based on the hardness of the work piece and literature review. The value of process parameter was depth of cut (0.2, 0.3, 0.4mm), feed rate (0.1, 0.2, 0.3mm/rev) and spindle speed (500, 750, 1000rpm) as shown in figure 3.12.

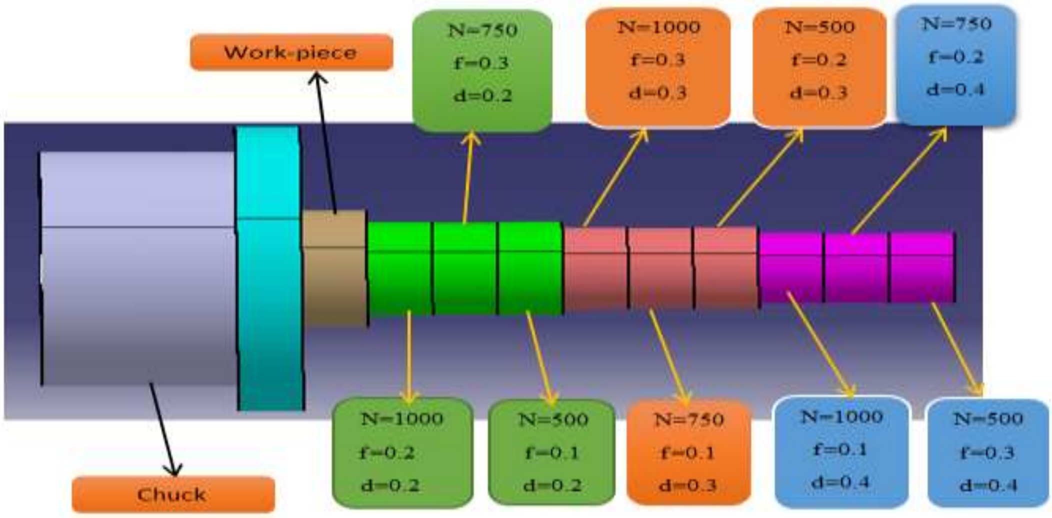

Figure 3.12: Schematic representation of machining by CATIA V5

3.2.13.4. Conducting Turning Process

Turning machining operation was achieved on DMTG computer numerical controls (CNC) lathe with CKE 6150 model which rotates the work piece and moves the cutting tool based on commands that are preprogrammed and offer very high precision was used for this study as shown in figure 3.13 below.

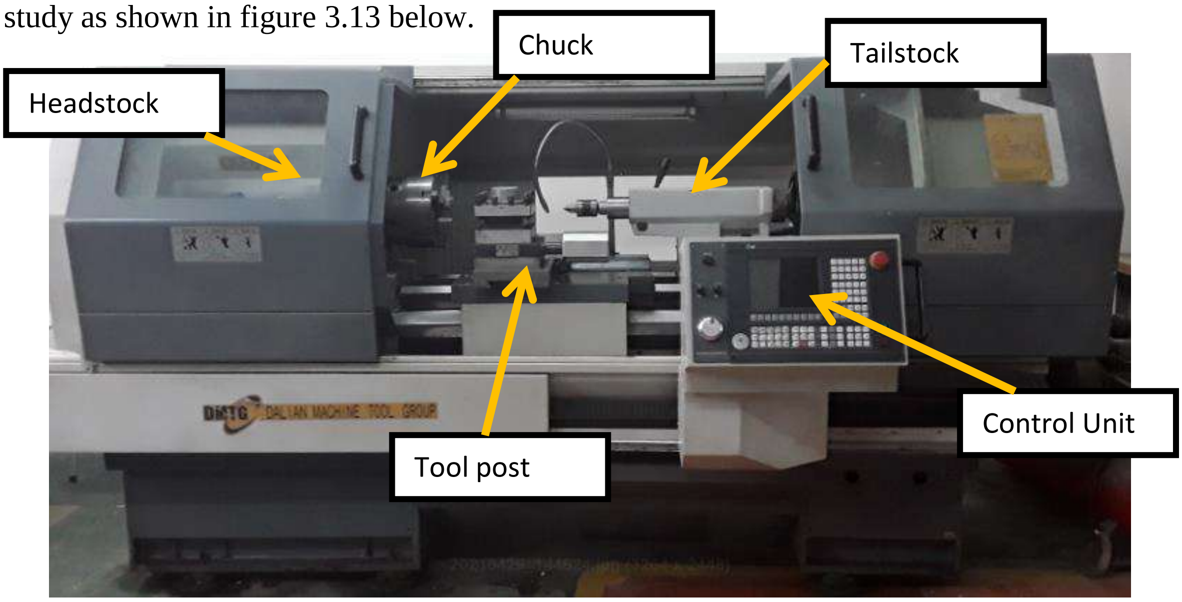

Figure 3.13: DMTG CNC Lathe Machine

3.2.13.5. Surface Roughness Measurement

During the machining cutting process parameters greatly influence the surface roughness of the machined composite. The final composite material of every machining process needs to have a low surface roughness (high surface finish quality). In this study, the surface roughness of all samples after turning was measured by VOGEL Surface Roughness Tester and analyzed by using Minitab 17 software to find the optimum cutting parameter combination which results in a good surface finish. During the measurement of surface roughness, every sample measurement was repeated at least three times at different new locations on the machined rod bar surface to get the exact surface roughness of the machined part.

Figure 3.13: Surface-Roughness Testing Equipment

3.2.13.6. Calculation of Material Removal Rate (MRR)

Material removal rate (MRR) is the amount of material removed per time unit and it directly determines the productivity of the machining process which maximizes the production rate. But high production rate only does not mean economic machining because increasing material removal rate usually results in high surface roughness, high tool wear rate, and high tool tip temperature which negatively affect the overall economy of the machining process. In this study, the following formula has been used to compute the material removal rate (Durga et.al, (2017)).

Material removal rate MRR = $\frac{\text{The total volume of material removed (V)}}{Total\ cutting\ time(t)}$

But, V = $\frac{\pi}{4}(D^2 - d^2) * L$ and t= $\frac{L}{Nf}$ where: D and d are initial and final work piece diameter, N is spindle speed and f is feed rate.

Then Material removal rate MRR = $\frac{\pi}{4}(D^2 - d^2) * Nf$ (3.6)

CHAPTER FOUR

RESULTS AND DISCUSSIONS

4.1. Introduction

In this analysis part, the results of the experimental work of the study have been discussed in detail in different sections and sub-sections in flow. The hardness test results, tensile strength test results, tensile toughness result, wear rate test result of developed composite with microstructural analysis, and also the surface roughness and material removal rate results for optimum composite during machining were reported. The result was analyzed as a single response characteristic for (hardness, tensile strength, tensile toughness, wear rate, surface roughness, and material removal rate) using Taguchi's S/N ratio and as a multi-response characteristic using Hybrid Taguchi Grey Relational Analysis (HTGRA) for both developments of composite and machining characteristics.

4.2. Analysis of Porosity of Composite

The porosity of developed composite material can be determined based on Eq. (3.4). The product quality can be determined by the criteria of "the smaller, the better" quality measurement (Das et al. (2020)). There was a difference between theoretical density and experimental density of composite due to the presents of voids and segregation of heavy particles towards the bottom as shown in figure 4.1. Porosity percentage increases with an increase in SiC particle addition because particles enter the melt as a group of particles trapping air in between them to form a void space (Bharath et al. (2014)). Porosity level is acceptable up to a maximum of 4 % have been reported for cast aluminum matrix composites (Gowri et al. (2018)).

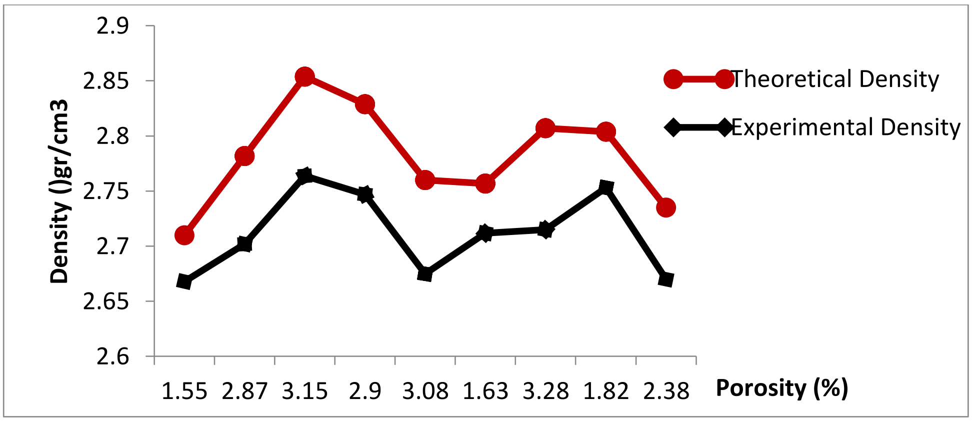

Figure 4.1: Porosity level and variations of theoretical and experimental density values.

Table 4.1: Porosity level and variations in theoretical and experimental density values

Designation	Theoretical Density gr/cm^3	Experimental Density gr/cm^3	Porosity (%)	S/N ratios of Porosity
S1	2.71	2.668	1.55	-3.8066
S2	2.782	2.702	2.87	-9.1576
S3	2.854	2.764	3.15	-9.9662
S4	2.829	2.747	2.90	-9.2480
S5	2.76	2.675	3.08	-9.7710
S6	2.757	2.712	1.63	-4.2438
S7	2.807	2.715	3.28	-10.3175
S8	2.804	2.753	1.82	-5.2014
S9	2.735	2.670	2.38	-7.5315

4.2.1. Analysis of S/N Ratio for Porosity of Composite

To measure and characterize the porosity of composite, the statistics formulas of "the smaller, the better" have been used. In the case of "smaller is the better", the ratio of signal noise can be given by equation (2.2).

Table 4.2: Signal to Noise Ratios of porosity of composite for Smaller is better

Level	Stirring Speed	Stirring Time	wt. % SiC	wt.% MoS2
1	**-7.643**	-7.791	**-4.417**	**-7.036**
2	-7.754	-8.043	-8.646	-7.906
3	-7.683	**-7.247**	-10.018	-8.139
Delta	0.111	0.796	5.601	1.102
Rank	**4**	**3**	**1**	**2**

The delta statistics from S/N Ratio for the porosity tabulated in table 4.2 shows the ranks of factors affecting the porosity based on the S/N ratios. The delta statistics were computed based on the difference between the highest and the lowest average value of each factor. Ranks were then assigned based on their delta value. The highest value of delta was assigned the first rank and represents the predominant factor affecting response. The analysis showed that the wt.% SiC was assigned a rank of 1 with a delta value of 5.601 signifying that it is the predominant factor that affects the porosity. The wt.% MoS2, stirring time, and stirring speed were assigned second (1.102), third (0.796), and fourth (0.111) ranks respectively.

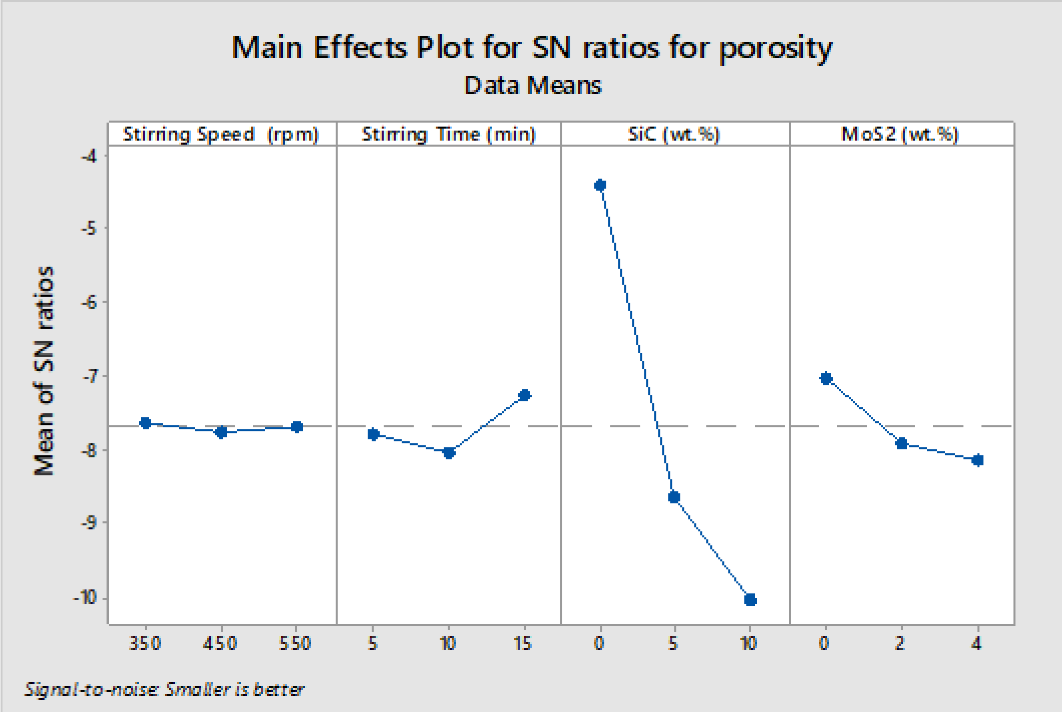

Figure 4.2: Main effects plots for S/N ratio of porosity of the composite

Figure 4.2 shows the optimal parameter combination of control factor's for the porosity smaller the better porosity. In the S/N ratio, the numerical value of the maximum point in each graph shows the best optimum combination of the factors and the above figure shows the maximum value for stirring speed at level 1, stirring time at level 3, wt.% SiC at level 1, wt.% MoS2 at level 1 are 350rpm, 15min, 0 wt.% SiC and 0 wt.% MoS2 respectively.

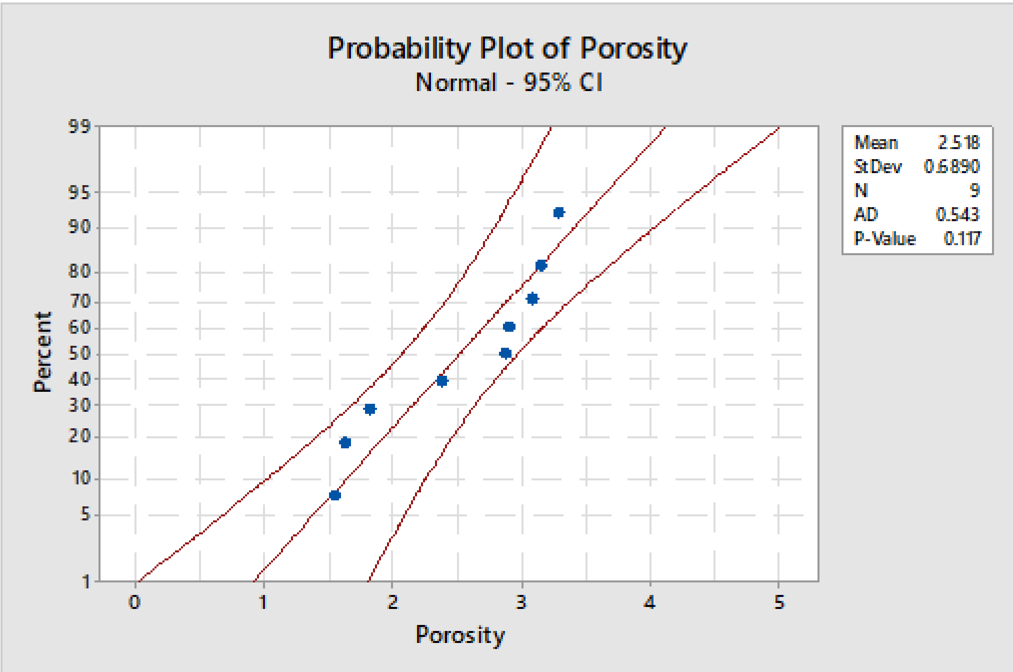

Figure 4.3: The normal probability plot for the porosity of composite

One of the assumptions in all the statistical models used in the design of experiments is that the experimental errors (residuals) are normally distributed and a normal probability plot of effects is used to judge the significance of effects. If all the residuals fall along a straight line drawn through the plotted points, it is inferred that the residuals/errors follow a normal distribution. Figure 4.3 shows the data points are relatively close to the fitted normal distribution line (the middle solid line of the graph). The normal probability plots of residuals depict that the residuals lie reasonably close to the normal probability lines and the p-value is greater than the significance level of 0.05 on the above figure 4.3, implying that residuals are distributed normally and the terms mentioned in the regression models are significant and adequate (Suresha and Sridhara 2012).

4.3. Analysis of Hardness

The hardness test was done using a Vickers hardness tester machine. To analyze hardness response, the experimental data using Taguchi's L9 OA is shown in table 4.3 were converted to S/N ratios. In this study, the effect of varying the control factors; stirring speed, stirring time, wt.% of SiC, and wt.% of MoS2 on the responses of hardness were analyzed. As higher values of hardness were desirable, larger the better-quality characteristic was selected to investigate the influence of factors on hardness responses.

Table 4.3 shows the separate signal-to-noise ratio of each sample in the design experiment. The largest values of the S/N ratios were indicated in sample number seven and the lowest value in sample number one with S/N ratios of 46.3738 and 41.8193 respectively. The respective highest and lowest hardness values were 208.30HV and 123.30HV. This results in when the wt.% of SiC increases (at a higher level) and wt.% of MoS2 is at 2wt.%, the hardness of the composite increases. In contrast the lowest hardness was recorded as the wt.% of SiC and wt.% of MoS2 are lower (at a lower level).

The hardness of composite increased due to increasing the contents of SiC particles and strong bonding between SiC particles and matrix due to enhanced wettability with the addition of MoS2. SiC particles increase the grain boundaries in composite and the grain size of the composite are reduced. Dislocation mobility will be restricted or challenged to move from grain to grain due to increased grain boundaries (decreased grain size) since grain boundaries act as a barrier to the motion of dislocation.

Also, SiC particle has an extremely low coefficient of thermal expansion, and how they strain the atomic lattice of the aluminum matrix, resulting in a dramatic increase in dislocation density. Dislocation density is the average distance between dislocation decreases and dislocation starts blocking the motion of each other. The hardness of composite material depends on the ability of dislocation to move and higher dislocation density results in a large number of dislocation interactions which increases the hardness of the composite. In this study, the addition of SiC particle content in the Al matrix showed enhancement in mechanical strength of composite and two main material hardening mechanisms have been attained i.e. grain size hardening and strain hardening. The addition of MoS2 also shows enhancement in hardness up to 2wt.% and shows decrement with 4wt.%, which means the role of MoS2 shows only facilitating the wettability, so an only a small amount is enough to enhance the wettability and bonding both matrix and reinforcement to each other and further increment leads to decrease the hardness of the composite.

In this study, hardness response variation is studied with the help of ANOVA and the signal-to-noise (S/N) ratio.

Table 4.3: Experimental results of hardness values

Designation	A	B	C	D	Experimental result of hardness value (HV)				Predicted S/N ratio result
					Trial 1	Trial 2	Trial 3	Average	
S1	350	5	0	0	121.0	129.2	119.7	123.30	41.8193
S2	350	10	5	2	196.1	177.5	175.2	182.90	45.2443
S3	350	15	10	4	207.3	197.4	208.5	204.40	46.2096
S4	450	5	5	4	185.8	161.4	174.1	173.80	44.8010
S5	450	10	10	0	178.6	222.6	197.4	199.50	45.9989
S6	450	15	0	2	161.4	164.4	214.7	180.17	45.1136
S7	550	5	10	2	207.3	210.2	207.3	208.30	46.3738
S8	550	10	0	4	158.4	164.4	163.4	162.60	44.2224
S9	550	15	5	0	178.6	175.2	187.1	180.30	45.1199

4.3.1. Effect of Process Parameter on Hardness

From the below figure 4.4, increasing the weight percentage of SiC increases the hardness of the developed composite at constant wt.% MoS2 and the hardness value for 0, 5, 10 wt.% of SiC at constant wt.% MoS2 (0 wt.%) are 123.3HV, 180.3HV, 199.5HV respectively. This result shows a better result than the previous studies by (Ajagol et al. (2018) and Ajith et al. (2020)). At the higher weight percentage of SiC, the higher value of hardness is shown. SiC has the most significant effect on hardness. SiC is a harder ceramic and the hardness of the composite also increases with its addition but, a high amount of SiC will lead to brittleness (Karvanis et al. (2016)).

MoS2 is used as a solid lubricant and it facilitates the wettability and bonding between the aluminum and silicon carbide particles due to its low coefficient of friction properties to enhance the obtained hardness result and the hardness is better when a small amount of MoS2 is added to Al-SiC composite. The hardness of the Al matrix increases as wt.% of MoS2 increases only up to 2% and after then it declines at 4 wt.% MoS2. The value of hardness for 0, 2, 4wt.% MoS2 at constant the wt.% of SiC (0 wt.%) are 123.3, 180.17, 162.6HV respectively as shown in figure 4.4. The highest hardness value of the developed composite was shown when the weight percentage of SiC is 10% wt of SiC and the wt.% of MoS2 is 2% and this result shows a better result than the previous studies by (Ajith et al. (2020)). From this analysis, the Al-SiC-MoS2 hybrid composite shows better enhancements in hardness than the Al-SiC composite.

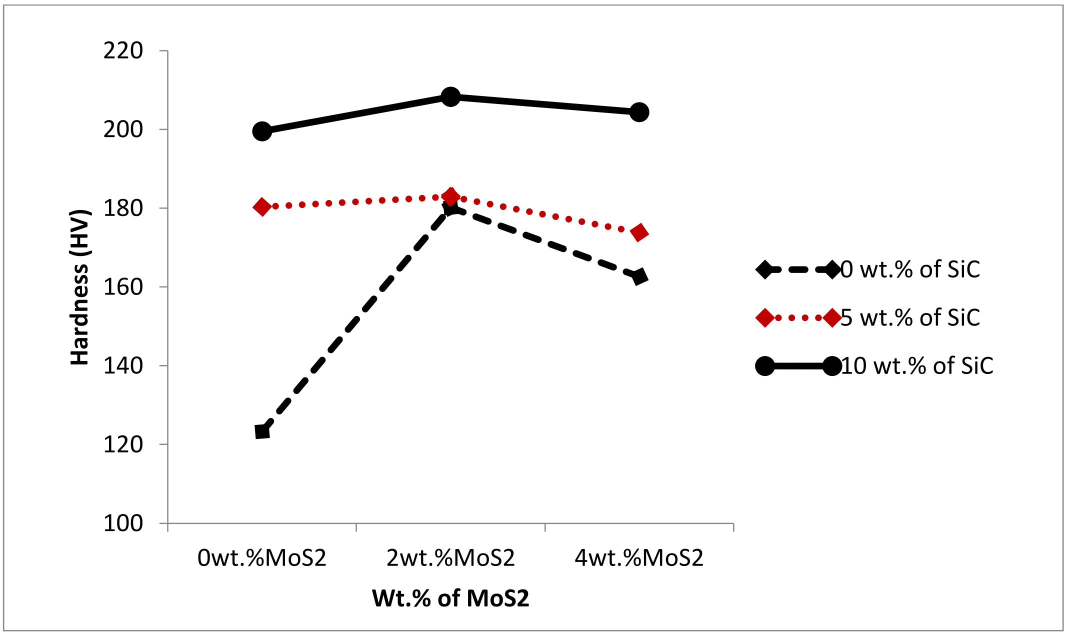

Figure 4.4: Effects of process parameters on hardness

4.3.1.1.Analysis of Variance (ANOVA) for Hardness

ANOVA is used to identify the most significant factors which affect the hardness of composite and the percent contribution of each factor was calculated. Where DoF = degree of freedom, SS= Sum of squares, MSS = Mean Sum of squares, and F = F- Ratio generated by using Minitab 17 software.

Table 4.4: Analysis of Variance of hardness of Composite

Source	DF	Adj SS	Adj MS	F-Value	P-Value	PC (%)
Stirring Speed (rpm)	1	236.9	236.9	1.40	0.303	4.44
Stirring Time (min)	1	274.7	274.7	1.62	0.272	5.14
SiC (wt.%)	1	3559.0	3559.0	20.98	0.010	66.66
MoS2 (wt.%)	1	589.4	589.4	3.47	0.136	11.04
Error	4	678.6	169.6			3.17
Total	8	5338.6				

R-sq = 87.29%, F0.05, 1, 8 = 5.32

Table 4.4 presents the percentage contribution of factors of stirring speed (4.44%), stirring time (5.14%), SiC (66.66%), and MoS2 (11.04%) on the hardness of the composite. This analysis was undertaken for a level of significance of 5%, i.e. for a level of confidence of 95%. It is observed from the above table 4.4, that wt.% of SiC has statistical significance and the highest percentage contribution (i.e. 66.66%) on the hardness value and followed by MoS2, stirring time, and stirring speed.

The ANOVA table also shows the significance of factors using the F-values and P-values. If the obtained F-value of a parameter is greater than the tabulated one, then that particular parameter has a significant influence over the response variable. From table 4.4, the F value of wt.% of SiC is 20.98 > 5.32, therefore, wt.% SiC has a significant influence on the hardness and stirring speed (1.40) < 5.32, stirring time (1.62) < 5.32, and MoS2 (3.47) < 5.32, therefore, stirring speed, stirring time, and MoS2 have no significant effect on hardness of the composite.

The analysis of variance (ANOVA) with p values also shows that wt.% of SiC are significant factors affecting the hardness (P=0.010 < 0.05), while stirring speed, stirring time, and SiC have almost no significance (P>0.05). The reason for the hardness increment in the composite was due to the higher hardness of SiC particles. Therefore, increasing the content of SiC particles will increase the hardness of the composite. R-squared measures how well the model fits the data. Since the R-square value is 87.29% and the regression model should fit observations.

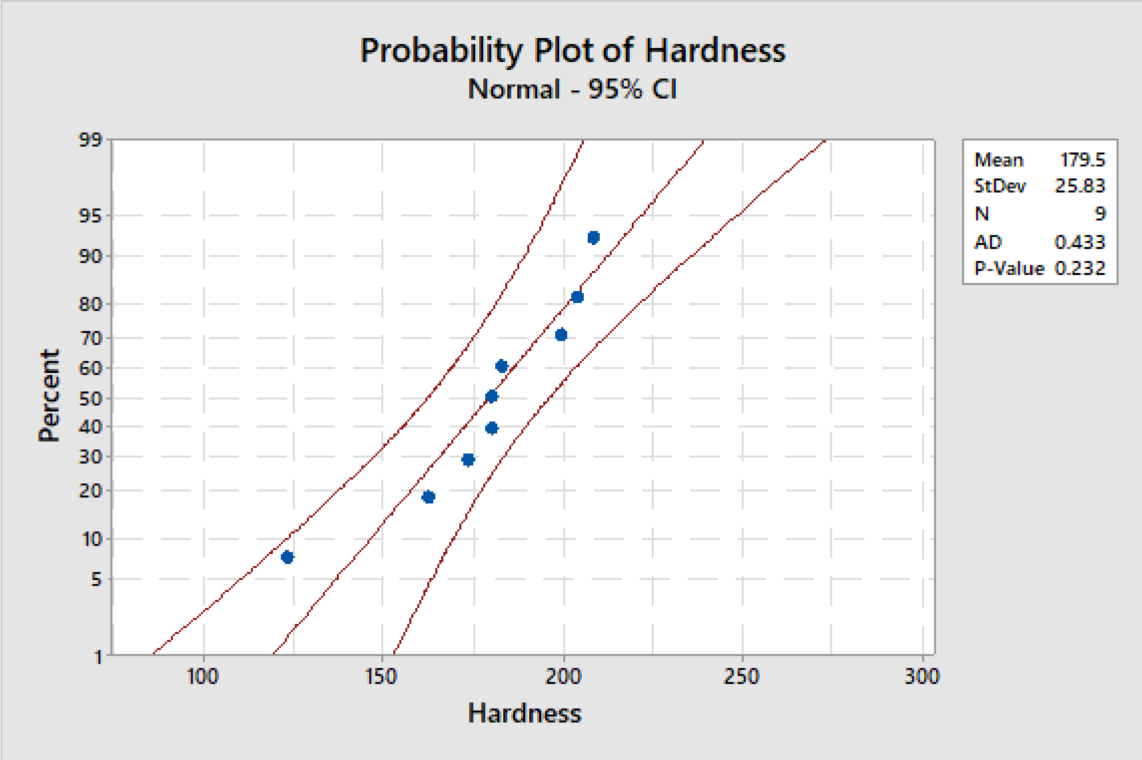

Figure 4.5: The normal probability plot for the hardness of composite

One of the assumptions in all the statistical models used in the design of experiments is that the experimental errors (residuals) are normally distributed and a normal probability plot of effects is used to judge the significance of effects. If all the residuals fall along a straight line drawn through the plotted points, it is inferred that the residuals/errors follow a normal distribution.

Figure 4.5 shows the data points are relatively close to the fitted normal distribution line (the middle solid line of the graph). The normal probability plots of residuals depict that the residuals lie reasonably close to the normal probability lines and the p-value is greater than the significance level of 0.05 on the above figure 4.5, implying that residuals are distributed normally and the terms mentioned in the regression models are significant and adequate (Suresha and Sridhara 2012).

4.3.2. Optimization of Process Parameters for Hardness

Taguchi Signal-to-Noise ratios (S/N) serve as objective functions for optimization in data analysis and prediction of optimum results for the hardness of the composite

4.3.2.1.Analysis of S/N Ratio for Hardness

To measure and characterize the hardness, the statistics formula of "the larger, the better" have been used. In the case of larger is the better, the ratio of signal noise can be given by equation (2.3).

Table 4.5: Signal to Noise Ratios for the hardness of composite (larger the better)

Level	Stirring Speed (rpm)	Stirring Time (min)	SiC (wt.%)	MoS2 (wt.%)
1	44.42	44.33	43.72	44.31
2	**45.30**	45.16	45.06	**45.58**
3	45.24	**45.48**	**46.19**	45.08
Delta	0.88	1.15	2.48	1.26
Rank	**4**	**3**	**1**	**2**

The delta statistics of the S/N ratio for the hardness tabulated in table 4.5 shows the ranks of the factors affecting responses based on the S/N ratios obtained using the Taguchi orthogonal array. The delta statistics were computed based on the difference between the highest and the lowest average value of each factor. The highest value of delta was assigned the first rank and represents the predominant factor affecting hardness. The analysis showed that, the wt.% SiC was assigned a rank of 1 with a delta value of 2.48 signifying that it is the predominant factor that affects the hardness. The wt.% MoS2, stirring time, and stirring speed were assigned as second (1.26), third (1.15), and fourth (0.88) ranks respectively.

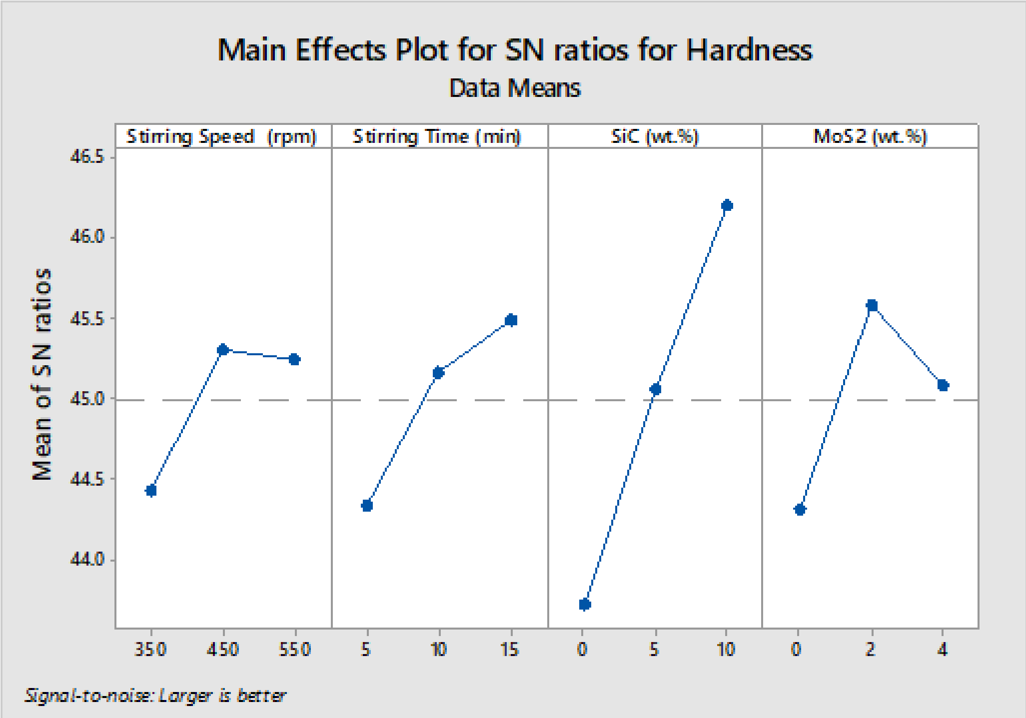

Figure 4.6: Main effects plots for S/N ratio of hardness

Figure 4.6 shows the optimal parameter combination of control factors for the hardness (higher the better hardness). Since the S/N ratio used for this study is larger is better and the highest S/N ratio was selected. In the S/N ratio, the numerical value of the maximum point in each graph shows the best optimum combination of the factors and the above figure shows the maximum value for stirring speed at level 2, stirring time at level 3, wt.% SiC at level 3, wt.% MoS2 at level 2 is 450rpm, 15min, 10% wt.% SiC, and 2% wt.% MoS2 respectively (i.e. **A2B3C3D2)** was selected.

4.3.2.2.Determining Optimum Conditions for Hardness

The optimum prediction condition for the S/N ratio in which, the higher hardness result of the composite obtains with the terms setting are shown in table 4.6. The selected optimum parameters in this study were **A2B3C3D2**.

Table 4.6: The optimum conditions for hardness result prediction-settings

Factors	Level	Value on level	Rank of affecting	Predicted values	
				S/N Ratio	Mean
Stirring speed (A)	2	450 rpm	4	**47.5893**	**228.88**
Stirring time (B)	3	10 min	3		
SiC (C)	3	10 wt.%	1		
MoS2 (D)	2	2 wt.%	2		

4.4. Analysis of Tensile Strength

The tensile strength test was done using UTM. To analyze tensile strength, experimental data Taguchi’s L9 OA in table 4.3 was converted to S/N ratios. In this study, the effect of varying the control factors; stirring speed, stirring time, wt.% of SiC, and wt.% of MoS2 on the responses of tensile strength were analyzed. As higher values of tensile strength were desirable, larger the better-quality characteristic was selected to investigate the influence of factors on the tensile strength. Table 4.7 shows the separate signal-to-noise ratio of each sample in the design experiment.

The largest values of the S/N ratios were indicated in sample number seven and the lowest value in sample number one with S/N ratios of 45.7753 and 37.5012 respectively. The respective highest and lowest tensile strength values were 194.43MPa and 75MPa respectively. This result shows that, when the wt.% of SiC increased (at a higher level) and wt.% of MoS2 are at 2wt.%, the tensile strength of the composite increased. In contrast, the lowest tensile strength was recorded as the wt.% of SiC and wt.% of MoS2 are lower (at the lower level).

The tensile strength of the composite is increased due to increasing the contents of SiC particles and strong bonding between SiC particles and matrix due to enhanced wettability with the addition of MoS2. SiC particles increase the grain boundaries in composite and the grain size of the composite are reduced. Dislocation mobility will be restricted or challenged to move from grain to grain due to increased grain boundaries (decreased grain size) since grain boundaries act as a barrier to the motion of dislocation. Also, SiC particles have an extremely low coefficient of thermal expansion, and how they strain the atomic lattice of the aluminum matrix, resulting in a dramatic increase in dislocation density. Dislocation density is the average distance between dislocation decreases and dislocation starts blocking the motion of each other. The strength of composite material depends on the ability of dislocation to move and higher dislocation density results in a large number of dislocation interactions which increases the strength of the composite. In this study, the addition of SiC particles content in Al matrix showed enhancement in mechanical strength of composite and two main strengthening mechanisms of material have been attained i.e. grain size hardening and strain hardening.

The addition of MoS2 also shows enhancement in tensile strength up to 2wt.% and shows decrement with 4wt.%, which means the role of MoS2 shows only facilitating the wettability, so an only a small amount is enough to enhance the wettability and bonding of both matrix and reinforcement to each other and further increment leads to decrease the tensile strength of the composite. In this study, tensile strength response variation is studied with the help of ANOVA and the signal-to-noise (S/N) ratio.

Table 4.7 Experimental results of tensile strength values of each sample

Designation	A	B	C	D	Ultimate tensile strength (MPa)	Predicted S/N ratio result
S1	350	5	0	0	75	37.5012
S2	350	10	5	2	129.13	42.2205
S3	350	15	10	4	171.24	44.6721
S4	450	5	5	4	104.6	40.3906
S5	450	10	10	0	180.85	45.1464
S6	450	15	0	2	89.76	39.0617
S7	550	5	10	2	194.43	45.7753
S8	550	10	0	4	82.41	38.3196
S9	550	15	5	0	118.9	41.5036

4.4.1. Effect of Process Parameter on Tensile Strength

From the figure 4.7, it is shown that increasing the weight percentage of SiC, increases the tensile strength of the developed composite at constant wt.% MoS2 and the tensile strength value for 0, 5, 10 wt% SiC at constant wt.% MoS2 (0 wt.%) are 75MPa, 118.9MPa, 180,85MPa respectively. This result shows a better result than the previous studies by (Ajagol et al. (2018) and Siddharthan et al. (2020)). At the higher weight percentage of SiC, the higher value of tensile strength is shown. Since SiC is a harder ceramic and Silicon carbide has the most significant effect on the tensile strength of aluminum reinforced silicon carbide metal matrix composite (Karvanis et al. (2016)).

MoS2 is used as a solid lubricant and it facilitates the wettability between the aluminum and silicon carbide due to its low friction coefficient to enhance the obtained tensile strength result and the tensile strength is better when a small amount of MoS2 is added to the Al-SiC composite. Tensile strength of Al matrix increases as wt.% of MoS2 increases only up to 2% and after then it declines at 4 wt.% of MoS2. The value of tensile strength for 0, 2, 4 wt.% of MoS2 at constant wt.% of SiC (0 wt.%) are 75, 89.76, 82.43MPa respectively. The highest tensile strength value of the developed composite was shown when the wt.% of SiC is 10% and the wt.% of MoS2 are 2% and this result shows a better result of tensile strength than the previous studies by (Ajith et al. (2020)). From this analysis, the Al-SiC-MoS2 hybrid composite shows better enhancements in tensile strength than the Al-SiC composite.

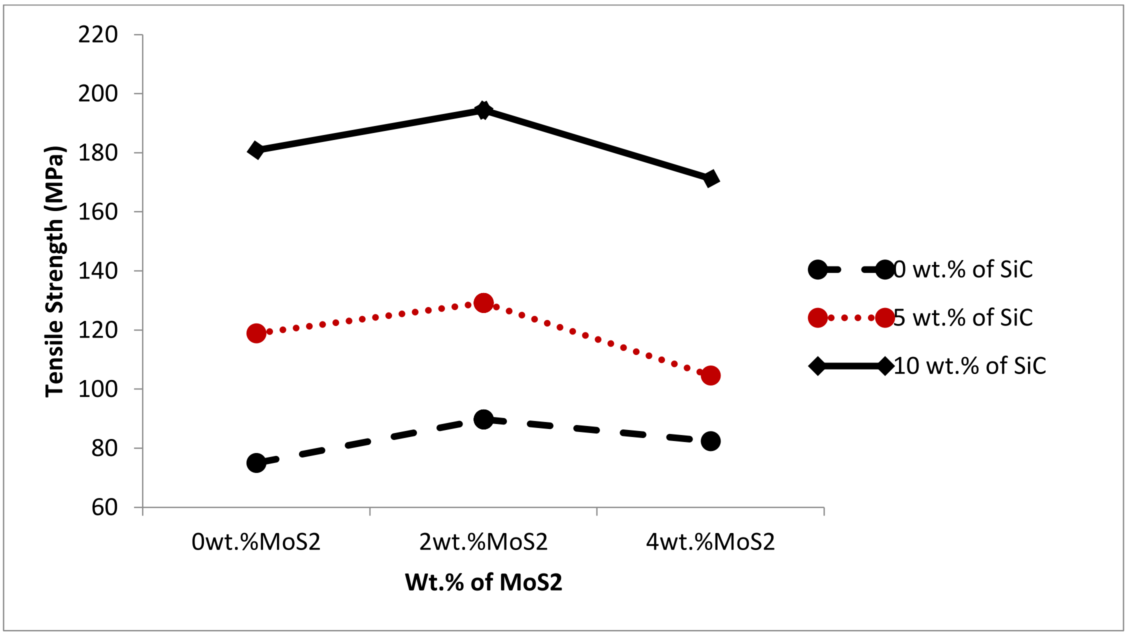

Figure 4.7: Effect of process parameter on tensile strength

4.4.1.1.Analysis of Variance (ANOVA) for Tensile strength

ANOVA is used to identify the most significant factors which affect the tensile strength of composite and the percent contribution of each factor. Where DoF = degree of freedom, SS= Sum of squares, MSS = Mean Sum of squares, and F = F- Ratio generated by using Minitab 17 software.

Table 4.8: Analysis of Variance for tensile strength

Source	DF	Adj SS	Adj MS	F-Value	P-Value	PC (%)
Stirring Speed (rpm)	1	5.7	5.7	0.02	0.887	0.035
Stirring Time (min)	1	45.4	45.4	0.18	0.692	0.28
SiC (wt.%)	1	14935.1	14935.1	59.85	0.002	93
MoS2 (wt.%)	1	69.2	69.2	0.28	0.626	0.43
Error	4	998.2	249.6			
Total	8	16053.6				100%

R-sq = 93.78%, F0.05, 1, 8 = 5.32

Table 4.8 presents percentage contribution of factors of stirring speed (0.0.35%), stirring time (0.28%), SiC (93%) and MoS2 (0.43%) on tensile strength of composite. This analysis was undertaken for a level of significance of 5%, i.e. for a level of confidence of 95%. From the table, it is shown that wt.% SiC has statistical significance and the highest percentage contribution (i.e 93%) on the tensile strength of composite and followed by MoS2, stirring time, and stirring speed.

The ANOVA table also shows the significance of factors using the F-values and P-values. If the obtained F-value of a parameter is greater than the tabulated one, then that particular parameter has a significant influence over the response variable. From table 4.8, the F value of wt.% of SiC is 59.85> F0.05, 1, 8 = 5.32, therefore, SiC has a significant influence over the tensile strength and stirring speed (0.02) < 5.32, stirring time (0.18) < 5.32, MoS2 (0.28) < 5.32, therefore, stirring speed, stirring time and MoS2 has no significant effect on tensile strength of composite.

The ANOVA with p values also shows that wt.% of SiC are significant factors affecting the tensile strength (P=0.002 < 0.05), while stirring speed, stirring time, and SiC have almost no significance (P>0.05). Therefore, increasing the wt.% of SiC particles increases the tensile strength of the composite. R-squared measures how well the model fits the data. From the above table 4.18, the R-square value is 93.78% and the model fits the data.

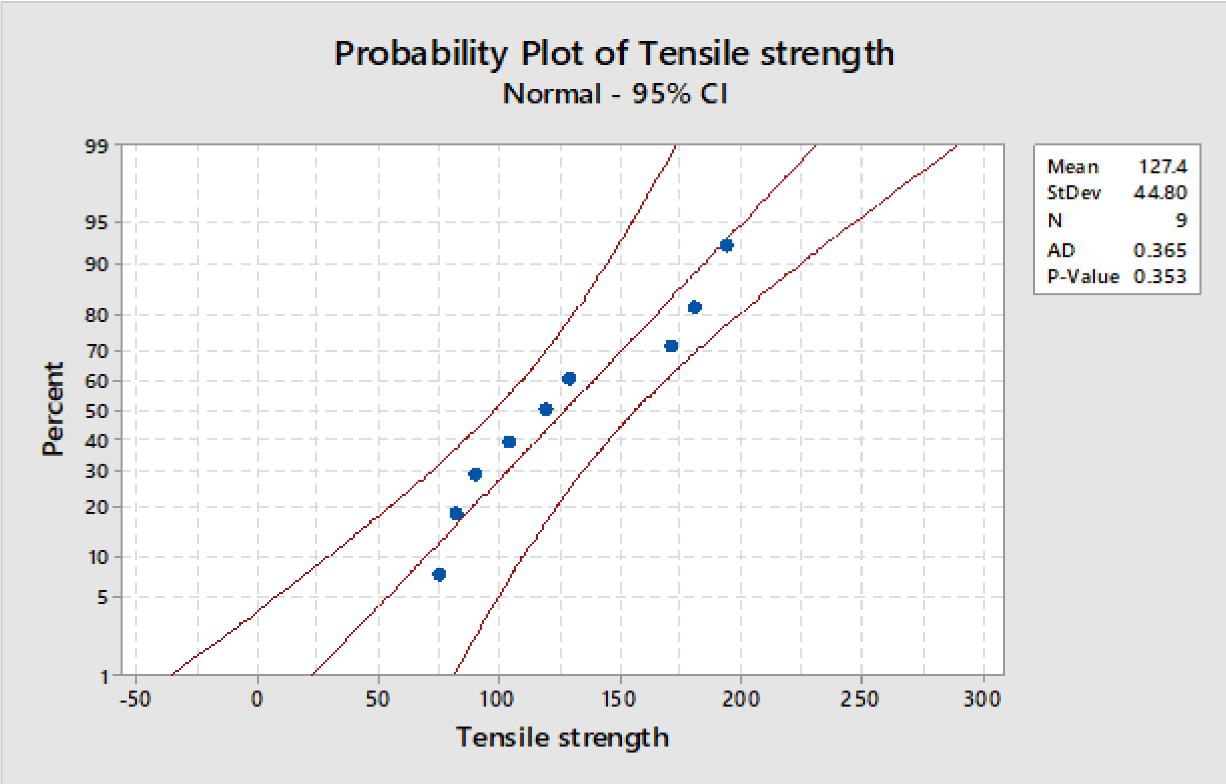

Figure 4.8: The normal probability plot for tensile strength

One of the assumptions in all the statistical models used in the design of experiments is that the experimental errors (residuals) are normally distributed and a normal probability plot of effects is used to judge the significance of effects. If all the residuals fall along a straight line drawn through the plotted points, it is inferred that the residuals/errors follow a normal distribution. Figure 4.8 shows the data points are relatively close to the fitted normal distribution line (the middle solid line of the graph). The normal probability plots of residuals depict that the residuals lie reasonably close to the normal probability lines and the p-value is greater than the significance level of 0.05 in the above figure 4.8, implying that residuals are distributed normally and the terms mentioned in the regression models are significant and adequate (Suresha and Sridhara 2012).

4.4.2. Optimization of Process Parameters for Tensile Strength

Taguchi Signal-to-Noise ratios are used as objective functions for optimization for data analysis and prediction of optimum results. In the Taguchi method, response variation is studied with the help of the signal-to-noise (S/N) ratio.

4.4.2.1.Analysis of S/N Ratio for Tensile Strength

To measure and characterize the tensile strength, the statistics formula of the larger, the better has been used. In the case of larger is the better the ratio of signal noise can be given by equation (2.3).

Table 4.9: Signal to Noise Ratios tensile strength of composite for larger is better

Level	Stirring Speed (rpm)	Stirring Time (min)	SiC (wt.%)	MoS2 (wt.%)
1	41.46	41.22	38.29	41.38
2	41.53	41.90	41.37	42.35
3	41.87	41.75	45.20	41.13
Delta	0.40	0.67	6.90	1.23
Rank	**4**	**3**	**1**	**2**

The delta statistics for the tensile strength tabulated in table 4.9 shows the ranks of factors affecting the responses based on the S/N ratios obtained via the Taguchi orthogonal array. The delta statistics were computed based on the difference between the highest and the lowest average value of each factor. The highest value of delta was assigned the first rank and represents the predominant factor affecting tensile strength. The analysis showed that the SiC was assigned a rank of 1 with a delta value of 6.90 signifying that it is the predominant factor that affects the tensile strength of the composite. The wt.% MoS2, stirring time, and stirring speed were assigned second (1.23), third (0.67), and fourth (0.40) ranks respectively.

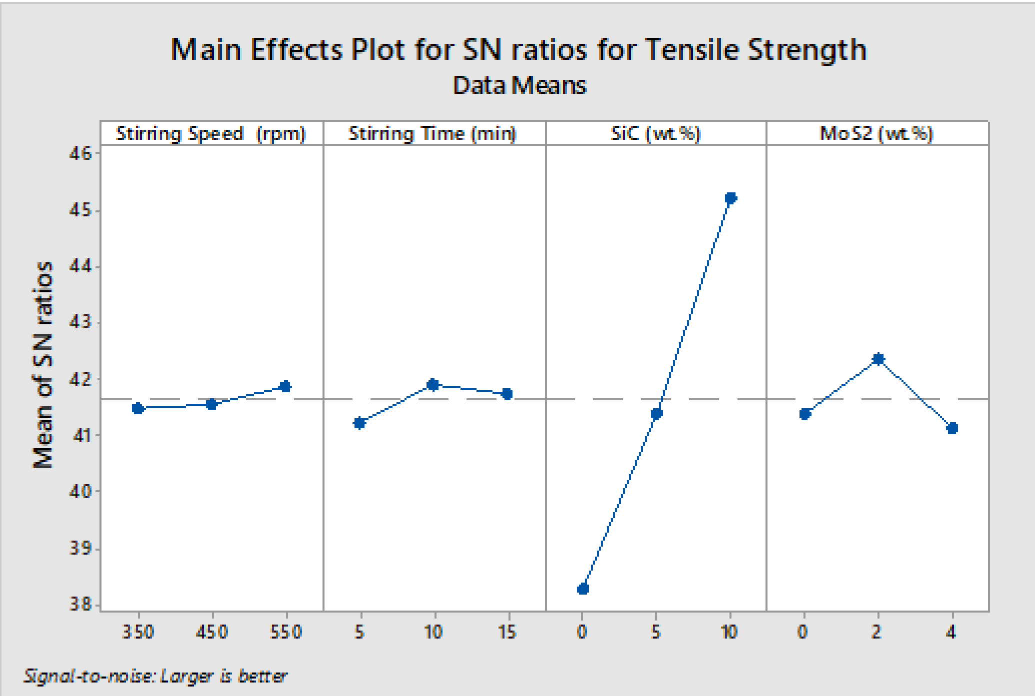

Figure 4.9: Main effects plots for S/N ratio of tensile strength

Figure 4.9 shows the optimal parameter combination of control factors for the tensile strength (higher the better tensile strength). Since the S/N ratio used for this study is larger is better and the highest S/N ratio was selected. In the S/N ratio, the numerical value of the maximum point in each graph shows the best optimum combination of the factors at that level and the above figure shows the maximum value for stirring speed at level 3, stirring time at level 2, wt.% SiC at level 3, wt.% MoS2 at level 2 are 550rpm, 10min, 10% wt.% SiC, and 2% wt.% MoS2 respectively (i.e. **A3B2C3D2)** was selected. The most effective parameter to increase the tensile strength is the SiC weight percentage when compared with other factors and stirring speed has the least effect on the tensile strength of the composite.

4.4.2.2.Determining Optimum Conditions for Tensile Strength

The optimum prediction condition for the S/N ratio in which, the higher tensile result of the composite obtains with the terms setting are shown in table 4.10. The selected optimum parameters in this study were at **A3B2C3D2**.

Table 4.10: The optimum conditions for tensile strength result prediction-settings

Factors	Level	Value on each level	Rank of affecting	Predicted values	
				S/N Ratio	Mean
Stirring speed (A)	3	550 rpm	4	**46.4484**	**200.55**
Stirring time (B)	2	10 min	3		
SiC (C)	3	10 wt.%	1		
MoS2 (D)	2	2 wt.%	2		

4.5. Analysis of Tensile Toughness (Impact Strength)

The response of tensile toughness (impact strength) was calculated with the help of the trapezoidal principle from the stress-strain curve as tensile toughness. To analyze tensile toughness, Taguchi’s L9 OA using the design of the experiment, the experimental data in table 4.3 were converted to S/N ratios. In this study, the effect of varying the control factors; stirring speed, stirring time, wt.% of SiC, and wt.% of MoS2 on the responses of tensile toughness were analyzed. As higher values of tensile toughness were desirable, larger the better-quality characteristic was selected to investigate the influence of factors on the tensile toughness. Table 4.11 shows the separate signal-to-noise ratio of each sample in the design experiment.

The largest values of the S/N ratios were indicated in sample number seven and the lowest value in sample number one with S/N ratios of 28.2995 and 22.9226 respectively. The respective highest and lowest tensile toughness values were 26J/mm^3 and 14J/mm^3 respectively. This result shows that, when the wt.% of SiC increased (at a higher level) and wt.% of MoS2 are at 2wt.%, the tensile toughness of the composite increased.

In contrast, the lowest tensile toughness was recorded as the wt.% of SiC and wt.% of MoS2 are lower (at a lower level). The tensile toughness of composite is increased due to increasing the contents of SiC particles and strong bonding between SiC particles and matrix due to enhanced wettability with the addition of MoS2. SiC particles increase the grain boundaries in composite and the grain size of the composite are reduced. In this study, tensile toughness response is studied using ANOVA and signal-to-noise (S/N) ratio.

Table 4.11: Experimental results of tensile toughness values of each sample

Designation	A	B	C	D	Tensile Toughness (J/mm^3)	Predicted S/N ratio result
S1	350	5	0	0	14	22.9226
S2	350	10	5	2	20	26.0206
S3	350	15	10	4	25	27.9588
S4	450	5	5	4	19	25.5751
S5	450	10	10	0	23	27.2346
S6	450	15	0	2	16	23.5218
S7	550	5	10	2	26	28.2995
S8	550	10	0	4	15	24.0824
S9	550	15	5	0	17	24.6090

4.5.1. Effect of Process Parameter on Tensile Toughness

From the figure below 4.10, it is shown that increasing the wt.% of SiC, increases the tensile toughness of composite and the tensile toughness value for 0, 5, and 10 wt% SiC at constant wt.% MoS2 (0 wt.%) are 14, 17, and 23 Joules respectively. This result shows a better result than the previous studies by (Radha and Vijaya Kumar (2015)). At the higher wt.% of SiC, the higher value of tensile toughness is shown. Silicon carbide has the most significant effect on the tensile toughness of aluminum reinforced silicon carbide metal matrix composite and since SiC is a harder ceramic material and tensile toughness of composite increases with its addition and decreases after some wt.% of SiC due to its brittleness property (Subramanya Reddy et al. (2017)).

MoS2 is used as a solid lubricant and it facilitates the wettability between the aluminum and silicon carbide due to its low friction coefficient properties to enhance the obtained toughness result at a small level and the tensile toughness is better when a small amount of MoS2 is added to Al-SiC composite. Tensile toughness of the Al matrix increases as the weight percentage of wt.% MoS2 increases only up to 2% and after then it declines at 4 wt.% MoS2. The value of tensile toughness for 0, 2, 4wt.% MoS2 at constant the weight percentage of SiC (0 wt.%) are 14, 16, and 15 Joules respectively shown in fig 4.10. The highest tensile toughness value of the developed composite was shown when the weight percentage of SiC is 10% wt of SiC and the weight percentage of MoS2 is 2% and this result shows a better result of tensile toughness (impact strength) than the previous studies by (Ajith et al. (2020)). From this analysis, the Al-SiC-MoS2 hybrid composite shows better enhancements in tensile toughness (impact strength) than the Al-SiC composite.

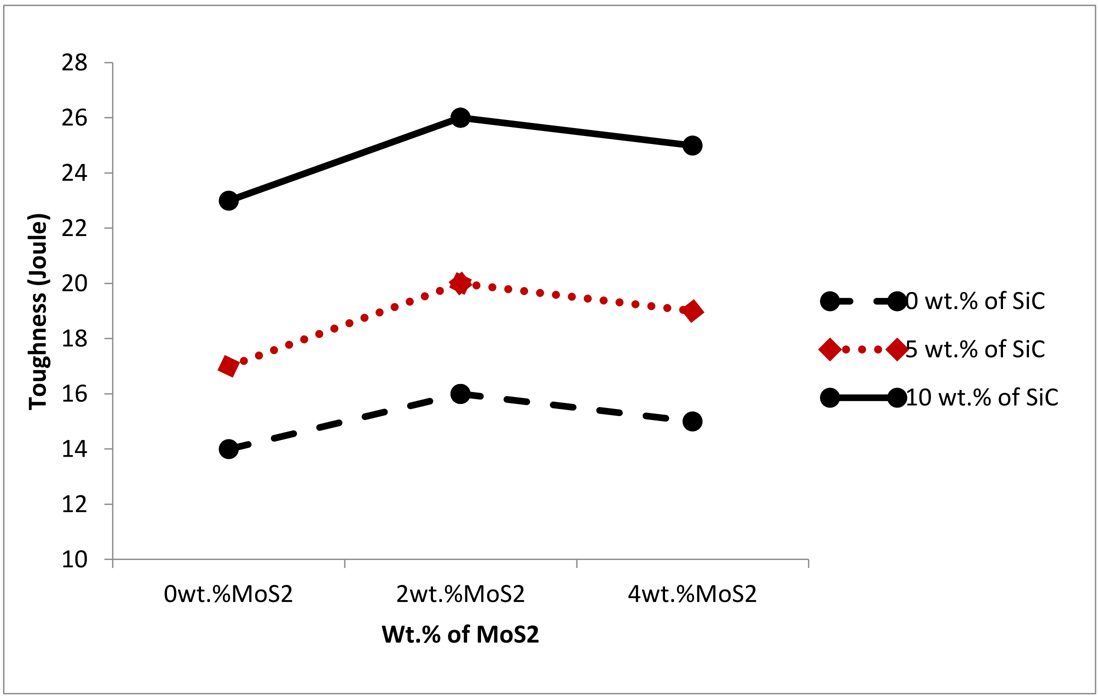

Figure 4.10: Effect of process parameter on tensile toughness

4.5.1.1.Analysis Of Variance (ANOVA) For Tensile Toughness

ANOVA is used to identify the most significant factors which affect the tensile toughness of composite and the percent contribution for each factor. Where DoF = degree of freedom, SS= Sum of squares, MSS = Mean Sum of squares, and F = F- Ratio

Table 4.12: Analysis of Variance of tensile toughness of Composite

Source	DF	Adj SS	Adj MS	F-Value	P-Value	PC (%)
Stirring Speed (rpm)	1	0.167	0.167	0.06	0.814	0.11
Stirring Time (min)	1	1.500	1.500	0.57	0.493	0.89
SiC (wt.%)	1	150.000	150.000	6.84	0.002	9.2
MoS2 (wt.%)	1	6.000	6.000	2.27	0.206	3.6
Error	4	10.556	2.639			6.2
Total	8	168.222				

R-sq = 93.73%, F0.05, 1, 8 = 5.32

Table 4.12 presents the percentage contribution variation of the main factors of stirring speed (0.11%), stirring time (0.89%), and wt.% SiC (89.2%) and wt.% MoS2 (3.6%) on tensile toughness of the composite. This analysis was undertaken for a level of significance of 5%, i.e. for a level of confidence of 95%. From the above table, it is shown that wt.% SiC has statistical significance and the highest percentage contribution (i.e. 89.2%) on the tensile toughness value and followed by wt.% MoS2, stirring time, and stirring speed.

The ANOVA table also shows the significance of factors using the F-values and P-values. If the obtained F-value of a parameter is greater than the tabulated one, then that particular parameter has a significant influence over the response variable. From table 4.12, the F value of wt.% SiC is 56.84 > F0.05, 1, 8 = 5.32, therefore, wt.% SiC has a significant influence over the tensile toughness. Stirring speed (0.06) < 5.32, stirring time (0.57) < 5.32, wt.% MoS2 (2.27) < 5.32, therefore, stirring speed, stirring time, and MoS2 have no significant effect on the tensile toughness of the composite.

The ANOVA with p values also shows that SiC is a significant factor affecting the tensile toughness (impact strength) (P=0.010 < 0.05), while stirring speed, stirring time, wt.% SiC has almost no significance (P>0.05). Therefore, increasing the content of SiC particles will increase the tensile toughness of the composite. The regression model fits the data well; because the R-square value is higher at 87.29%.

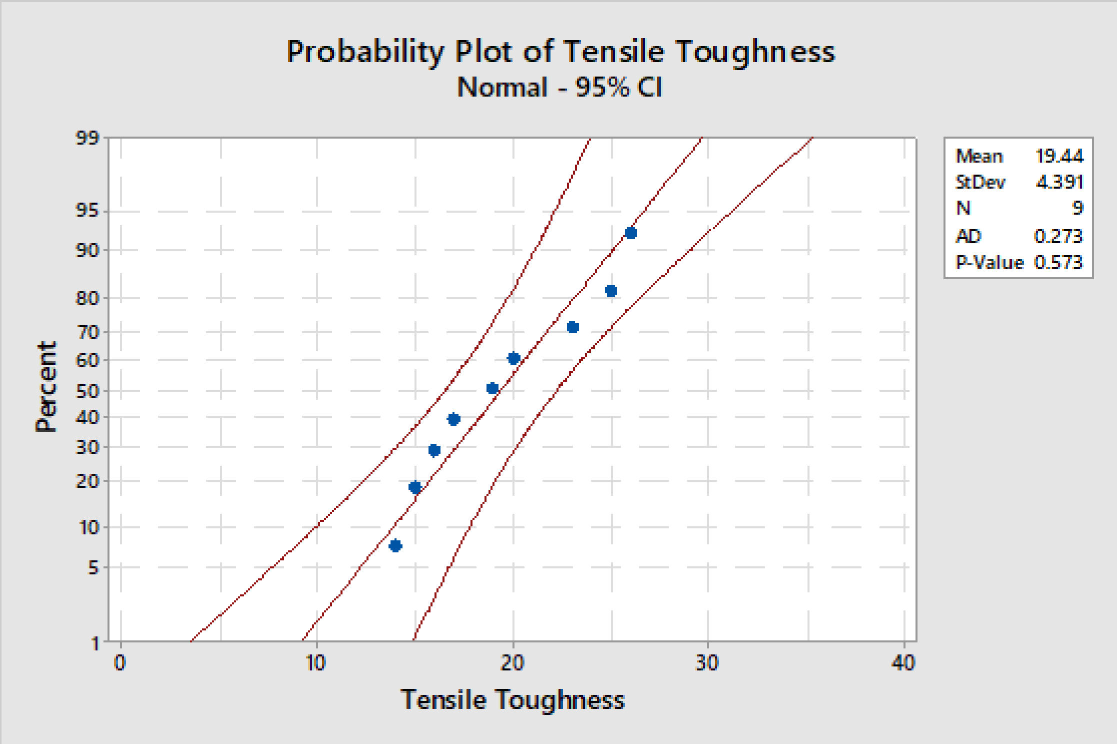

Figure 4.11: The normal probability plot for tensile toughness

One of the assumptions in all the statistical models used in the design of experiments is that the experimental errors (residuals) are normally distributed and a normal probability plot of effects is used to judge the significance of effects. If all the residuals fall along a straight line drawn through the plotted points, it is inferred that the residuals/errors follow a normal distribution. Figure 4.11 shows the data points are relatively close to the fitted normal distribution line (the middle solid line of the graph). The normal probability plots of residuals depict that the residuals lie reasonably close to the normal probability lines and the p-value is greater than the significance level of 0.05 on the above figure 4.11, implying that residuals are distributed normally and the terms mentioned in the regression models are significant and adequate (Suresha and Sridhara (2012)).

4.5.2. Optimization of Process Parameters for Tensile Toughness

Taguchi Signal-to-Noise ratios serve as objective functions for optimization, help in data analysis, and prediction of optimum results of the tensile toughness response variation.

4.5.2.1. Analysis of S/N Ratio for Tensile Toughness

To measure and characterize the impact strength (tensile toughness), the statistics formula of the larger, the better has been used. In the case of larger is the better, the ratio of signal noise can be given by equation (2.3).

Table 4.13: Signal to Noise Ratios for tensile toughness of composite (larger the better)

Level	Stirring Speed (rpm)	Stirring Time (min)	SiC (wt.%)	MoS2 (wt.%)
1	25.63	25.60	23.51	24.92
2	25.44	**25.78**	25.40	**25.95**
3	**25.66**	25.36	**27.83**	25.87
Delta	0.22	0.42	4.32	1.03
Rank	**4**	**3**	**1**	**2**

The delta statistics of the S/N ratio for the tensile toughness tabulated in table 4.13 shows the ranks of the factors affecting the responses based on the S/N ratios obtained via the Taguchi orthogonal array. The delta statistics were computed based on the difference between the highest and the lowest average value of each factor. The highest value of delta was assigned the first rank and represents the predominant factor affecting tensile toughness. The analysis showed that, the wt.% SiC was assigned a rank of 1 with a delta value of 4.32 signifying that it is the predominant factor that affects the tensile toughness of the cast composite. The wt.% MoS2, stirring time, and stirring speed were assigned second (1.03), third (0.42), and fourth (0.22) ranks respectively.

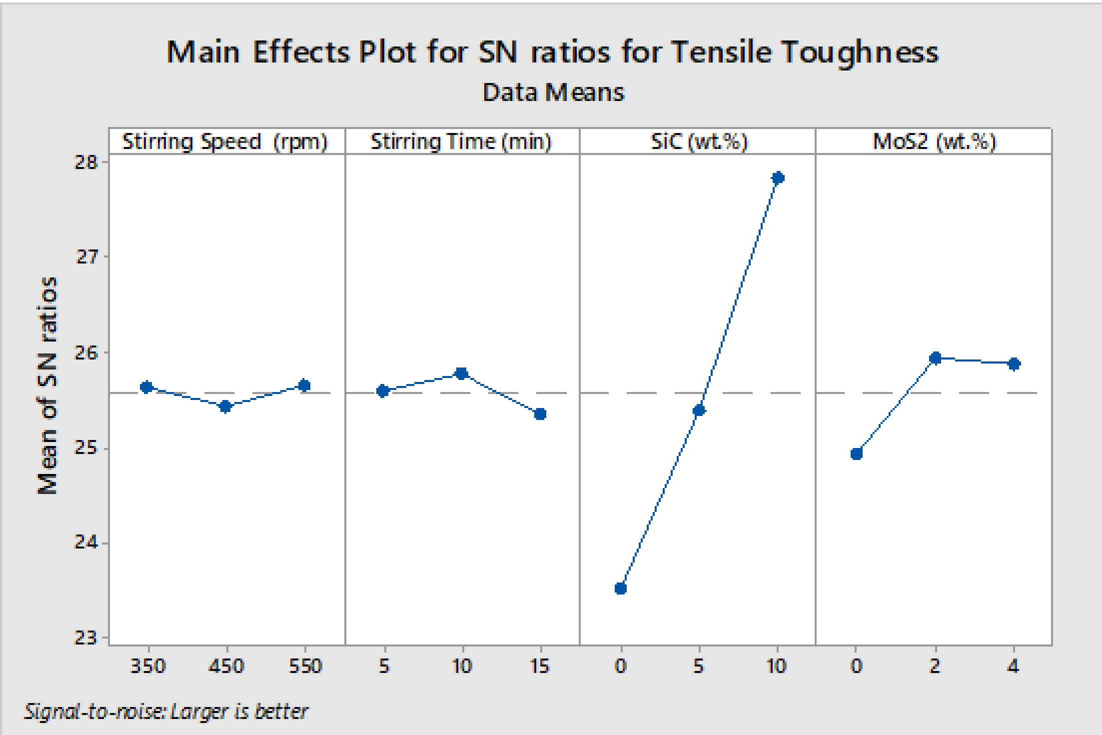

Figure 4.12: Main effects plots for S/N ratio of tensile toughness

Figure 4.12 shows the control factor‘s main effect plot for the S/N ratio and the optimal parameter combination on tensile toughness (higher the better tensile toughness).

Since the S/N ratio used for this study is larger the better and highest S/N ratio was selected. In the S/N ratio, the numerical value of the maximum point in each graph shows the best optimum combination of the factors at that level and the above figure shows the maximum value for stirring speed at level 3, stirring time at level 2, wt.% SiC at level 3, wt.% MoS2 at level 2 are 550rpm, 10min, 10% wt.% SiC, and 2% wt.% MoS2 respectively (i.e. **A3B2C3D2)** was selected.

4.5.2.2.Determining Optimum Conditions for Tensile Toughness

The optimum prediction condition for the S/N ratio in which, the higher tensile toughness result of the composite obtains with the terms setting shown in table 4.14. The selected optimum parameters in this study were at **A3B2C3D2**.

Table 4.14: The optimum conditions for tensile toughness result prediction-settings

Factors	Level	Value on level	Rank of affecting	Predicted values	
Stirring speed (A)	3	550 rpm	4	S/N Ratio	Mean
Stirring time (B)	2	10 min	3	**28.4796**	**26**
SiC (C)	3	10 wt.%	1		
MoS2 (D)	2	2 wt.%	2		

4.6. Analysis of Wear Rate

The wear rate test was done using Pin on disc apparatus testing machine. The wear rate study was conducted based on the mass loss analysis, Taguchi's L9 OA using the design of the experiment; the experimental data in table 4.15 were converted to S/N ratios. In this study, the effect of varying the control factors; stirring speed, stirring time, wt.% of SiC, and wt.% of MoS2 on the responses of wear rate were analyzed. As lower values of wear rate were desirable, smaller the better-quality characteristic was selected to investigate the influence of factors on the wear rate.

Table 4.15 shows the separate signal-to-noise ratio of each sample in the design experiment. The largest values of the S/N ratios were indicated in sample number three and the lowest value in sample number one with S/N ratios of 0.0000 and -20.0000 respectively. The respective highest and lowest wear rate values were 10 $x10^{-9}$Kg/m and 1 $x10^{-9}$Kg/m respectively. This result shows that, when the wt.% of SiC increased (at a higher level) and wt.% of MoS2 increased (higher level), the wear rate of the composite decreased. In contrast, the highest wear rate was recorded as the wt.% of SiC and wt.% of MoS2 are lower (at a lower level).

The wear resistance of composite is increased due to increasing the content of SiC particles and MoS2 reinforcement because the wear resistance of carbides is very high and the hard-reinforcing particles work to resist wear on the surface of the cast hybrid composite samples. Another reason for the improved wear resistance of the cast AMC is the adequate interfacial bonding between the hybrid reinforcements and the aluminum matrix due to the addition of MoS2 which resists the pull-out of the hybrid reinforcements during the relative movement between two contacting surfaces. The addition of MoS_2 reinforcement in Al6061/SiC composites as a hybrid reinforcement further increases the wear and friction resistance of the composite. In this study, wear rate response variation is studied with the help of ANOVA and the signal-to-noise (S/N) ratio.

Table 4.15: Experimental results of wear rate values for each sample.

Designation	Weight before and after wear test in gram			Calculated W.R (wear rate) ($x10^{-9}$Kg/m)	Predicted S/N ratio result
	W_b	W_a	W_L		
S1	0.8594	0.8563	0.0031	10	-20.0000
S2	0.8464	0.8444	0.0020	7	-16.9020
S3	0.8642	0.8638	0.0004	1	0.0000
S4	0.8613	0.8596	0.0017	6	-15.5630
S5	0.8702	0.8688	0.0012	4	-12.0412
S6	0.8562	0.8534	0.0028	9.002	-19.0868
S7	0.8486	0.8477	0.0009	3	-9.5424
S8	0.8522	0.8496	0.0026	9	-19.0849
S9	0.8630	0.8496	0.0024	8	-18.0618

4.6.1. Effect of Process Parameter on Wear Rate

From the figure below 4.13, it is shown that increasing the weight percentage of SiC, the wear rate of the developed composite decreased (increased wear resistance), and the wear rate value for 0, 5, 10 wt% SiC at constant wt.% MoS2 (0 wt.%). are 10, 8, $4x10^{-9}$kg/m respectively. . This result shows a better result than the previous studies by (Siddharthan et al. (2020)). At the higher weight percentage of SiC, the smaller value of wear rate is shown. SiC is a hard ceramic and wear-resistant material and Silicon carbide have the most significant effect on the wear rate of aluminum reinforced silicon carbide metal matrix composite and the wear rate of the composite decreases due to the addition of SiC (Md. Habibur Rahman et. al. (2014)).

MoS2 used as solid lubricant and lubrication is one way of wear prevention and also it facilitates the wettability between the aluminum and silicon carbide due to its low friction coefficient properties to enhance the obtained wear resistance of composite by decreasing the wear rate and wear rate is smaller when weight percentage of MoS2 is increased to Al-SiC composite.

The wear rate of the Al matrix decreases as the weight percentage of wt.% MoS2 increases. The value of wear rate for 0, 2, 4wt.% MoS2 at constant weight percentage of SiC (0 wt.%) are 10, 9.002, 9×10^{-9}kg/m respectively shown in figure 4.13. The smallest wear rate value of the developed composite was shown when the weight percentage of SiC is 10% wt of SiC and the weight percentage of MoS2 is 4% and this result shows a better result of wear rate than the previous studies by (Ajith et al. (2020)). From this analysis, the Al-SiC-MoS2 hybrid composite shows higher enhancements in decreasing wear rate than the Al-SiC composite.

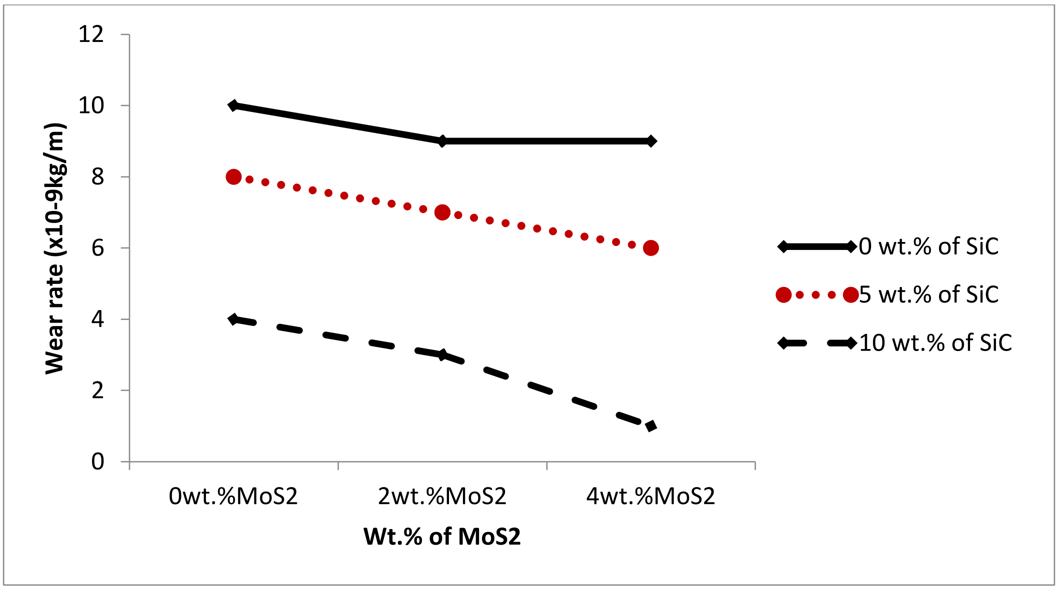

Figure 4.13: Effect of process parameter on the wear rate

4.6.1.1.Analysis Of Variance (ANOVA) For Wear Rate

ANOVA is used to identify the most significant factors which affect the wear rate of composite and the percent contribution of each factor. Where DoF = degree of freedom, SS= Sum of squares, MSS = Mean Sum of squares, and F = F- Ratio generated by using Minitab 17 software.

Table 4.16: Analysis of Variance of wear rate of Composite

Source	DF	Adj SS	Adj MS	F-Value	P-Value	PC (%)
Stirring Speed (rpm)	1	0.1660	0.1660	0.27	0.633	0.22
Stirring Time (min)	1	0.6667	0.6667	1.07	0.360	0.88
SiC (wt.%)	1	66.6800	66.6800	106.77	0.000	86.9
MoS2 (wt.%)	1	6.0000	6.0000	9.61	0.036	8.8
Error	4	2.4980	0.6245			3.2
Total	8	76.0107				

R-sq = 96, $F_{0.05, 1, 8} = 5.32$

Table 4.16 presents the percentage contribution of factors of stirring speed (0.22%), stirring time (0.88%), SiC (86.9%), and MoS2 (8.8%) on the wear rate of composite. This analysis was undertaken for a level of significance of 5%, i.e. for a level of confidence of 95%. From the ANOVA table, it is shown that wt.% SiC has statistical significance and has the highest percentage contribution (i.e. 86.9%) on the wear rate value and followed by wt.% MoS2, stirring time, and stirring speed.

The ANOVA table also shows the significance of factors using the F-values and P-values. If the obtained F-value of a parameter is greater than the tabulated one, then that particular parameter has a significant influence over the response variable. From table 4.16, the F value of wt.% SiC is 106.77 > 5.32, and, wt.% MoS2 (9.61) > 5.32, therefore, wt.% SiC and wt.% MoS2 have a significant influence over the wear rate. The result of the F-value for stirring speed (0.27) < 5.32, stirring time (1.07) < 5.32, therefore, stirring speed, and stirring time have no significant effect on the wear rate of composite.

The ANOVA with p values also shows that wt.% SiC (P=0.000 < 0.05), and wt.% MoS2 (P=0.036 < 0.05) and then both wt.% SiC and wt.% MoS2 are significant factors affecting the wear rate while stirring speed, and stirring time, have almost no significance (P>0.05). The reason for wear rate decrement in the composite was due to higher wear resistance properties in the contents of SiC and lubricant properties in the contents of MoS2. R-square value is 87.29% then, the model fits the data.

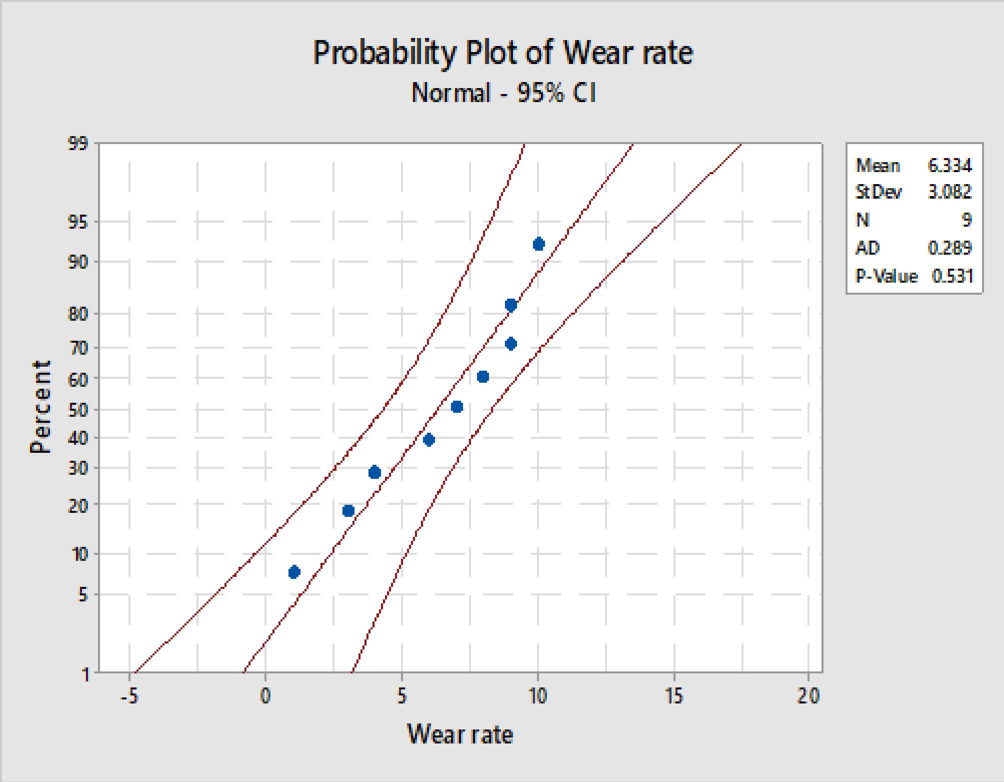

Figure 4.14: The normal probability plot for wear rate

A normal probability plot of effects is used to judge the significance of effects. If all the residuals fall along a straight line drawn through the plotted points, it is inferred that the residuals/errors follow a normal distribution. Figure 4.14 shows the data points are relatively close to the fitted normal distribution line (the middle solid line of the graph). The normal probability plots of residuals depict that the residuals lie reasonably close to the normal probability lines and the p-value is greater than the significance level of 0.05 on the above figure 4.14, implying that residuals are distributed normally and the terms mentioned in the regression models are significant and adequate (Suresha and Sridhara (2012)).

4.6.2. Optimization of Process Parameters for Wear Rate

Taguchi Signal-to-Noise ratios (S/N), which are log functions of the desired output, serve as objective functions for optimization and help in data analysis and prediction of optimum results. In the Taguchi method, wear rate response variation is studied with the help of the signal-to-noise (S/N) ratio.

4.6.2.1.Analysis of S/N Ratio for Wear Rate

To measure and characterize the wear rate, the statistics formula of —the smaller, the better has been used. In the case of smaller is the better, the ratio of signal noise can be given by equation (2.2).

Table 4.17: Signal to Noise Ratios for wear rate of composite for smaller is better

Level	Stirring Speed (rpm)	Stirring Time (min)	SiC (wt.%)	MoS2 (wt.%)
1	-12.301	-15.035	-19.391	-16.701
2	-15.564	-16.009	-16.842	-15.177
3	-15.563	-12.383	-7.195	-11.549
Delta	3.263	3.626	12.196	5.152
Rank	**4**	**3**	**1**	**2**

The delta statistics of the S/N ratio for the wear rate depicted in table 4.17 shows the ranks of factors affecting responses based on the S/N ratios obtained via the Taguchi orthogonal array. The delta statistics were computed based on the difference between the highest and the lowest average value of each factor. The highest value of delta was assigned the first rank and represents the predominant factor affecting wear rate. The analysis showed that, the wt.% SiC was assigned a rank of 1 with a delta value of 12.196 signifying that it is the predominant factor that affects the wear rate of the cast composite. The wt.% MoS2, stirring time, and stirring speed were assigned second (5.152), third (3.626), and fourth (3.263) ranks respectively.

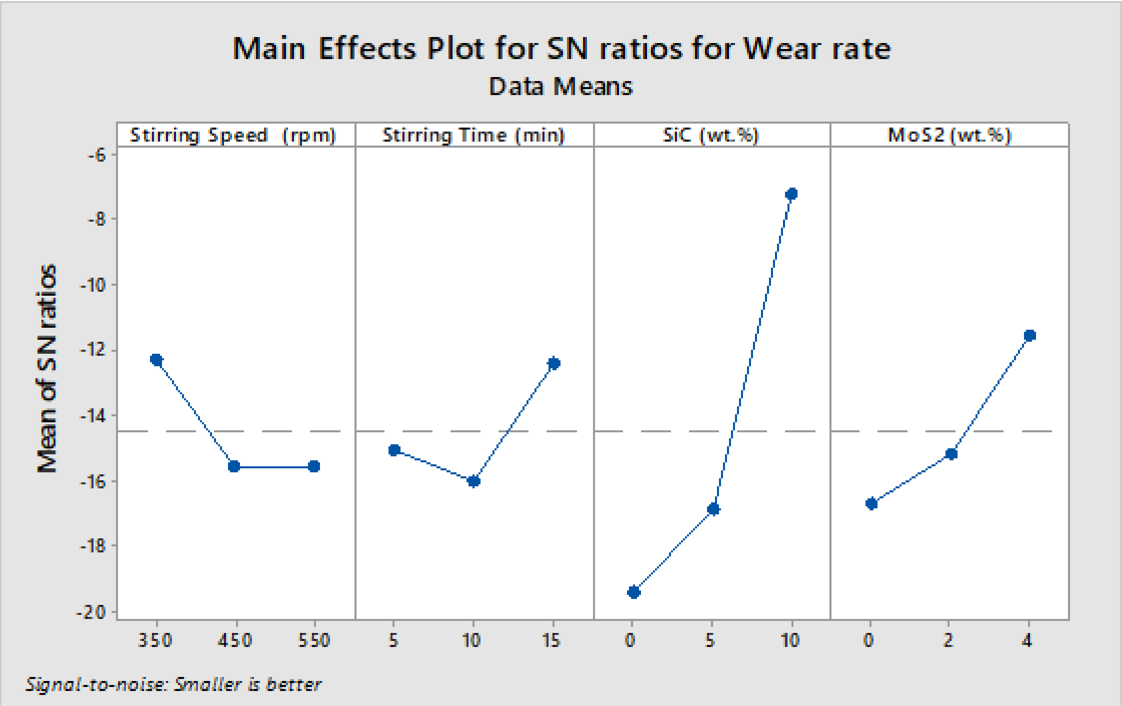

Figure 4.15: Main effects plots for S/N ratio of wear rate

Figure 4.15 shows the control factor‘s main effect plot for the S/N ratio and the optimal parameter combination on the wear rate of composite (lower the better wear rate). Since the S/N ratio used for this study is smaller is better, and the highest S/N ratio was selected. In the S/N ratio, the numerical value of the maximum point in each graph shows the best optimum combination of the factors at that level and the above figure shows the maximum value for stirring speed at level 1, stirring time at level 3, wt.% SiC at level 3, wt.% MoS2 at level 3 are is 350rpm, 15min, 10% wt.% SiC, and 3% wt.% MoS2 respectively (i.e.: **A1B3C3D3)** was selected. The most effective parameter to increase the tensile toughness is the SiC weight percentage when compared with other factors and stirring speed has the least effect on the tensile toughness.

4.6.2.2.Determining Optimum Conditions for Wear Rate

The optimum prediction condition for the S/NL ratio in which, the lower wear rate result of the composite obtains with the terms setting is shown in table 4.18. The selected optimum parameters in this study were at a lower stirring speed, at a higher stirring time, and higher wt.% SiC and at higher wt.% MoS2 which is at **A1B3C3D3**.

Table 4.18: The optimum conditions for wear rate result prediction-settings

Factors	Level	Value on each level	Rank of affecting	Predicted values	
				S/N Ratio	Mean
Stirring speed (A)	1	350 rpm	4	**-0.0000000**	**1**
Stirring time (B)	3	15 min	3		
SiC (C)	3	10 wt.%	1		
MoS2 (D)	3	4 wt.%	2		

4.7. Multi-Response Optimization for Developed Composite

Grey relational analysis is used for solving interrelationships among the multiple responses. In this approach, a grey relational grade is obtained for analyzing the relational degree of the multiple responses.

Step 1: Transformation of data into S/N ratios

Table 4.19: Experimental results and S/N ratio of response values

Designation	Experimental result				S/N ratio			
	Hardness	Tensile strength	Toughness	Wear rate	Hardness	Tensile strength	Toughness	Wear rate
S1	123.30	75	14	10	41.8193	37.5012	22.9226	-20.0000
S2	182.90	129.13	20	7	45.2443	42.2205	26.0206	-16.9020
S3	204.40	171.24	25	1	46.2096	44.6721	27.9588	0.0000
S4	173.80	104.6	19	6	44.8010	40.3906	25.5751	-15.5630
S5	199.50	180.85	23	4	45.9989	45.1464	27.2346	-12.0412
S6	180.17	89.76	15	9.002	45.1136	39.0617	23.5218	-19.0868
S7	208.30	194.43	26	3	46.3738	45.7753	28.2995	-9.5424
S8	162.60	82.41	16	9	44.2224	38.3196	24.0824	-19.0849
S9	180.30	118.9	17	8	45.1199	41.5036	24.6090	-18.0618

Step 2: Normalization of S/N values

Normalization of S/N values is the generation of grey relational within 0 and 1. If the response in the original sequence is "larger is better", then it is normalized using Eq. (2.5), and "smaller is better", then Eq. (2.7) is used for normalization (Mishra et al. (2015)).

Table 4.20: Normalized data of the experimental results

Designation	Normalized S/N ratio			
	Hardness	Tensile strength	Toughness	Wear rate
S1	0	0	0	1
S2	0.752	0.571	0.576	0.8451
S3	0.964	0.866	0.936	0
S4	0.655	0.13	0.493	0.778
S5	0.918	0.923	0.802	0.602
S6	0.723	0.188	0.111	0.954
S7	1	1	1	0.477
S8	0.527	0.123	0.215	0.954
S9	0.725	0.483	0.313	0.903

Step 3: Computation of grey relational coefficient (GC*ij*)

Grey relational coefficient (GRC) determined using Eq. (2.8)

Table 4.21: Deviation sequence and Grey relational coefficient with ∂= 0.5

Designation	Deviation sequence				GRC (Grey relational coefficient)			
	Hardness	Tensile strength	Toughness	Wear rate	Hardness	Tensile strength	Toughness	Wear rate
S1	1	1	1	0	0.333	0.333	0.333	1
S2	0.248	0.429	0.424	0.155	0.668	0.538	0.541	0.763
S3	0.036	0.134	0.064	1	0.933	0.788	0.886	0.333
S4	0.345	0.87	0.507	0.222	0.592	0.365	0.496	0.693
S5	0.082	0.077	0.198	0.398	0.859	0.866	0.716	0.557
S6	0.277	0.812	0.889	0.046	0.643	0.382	0.360	0.916
S7	0	0	0	0.523	1	1	1	0.489
S8	0.473	0.877	0.785	0.046	0.514	0.363	0.389	0.916
S9	0.275	0.517	0.687	0.097	0.645	0.492	0.421	0.838

Step 4: Determination of grey relational grade (GRG) and its order sequencing.

Grey relational coefficient (GRC) determined using Eq. (2.9) and where m (4 in this case) is the number of responses

Table 4.22: Grey relational grades and their order

Designation	GRG				GRG	Rank
	Hardness	Tensile strength	Toughness	Wear rate		
S1	0.333	0.333	0.333	1	0.499	9
S2	0.668	0.538	0.541	0.763	0.628	4
S3	0.933	0.788	0.886	0.333	0.735	3
S4	0.592	0.365	0.496	0.693	0.537	8
S5	0.859	0.866	0.716	0.557	0.750	2
S6	0.643	0.382	0.360	0.916	0.575	6
S7	1	1	1	0.489	0.872	1
S8	0.514	0.363	0.389	0.916	0.546	7
S9	0.645	0.492	0.421	0.838	0.599	5

4.7.1. Optimization of Process Parameters for Grey Relational Grade

Taguchi Signal-to-Noise ratios (S/N), which are log functions of the desired output, serve as objective functions for optimization and help in data analysis and prediction of optimum results. In the Taguchi method, GRG response variation is studied with the help of the Mean and signal-to-noise (S/N) ratio.

4.7.1.1.Analysis of S/N Ratio for Grey Relational Grade

To measure and characterize the hardness, the statistics formula of the larger, the better has been used. In the case of larger is the better, the ratio of signal noise can be given by equation (2.3).

Table 4.24: Signal to Noise Ratios for GRG for larger is better

Level	Stirring Speed (rpm)	Stirring Time (min)	SiC (wt.%)	MoS2 (wt.%)
1	-4.251	-4.209	-5.367	-4.329
2	-4.235	-3.932	-4.631	-3.346
3	-3.632	-3.977	-2.121	-4.444
Delta	0.619	0.277	3.246	1.098
Rank	**3**	**4**	**1**	**2**

The delta statistics of the S/N ratio for the GRG response depicted in table 4.24 shows the ranks of factors affecting the responses based on the S/N ratios obtained via the Taguchi orthogonal array. The highest value of delta was assigned the first rank and represents the predominant factor affecting GRG response. The analysis showed that wt.% SiC was assigned as rank 1 with a delta value of 3.246 signifying that it is the predominant factor that affects GRG response. The wt.% MoS2, stirring speed, and stirring time were assigned second (1.098), third (0.619), and fourth (0.277) ranks respectively. For predicting the optimum GRG, four factors of parameters are selected **A3B2C3D2** (i.e. 550 rpm stirring speed, 10 min stirring time, 10 wt.% SiC and 2 wt.%MoS2).

Figure 4.16 shows the control factor‘s main effect plot for the S/N ratio and the optimal parameter combination on the GRG response (larger the better GRG response). Since the S/N ratio used for this study is larger is better and the highest S/N ratio was selected. In the S/N ratio, the numerical value of the maximum point in each graph shows the best optimum combination of the factors at that level and the below figure shows the maximum value for stirring speed at level 3, stirring time at level 2, wt.% SiC at level 3, wt.% MoS2 at level 2 is 550rpm, 10min, 10% wt.% SiC, and 2% wt.% MoS2 respectively (i.e. **A3B2C3D2)** was selected.

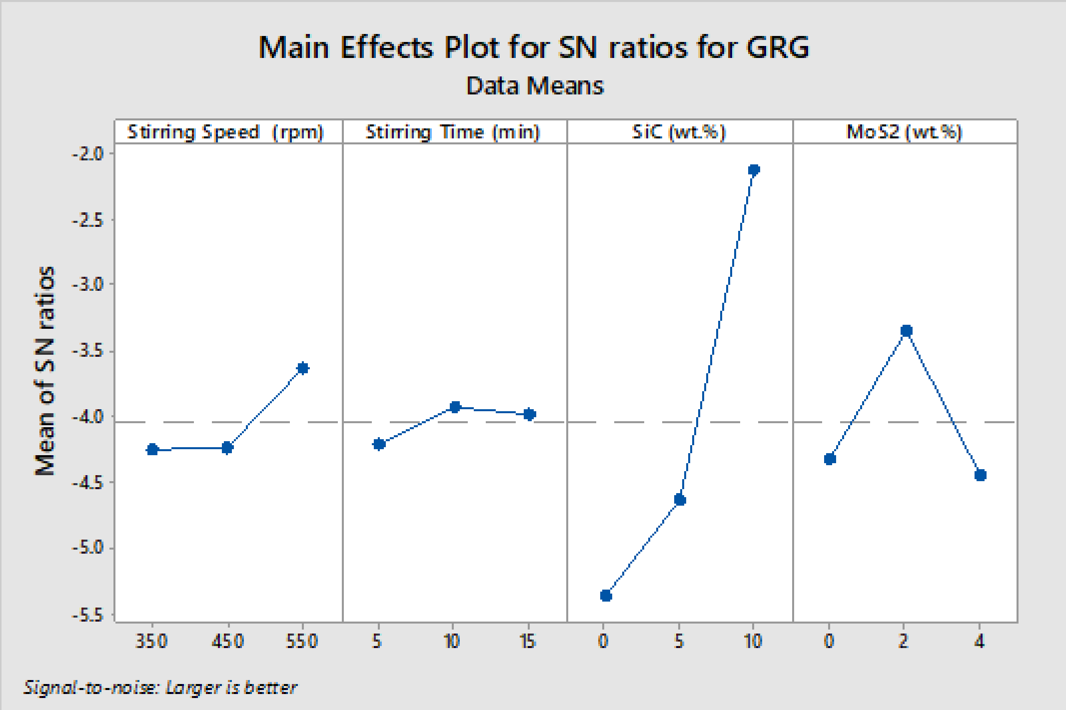

Figure 4.16: Main effects plots for S/N ratio of GRG response

The normal probability plot of effects is used to judge the significance of effects. Figure 4.17 shows the data points are relatively close to the fitted normal distribution line and the p-value is greater than the significance level of 0.05 on the figure 4.17, implying that residuals are distributed normally and the terms mentioned in the regression models are significant and adequate (Suresha and Sridhara (2012)).

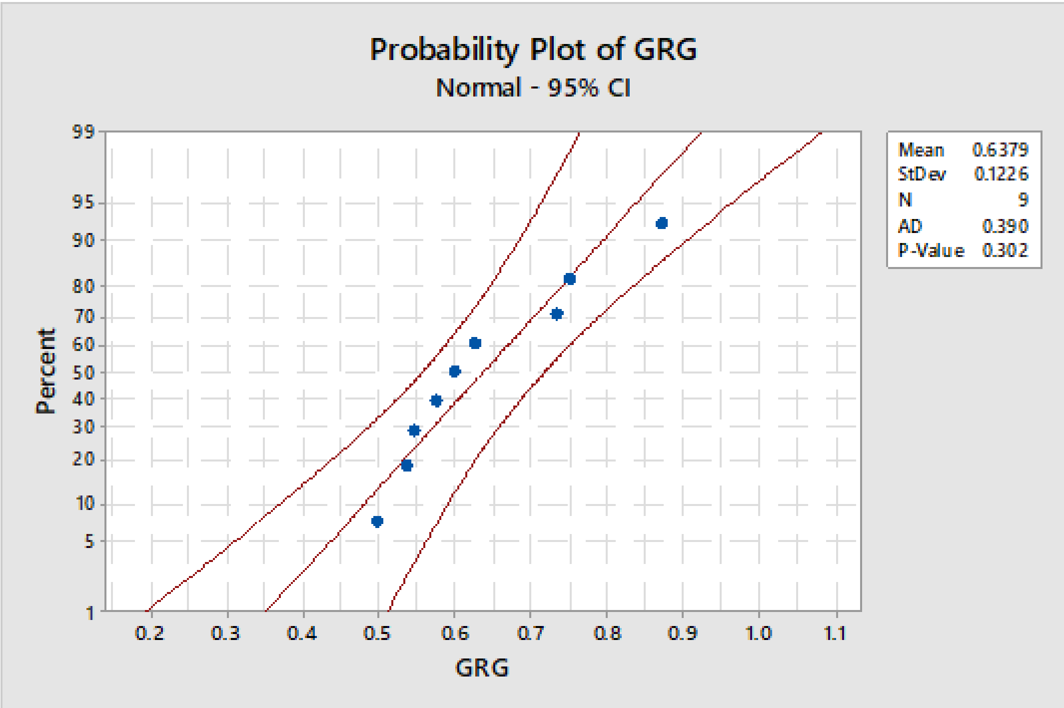

Figure 4.17: The normal probability plot for GRG

4.7.1.2.Determining Optimum Conditions for GRG

The optimum prediction condition for the S/NL ratio in which, the higher GRG response result of the composite obtains with the terms setting is shown in table 4.25. The selected optimum parameters in this study were higher stirring speed, and medium stirring time, at higher wt.% SiC and at medium wt.% MoS2 which is at **A3B2C3D2**.

Table 4.25: The optimum conditions for GRG response result prediction-settings

Factors	Level	Value on each level	Rank of affecting	Predicted values	
				S/N Ratio	Mean
Stirring speed (A)	3	550 rpm	3	-0.912189	**0.877333**
Stirring time (B)	2	10 min	4		
SiC (C)	3	10 wt.%	1		
MoS2 (D)	2	2 wt.%	2		

4.8. Analysis of Particle Distribution in Matrix

The microstructural image was analyzed by determining the grain particle size area for scaled dimension using "ImageJ" software. The software considers and counts all the particles, pores, and cracks in the Al matrix as grain particles and determines the volume fraction of particles in the Al matrix. The data recorded from this software were the total area of analyzed images, the total number of grain particles, total area of grain particles, the average area of grain particles, and the volume fraction of grain particles. The volume fraction of grain particles was proportional as per the analysis. Sample 3 which has the higher wt.% of SiC and MoS2 shows the higher volume fraction and Sample 1 which has no weight percentage of SiC and MoS2 shows the smaller volume fraction as shown in table 4.26

Table 4.26: Microstructural analysis of grain particles in the composite

Designation	Total area of images (μm2)	Total counted grain particles	Total grain particle area (μm2)	Average grain particle size area (μm2)	Volume fraction area of the grain particle size (%)
S1	624679.7	500	9264	18.528	1.483
S2	1261693	1809	134875	74.558	10.690
S3	1970589.4	2930	369052	125.956	18.728
S4	1360391.2	998	155071	155.382	11.399
S5	1866556.6	2551	248700	97.491	13.324
S6	1281421.4	1762	56075	31.825	4.376
S7	1697183.9	2091	239863	114.712	14.133
S8	1628568.9	1930	95369	49.414	5.856
S9	837422.7	1846	75837	41.082	9.056

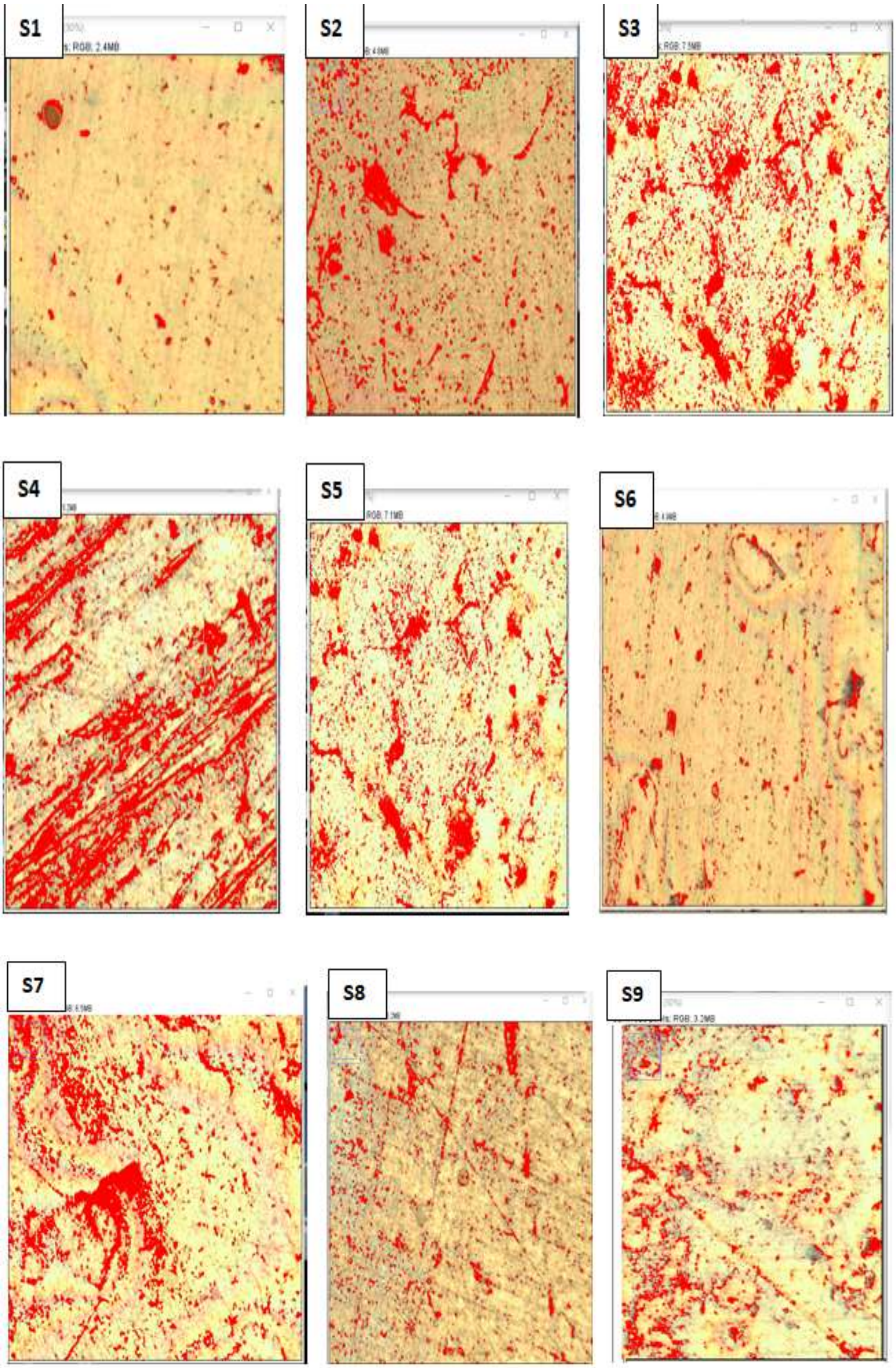

Figure 4.18: Optical microscopic images showing the reinforcement particle distribution.

4.9. Investigation of Machining Characteristics for Optimum Composite

The main challenge of AMMC material is its machining characteristics. The presence of ceramic reinforcement particles in aluminum metal matrix composites makes the composite difficult to machine due to the presence of hard abrasive ceramic reinforcing. Ceramic reinforcements build them stronger and stiffer than the base matrix and they lead to rapid tool wear and also poor surface finish (Duong et al. (2016)). Therefore, it needs to study the influence of process parameters on its machinability in a dry environment.

4.10. Analysis of Surface Roughness

Taguchi's orthogonal arrays are highly fractional orthogonal designs. Orthogonal array designs focus primarily on main effects. These designs are used to estimate the main effects using only a few experimental runs. In the Taguchi method, surface roughness response variation is studied with the help of the signal-to-noise (S/N) ratio.

Table 4.27: Experimental results of surface roughness each section.

Designation	N(rpm)	f(mm/rev)	d (mm)	Ra(in μm)				Predicted S/N ratio result
				Tr1	Tr1	Tr1	Ave	
Section 1	500	0.1	0.2	2.02	1.88	2.4	2.10	-6.4444
Section 2	500	0.2	0.3	2.76	2.6	3.1	2.82	-9.0050
Section 3	500	0.3	0.4	4.5	4.1	4.9	4.50	-13.0643
Section 4	750	0.1	0.3	1.7	1.73	1.82	1.75	-4.8608
Section 5	750	0.2	0.4	2.4	2.3	2.8	2.50	-7.9588
Section 6	750	0.3	0.2	3.25	2.7	2.9	2.95	-9.3964
Section 7	1000	0.1	0.4	1.35	1.1	1.3	1.25	-1.9382
Section 8	1000	0.2	0.2	2.02	1.82	1.8	1.88	-5.4832
Section 9	1000	0.3	0.3	2.75	2.6	2.9	2.75	-8.7867

4.10.1. Effect of Cutting Parameters on Surface Roughness

Figure 4.19 and 4.20 shows the variation of average surface roughness against spindle speed, depth of cut and feed rate respectively. From the figure 4.19, the average surface roughness decreases as the spindle speed increases and vice versa. Surface roughness attains minimum when spindle speed increases to its maximum i.e. 1000rpm. Surface roughness attains minimum when spindle speed and feed rate are 1000rpm.and 0.1mm/rev respectively. Average surface roughness attains maximum when spindle speed and feed rate are 500rpm and 0.3mm/rev respectively

Hence the graphs shown in figure 4.19 shows the concept that the average surface roughness can be highly reduced by higher spindle speed and lowering feed rate.

From the figure 4.20, the average surface roughness decreases as the depth of cut and feed rate increases and vice versa. Surface roughness attains minimum when feed rate and depth of cut are 0.1mm/rev and 0.4mm respectively. Average surface roughness attains maximum when feed rate and depth of cut are 0.3mm/rev and 0.4mm respectively. Hence the graphs shown on figure 4.20 shows the concept that the average surface roughness can be highly reduced by lowering feed rate and lowering depth of cut.

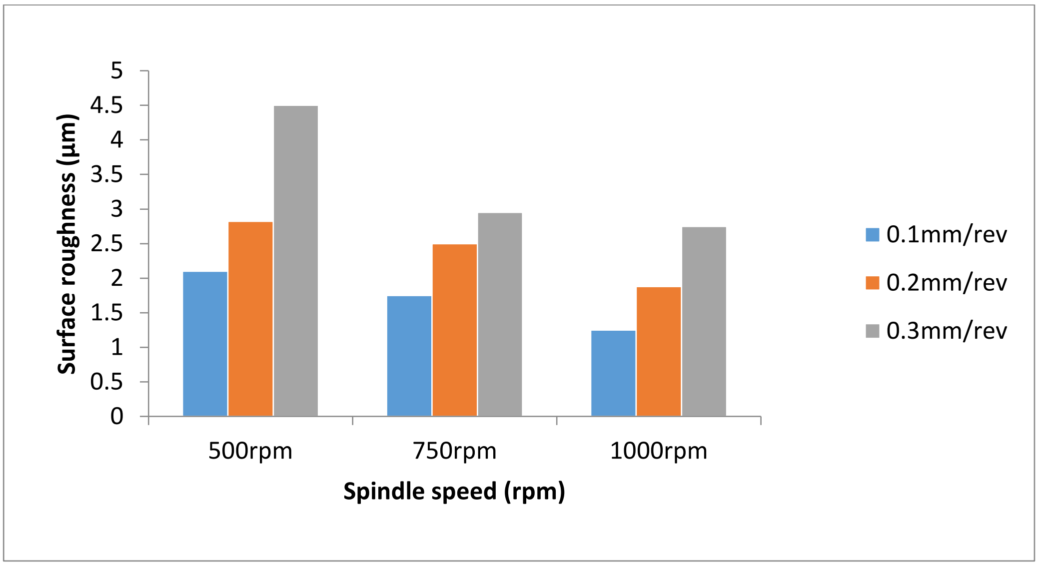

Figure 4.19: Effects of Spindle speed vs. feed rate on surface roughness

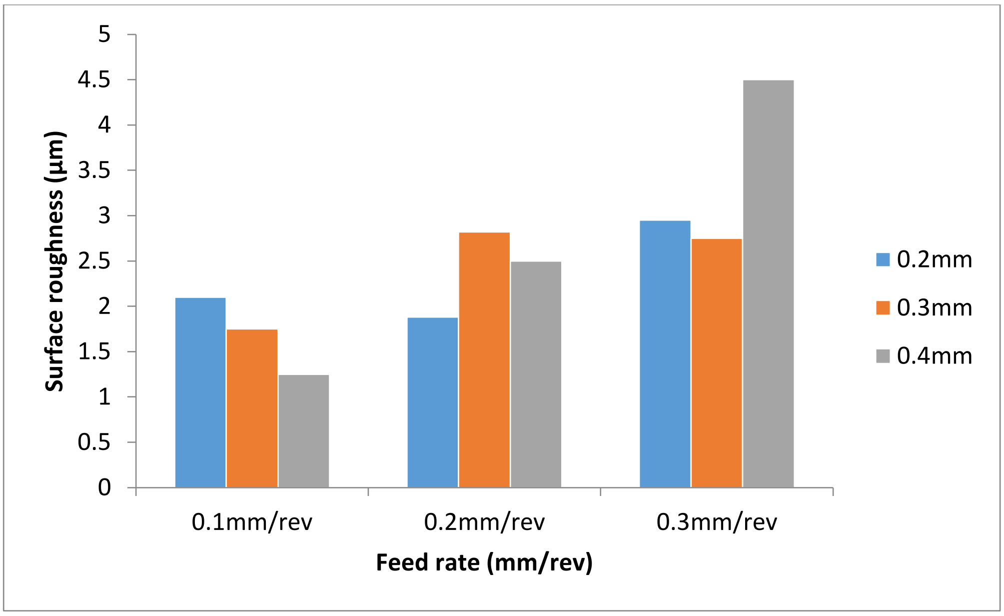

Figure 4.20: Effects of feed rate vs. depth of cut on surface roughness

4.10.1.2.Analysis Of Variance (ANOVA) For Surface Roughness

Analysis of variance (ANOVA) is used to identify the most significant factors which affect the surface roughness and the percent contribution of each factor. Where DoF = degree of freedom, SS= Sum of squares, MSS = Mean Sum of squares, and F = F- Ratio generated by using Minitab 17 software.

Table 4.28: Analysis of Variance of surface roughness

Source	DF	Adj SS	Adj MS	F-Value	P-Value	PC (%)
Spindle speed (N)	1	2.0886	2.08860	32.35	0.002	29.68
Feed rate (f)	1	4.3350	4.33500	67.15	0.000	61.6
Depth of cut (d)	1	0.2904	0.29040	4.50	0.087	4.14
Error	5	0.3228	0.06456			4.58
Total	8	7.0368				100

R-sq = 95.41%, $F_{0.05, 1, 8} = 5.32$

Table 4.28 presents the percentage contribution variation of factors of spindle speed (29.68%), feed rate (61.6%), and depth of cut (4.14%) on surface roughness. This analysis was undertaken for a level of significance of 5%, i.e. for a level of confidence of 95%. It is observed that feed rate has statistical significance and has the highest percentage contribution (i.e. 61.6%) on the surface roughness value and followed by spindle speed and depth of cut.

The ANOVA table also consists of the F-values and P-values. By comparing the F-values with the tabulated ones (critical F-value), the significance of the factors can be understood. If the obtained F value of a parameter is greater than the tabulated one, then that particular parameter has a significant influence over the response variable. From table 4.28, the F value of spindle speed is (32.35) > $F_{0.05, 1, 8} = 5.32$, feed rate (67.15) > 5.32, and depth of cut (4.5) < 5.32. Therefore, spindle speed and feed rate have a significant influence on surface roughness, and depth of cut has no significant effect on surface roughness. The analysis of variance with p values also shows that the p value of spindle speed, feed rate, and depth of cut are (P=0.002 < 0.05), (P=0.000< 0.05), and (P=0.089 > 0.05) respectively. Therefore, spindle speed and feed rate are significant factors affecting the surface roughness while depths of cut are not significant factors affecting the surface roughness. R-squared measures how well the model fits the data. Since the R-square value is 95.41% and the model fits the data.

4.10.2. Optimization of Process Parameters for Surface Roughness

Taguchi Signal-to-Noise ratios (S/N) serve as objective functions for optimization. In the Taguchi method, Surface roughness response variation is studied with the help of the signal-to-noise (S/N) ratio.

4.10.2.2. Analysis of S/N Ratio for Surface Roughness

To measure and characterize the Surface roughness, the statistics formula of the smaller, the better has been used. In the case of smaller is the better, the ratio of signal noise can be given by equation (2.2).

Table 4.29: Signal to Noise Ratios for Surface roughness for smaller is better

Level	Spindle speed (N)	Feed rate (f)	Depth of cut (d)
1	-9.505	**-4.414**	**-7.108**
2	-7.405	-7.482	-7.551
3	**-5.403**	-10.416	-7.654
Delta	4.102	6.001	0.546
Rank	**2**	**1**	**3**

The delta statistics of S/N ratio for the surface roughness depicted in table 4.29 shows the ranks of factors affecting surface roughness responses based on the S/N ratios obtained via the Taguchi orthogonal array. The delta statistics were computed based on the difference between the highest and the lowest average value of each factor.

The highest value of delta was assigned as the first rank and represents the predominant factor affecting surface roughness. The analysis showed that the feed rate was assigned a rank of 1 with a delta value of 6.001 signifying that it is the predominant factor that affects the surface roughness and followed by spindle speed and depth of cut. The most effective parameter to reduce surface roughness is the feed rate when compared with other factors and depth of cut has the least effect on the surface roughness.

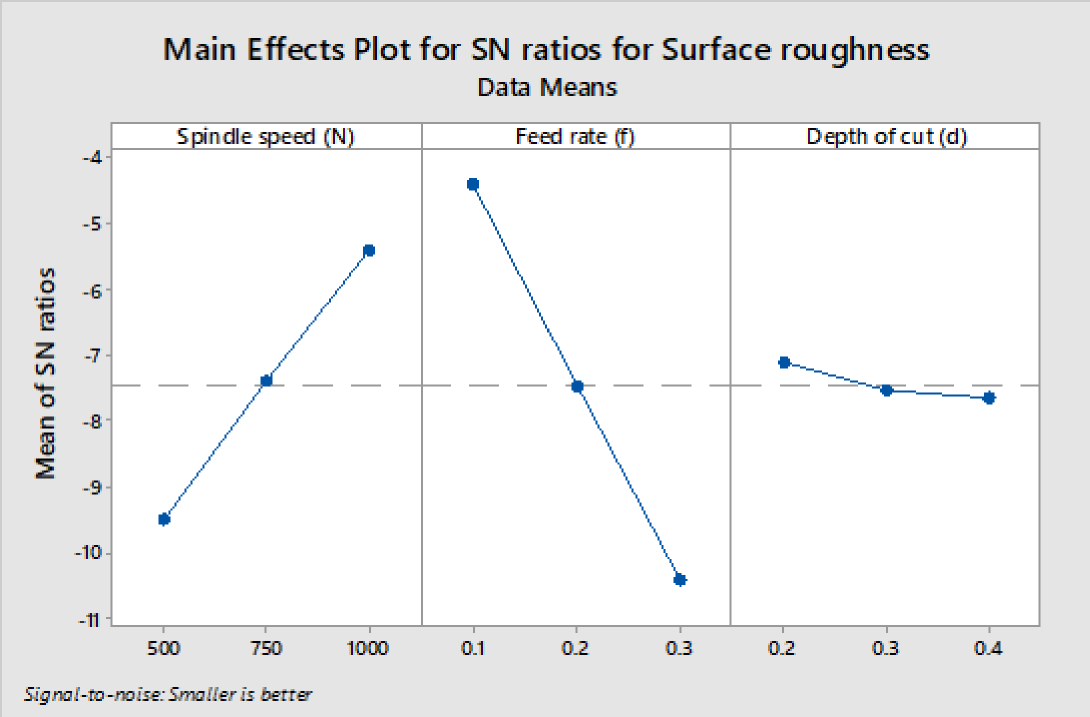

Figure 4.21: Main effects plots for S/N ratio of Surface roughness

Figure 4.21 shows the optimal parameter combination on the smaller surface roughness is the optimum combination of the factors is 1000rpm, 0.1mm/rev, and 0.2mm (i.e.: N3f1d1**)**. The numerical value of the maximum point in each graph shows the best value of that particular parameter at that level. Since the S/N ratio used for this study is smaller is better and the highest S/N ratio was selected as shown in the graph in figure 4.21. That is, spindle speed at level 3, feed rate at level 1, and depth of cut at level 1 (i.e.: **N3f1d1)** were selected.

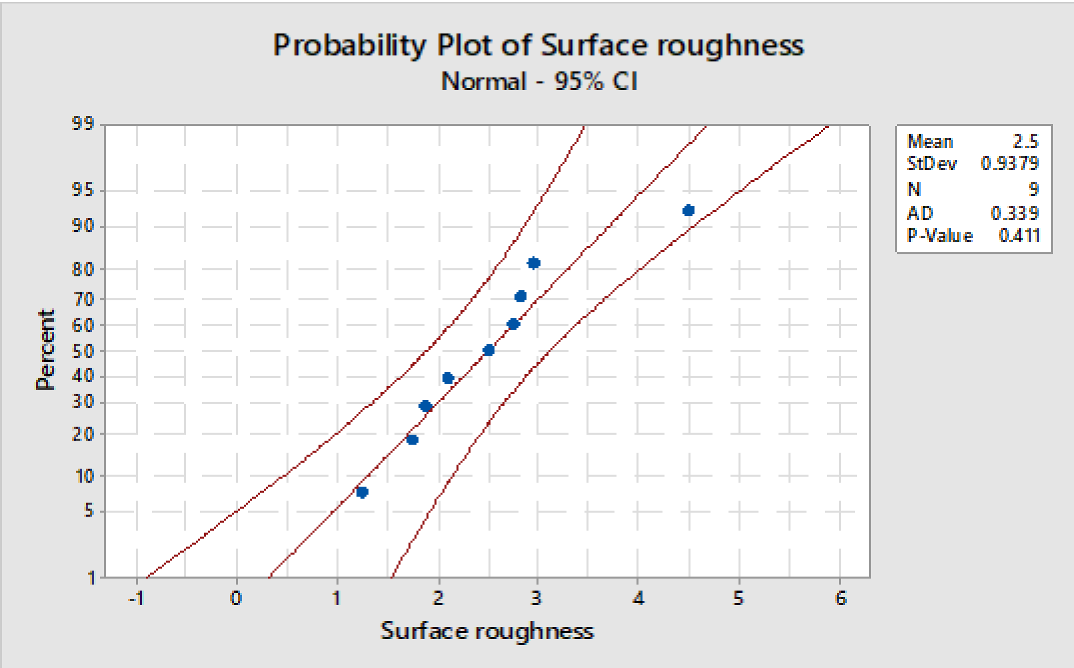

Figure 4.22: The normal probability plot for surface roughness

A normal probability plot of effects is used to judge the significance of effects. Figure 4.22 shows the data points are relatively close to the fitted normal distribution line (the middle solid line of the graph). The normal probability plots of residuals depict that the residuals lie reasonably close to the normal probability lines and the p-value is greater than the significance level of 0.05 on the above figure 4.22, implying that residuals are distributed normally and the terms mentioned in the regression models are significant and adequate (Suresha and Sridhara 2012).

4.10.2.3.Determining optimum conditions for Surface roughness

The optimum prediction condition for the S/NL ratio in which, the higher MRR result obtains with the terms setting in table 4.30. As shown in table 4.14, the selected optimum parameters in this study were at higher spindle speed, at lower feed rate, and at lower depth of cut which is at **N3f1d1**.

Table 4.30: The optimum conditions for surface roughness result prediction-settings

Factors	Level	Value of level	Rank of affecting	Predicted values	
				S/N Ratio	Mean
Spindle speed (N)	3	1000 rpm	2	-2.05008	0.97
Feed rate (f)	1	0.1 mm/rev	1		
Depth of cut (d)	1	0.2 mm	3		

4.11. Analysis of Material Removal Rate

In the Taguchi method, MRR response variation is studied with the help of signal-to-noise (S/N) ratio and ANOVA.

Table 4.31: Experimental results of MRR in each section

Designation	N(rpm)	F(mm/rev)	d (mm)	MRR (mm^3/min)	Predicted S/NL ratio result
Section 1	500	0.1	0.2	628	55.9592
Section 2	500	0.2	0.3	1884	65.5016
Section 3	500	0.3	0.4	3768	71.5222
Section 4	750	0.1	0.3	1413	63.0028
Section 5	750	0.2	0.4	3768	71.5222
Section 6	750	0.3	0.2	2826	69.0234
Section 7	1000	0.1	0.4	2512	68.0004
Section 8	1000	0.2	0.2	2512	68.0004
Section 9	1000	0.3	0.3	5652	75.0440

4.11.1. Effects of Cutting Parameter on Material Removal Rate

Figure 4.23 and 4.24 shows the variation of MRR against spindle speed, depth of cut and feed rate respectively. From the figure 4.23, the MRR increases as the spindle speed and feed rate increases and vice versa. The MRR is maximum when the spindle speed and feed rate are 1000rpm and 0.3mm/rev respectively. The MRR increases with increase in spindle speed and feed rate. Hence the graph shown on figure 4.23 shows that the concept that the MRR can be highly increased by higher feed rate, and higher spindle speed.

From the figure 4.24, the MRR increases as the spindle speed and feed rate increases and vice versa. The MRR is maximum when the feed rate and depth of cut are 0.3mm/rev and 0.4mm respectively. The MRR increases with increase in feed rate and depth of cut. Hence the graph shown on figure 4.24 shows that the concept that the MRR can be highly increased by higher feed rate, and higher depth of cut.

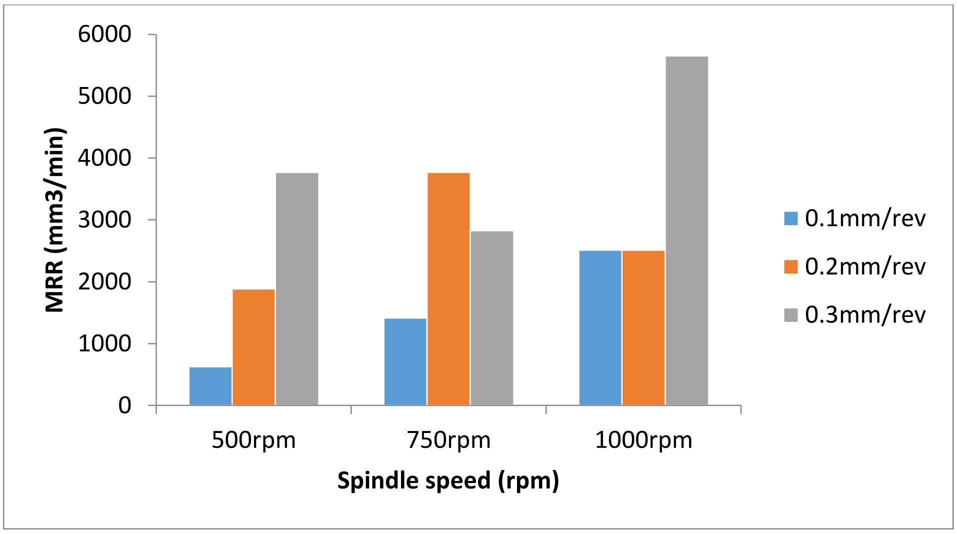

Figure 4.23: Effect of spindle speed vs. feed rate on material removal rate

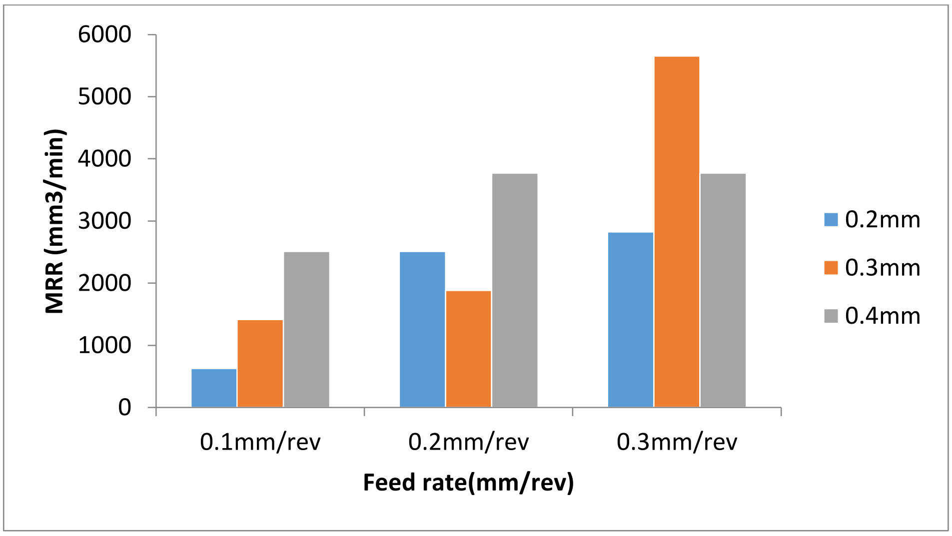

Figure 4.24: Effect of feed rate vs. depth of cut on material removal rate

4.11.1.2.Analysis of variance (ANOVA) for Material Removal Rate

Analysis of variance (ANOVA) is used to identify the most significant factors which affect the MRR. It was calculated and reported in table 4.32 for MRR and the percent contribution for each factor was calculated. Where DoF = degree of freedom, SS= Sum of squares, MSS = Mean Sum of squares, and F = F- Ratio generated by using Minitab 17 software.

Table 4.32: Analysis of Variance of MRR of machining

Source	DF	Adj SS	Adj MS	F-Value	P-Value	PC (%)
Spindle speed (N)	1	779718	779718	8.40	0.034	17.86
Feed rate (f)	1	2398314	2398314	25.83	0.004	54.95
Depth of cut (d)	1	721941	721941	7.78	0.039	16.55
Error	5	464231	92846			10.64
Total	8	4364204				100

R-sq = 89.36%, $F_{0.05, 1, 8} = 5.32$

Table 4.32 presents the percentage contribution variation of factors of spindle speed (17.86%), feed rate (54.95%), and depth of cut (16.55%) on MRR. It is observed that the feed rate has statistical significance on the MRR value. This analysis was undertaken for a level of significance of 5%, i.e. for a level of confidence of 95%. Feed rate has the highest percentage contribution (i.e. 54.95%) followed by spindle speed and depth of cut.

The ANOVA table also consists of the F-values and P-values. By comparing the F-values with the tabulated ones (critical F-value), the significance of the factors can be understood. If the obtained F value of a parameter is greater than the tabulated one, then that particular parameter has a significant influence over the response variable. From table 4.32, the F value of spindle speed is 8.40 > $F_{0.05, 1, 8} = 5.32$, (1.62) < $F_{0.05, 1, 8} = 5.32$, feed rate (25.83) <$F_{0.05, 1, 8} = 5.32$, depth of cut (7.78) < $F_{0.05, 1, 8} = 5.32$. Therefore, spindle speed, feed rate, and depth of cut have a significant influence over MRR.

The analysis of variance (ANOVA) with p values also shows that spindle speed, feed rate, and depth of cut are significant factors affecting the MRR spindle speed(P=0.034 < 0.05), and feed rate(P=0.004< 0.05), and depth of cut (P=0.039 < 0.05). R-squared measures how well the model fits the data. Since the R-square value is 87.29% and the regression model should fit observations.

4.11.2. Optimization of Cutting Parameters for Material Removal Rate

Taguchi Signal-to-Noise ratios (S/N), which are log functions of the desired output, serve as objective functions for optimization and help in data analysis and prediction of optimum results. In the Taguchi method, MRR response variation is studied with the help of the signal-to-noise (S/N) ratio.

4.11.2.2.Analysis of S/N Ratio for MRR

To measure and characterize the MRR, the statistics formula of ―the larger, the better has been used, because a high value of experimental MRR is desired for experimentally investigated data to be transformed into SNs-ratio. In the case of ―larger is the better, the ratio of signal noise can be given by equation (2.3).

Table 4.33: Signal to Noise Ratios for MRR for larger is better

Level	Spindle speed (N)	Feed rate (f)	Depth of cut (d)
1	64.33	62.32	64.33
2	67.85	68.34	67.85
3	**70.35**	**71.86**	**70.35**
Delta	6.02	9.54	6.02
Rank	**3**	**1**	**2**

The delta statistics of the S/N ratio for the MRR depicted in table 4.33 shows the ranks of the individual responses based on the S/N ratios obtained via the Taguchi orthogonal array. The delta statistics were computed based on the difference between the highest and the lowest average value of each factor. Ranks were then assigned according to the delta value. The highest value of delta was assigned the first rank and represents the predominant factor affecting MRR. The analysis showed that the feed rate was assigned a rank of 1 with a delta value of 9.54 signifying that it is the predominant factor that affects the MRR and followed by the depth of cut and spindle speed with delta value (6.02) and fourth (6.02) respectively.

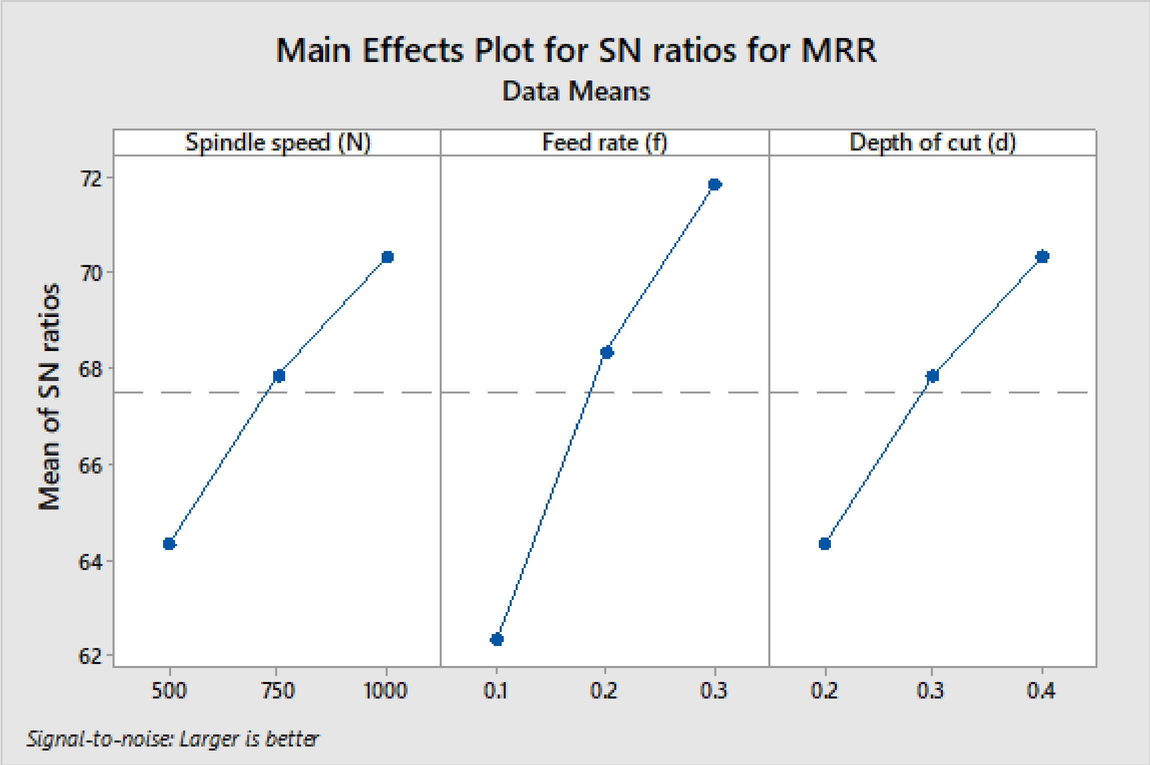

Figure 4.25: Main effects plots for S/N ratio of MRR

Figure 4.25 shows the optimal parameter combination on the higher MRR is the optimum combination of the factors is 1000rpm, 0.3mm/min, and 0.4mm (i.e.: **N3f3d3)**. The control factor's main effect plot for the MRR S/N ratio is shown in figure 4.23. The numerical value of the maximum point in each graph shows the best value of that particular parameter at that level. The most effective parameter to increase the MRR is the feed rate weight percentage when compared with other factors and spindle speed has the least effect on the MRR which is similar to the result obtained from the analysis of the mean. Since the S/N ratio used for this study is larger is better and the highest S/N ratio was selected as shown in the graph in figure 4.25. That is, spindle speed at level 3, feed rate at level 3, and depth of cut at level 3 (i.e.: **N3f3d3)** were selected.

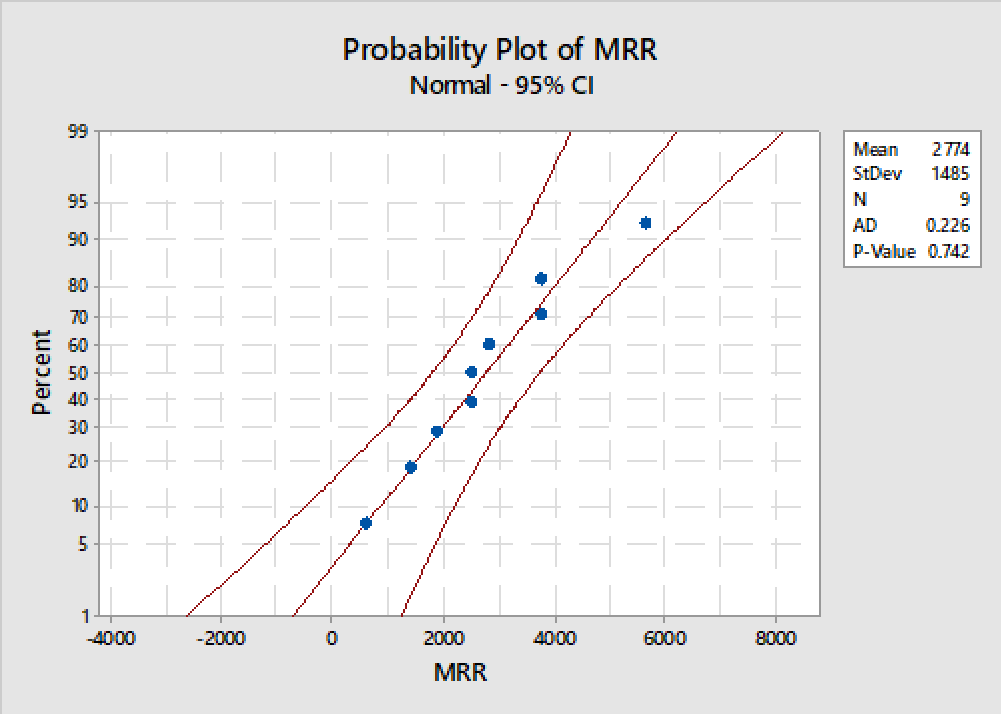

Figure 4.26: The normal probability plot for MRR

The normal probability plot of effects is used to judge the significance of effects. If all the residuals fall along a straight line drawn through the plotted points, it is inferred that the residuals/errors follow a normal distribution. Figure 4.26 shows the data points are relatively close to the fitted normal distribution lines and the p-value is greater than the significance level of 0.05 on the above figure 4.26, implying that residuals are distributed normally and the terms mentioned in the regression models are significant and adequate (Suresha and Sridhara 2012).

4.11.2.3.Determining Optimum Conditions for MRR

The optimum prediction condition for the higher MRR result obtains with the terms setting in table 4.34. The selected optimum parameters in this study were at **N3f3d3**.

Table 4.34: The optimum conditions for MRR result prediction-settings

Factors	Level	Value of level	Rank of affecting	Predicted values	
				S/N Ratio	Mean
Spindle speed (N)	3	1000 rpm	3	**77.5428**	**5442.67**
Feed rate (f)	3	0.3 mm/rev	1		
Depth of cut (d)	3	0.4 mm	2		

4.12. Multi Response Optimization for Machining Performance

Hybrid Taguchi-based grey relational analysis (HTGRA) is used for the optimization of the fabrication process parameters (spindle speed, feed rate, and depth of cut). In the grey relational analysis, the grey relational grade is used to optimize a multi-response system. The use of GRA includes the following steps:

Step 1: Transformation of data into S/N ratios

Table 4.35: Experimental results and S/N ratio of surface roughness (Ra) and MRR values

Designation	Experimental result		Predicted S/N ratio result	
	Ra (µm)	MRR (mm^3/min)	Ra	MRR
Section 1	2.10	628	-6.4444	55.9592
Section 2	2.82	1884	-9.0050	65.5016
Section 3	4.50	3768	-13.0643	71.5222
Section 4	1.75	1413	-4.8608	63.0028
Section 5	2.50	3768	-7.9588	71.5222
Section 6	2.95	2826	-9.3964	69.0234
Section 7	1.25	2512	-1.9382	68.0004
Section 8	1.88	2512	-5.4832	68.0004
Section 9	2.75	5652	-8.7867	75.0440

Step 2: Normalization of S/N values

Normalization of S/N values is the generation of grey relational. It generates a normalized data sequence for the experimental results within 0 and 1. If the response in the original sequence is "larger is better" Eq. (2.5) and if the response is "smaller is better" then Eq. (2.6) is used for its normalization (Mishra et al. (2015).

Table 4.36: Normalized data of the experimental results

Designation	Normalized S/N ratio	
	Ra (µm)	MRR (mm^3/min)
Section 1	0.405	0
Section 2	0.635	0.5
Section 3	1	0.815
Section 4	0.263	0.369
Section 5	0.541	0.815
Section 6	0.67	0.684
Section 7	0	0.63
Section 8	0.318	0.63
Section 9	0.61	1

Step 3: Determination of deviation sequence and grey relational coefficient.

The grey relational coefficient (GRC) for the normalized S/N ratio values is determined using the Eq. (2.8)

Table 4.37: Deviation sequence and Grey relational coefficient with ∂= 0.5

Designation	Deviation sequence (Δ)		Grey relational coefficient (GRC)	
	Ra (µm)	MRR (mm^3/min)	Ra (µm)	MRR (mm^3/min)
S1	0.595	1	0.456	0.333
S2	0.365	0.5	0.578	0.5
S3	0	0.185	1	0.730
S4	0.737	0.631	0.404	0.442
S5	0.459	0.185	0.521	0.490
S6	0.33	0.316	0.602	0.454
S7	1	0.37	0.333	0.600
S8	0.682	0.37	0.423	0.542
S9	0.39	0	0.562	0.470

Step 4: Determination of grey relational grade (GRG) and its order of sequencing

The grey relational grade is determined using the formula on Eq. (2.9). Where *m* is the number of responses

Table 4.38: Grey relational grades and their order

Designation	GRC (Grey relational coefficient)		GRG (Grey relational grades)	Order
	Ra (µm)	MRR (mm^3/min)		
S1	0.456	0.333	0.394	9
S2	0.578	0.5	0.539	2
S3	1	0.730	0.865	1
S4	0.404	0.442	0.423	8
S5	0.521	0.490	0.505	5
S6	0.602	0.454	0.528	3
S7	0.333	0.600	0.466	7
S8	0.423	0.542	0.482	6
S9	0.562	0.470	0.516	4

4.12.1. Optimization of Cutting Parameters for Grey Relational Grades

4.12.1.1.Analysis of S/N Ratio for GRG

To measure and characterize the GRG, the statistics formula of the larger, the better has been used and the data are transformed into SNs-ratio.

Table 4.39: Signal to Noise Ratios for GRG for larger is better

Level	Spindle speed (N)	Feed rate (f)	Depth of cut (d)
1	-4.906	-7.399	-6.659
2	-6.318	-5.880	-6.196
3	-6.239	-4.185	-4.609
Delta	1.412	3.214	2.050
Rank	**3**	**1**	**2**

The delta statistics of the S/N ratio for the grey relational grade tabulated in table 4.39 shows the ranks of factors affecting the responses based on the S/N ratios obtained via the Taguchi orthogonal array. The delta statistics were computed based on the difference between the highest and the lowest average value of each factor. The highest value of delta was assigned the first rank and represents the predominant factor affecting grey relational grade response. The analysis showed that the feed rate was assigned the rank of 1 with a delta value of 3.214 signifying that it is the predominant factor that affects the grey relational grade response and followed by the depth of cut and spindle speed with a delta value (2.050) and fourth (1.412) respectively.

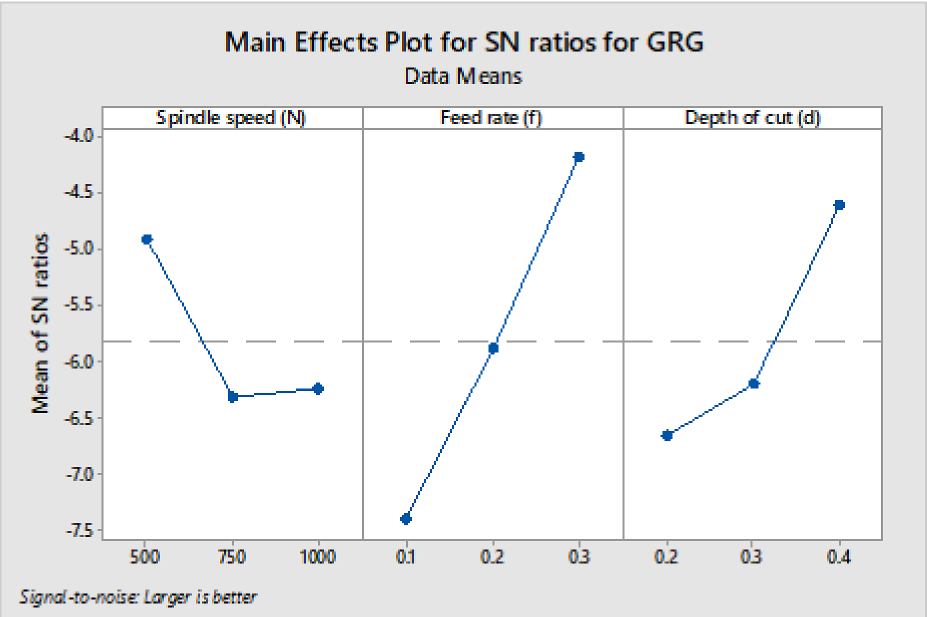

Figure 4.27: Main effects plots for S/N ratio of GRG

Figure 4.27 shows the control factor's main effect plot for the grey relational grade and optimal parameter combination on the grey relational grade (higher the better grey relational grade). Since the S/N ratio used for this study is larger is better and the highest S/N ratio was selected and the numerical value of the maximum point in each graph shows the best value of that particular parameter at that level for the optimum combination of the factors of spindle speed at level 1, feed rate at level 3, and depth of cut at level 3 are 1000rpm, 0.3mm/min, and 0.4mm respectively (i.e. N1f3d3) was selected. The most effective parameter of the grey relational grade is the feed rate when compared with other factors and spindle speed has the least effect on the grey relational grade. The optimum prediction condition for the higher GRG result of the composite obtained with the terms setting are (i.e. **N1f3d3).**

4.12.1.2.Determining Optimum Conditions for GRG

The optimum prediction condition for the higher GRG result obtains with the terms setting in table 4.40. The selected optimum parameters in this study were at N1f3d3.

Table 4.40: The optimum conditions for GRG result prediction-settings

Factors	Level	Value of level	Rank of affecting	Predicted values	
				S/N Ratio	Mean
Spindle speed (N)	1	500 rpm	3	**-2.05692**	**0.799222**
Feed rate (f)	3	0.3 mm/rev	1		
Depth of cut (d)	3	0.4 mm	2		

CHAPTER FIVE

CONCLUSIONS AND RECOMMENDATIONS

5.1. Summary of Finding and Conclusions

In this experimental study, aluminum-based MMCs at varying stirring speeds (350, 450, 550rpm), stirring time (5, 10, 15min), wt.% of SiC particles (0, 5, 10 wt.%), and wt.% of MoS2 powder (0, 2, 4 wt.%) were successfully prepared using stir casting fabrication technique. Microstructural aspects, hardness, tensile strength, and wear characteristics of the prepared composites were studied. Based on the experimental evaluation, the optimum composite was selected and investigated on its machining characteristics to study the influence of cutting parameters spindle speed (500, 750, 1000rpm), feed rate (0.1, 0.2, 0.3mm/rev), and depth of cut (0.2, 0.3, 0.4mm) on surface roughness and material removal rate (MRR) in dry turning condition. From the observations, the following conclusions were made. The analysis of mechanical properties like hardness, tensile strength, tensile toughness and wear resistance were done with the help of ANOVA and S/N ratio and both analyzing methods show the same results in the rank of factors affecting the response.

- Optical micrographs showed homogenous dispersion of particles in Al matrix Porosities were found and it is higher for reinforcement contents are higher.
- From the ANOVA analysis, the addition of SiC in composite showed better hardness, tensile strength, tensile toughness, and wear resistance. Wt.% of SiC are the only and the most significant factors affecting the hardness, tensile strength, and toughness of composite and followed by wt.% of MoS2, stirring time, and stirring speed. In the case of wear resistance, only wt.% of SiC and wt.% of MoS2 are the significant factors and wt.% of SiC is the most significant factor affecting wear rate and followed by wt.% of MoS2, stirring time, and stirring speed. This means, that the higher value of hardness, tensile strength, tensile toughness, and lower wear rate have been obtained at 10 wt.% of SiC contents in the composite. The addition of MoS2 in composite showed better hardness, tensile strength, and tensile toughness only up to 2 wt.% of MoS2 and in the case of wear rate addition of MoS2 in composite up to 4% showed better wear resistance than unreinforced Al matrix. This means, that the highest value of hardness, tensile strength, and tensile toughness has been obtained at 2wt.% of MoS2 and the lowest wear rate has been obtained at 4wt.% of MoS2 contents in the composite.

- Therefore, the maximum hardness = 208.30HV has been obtained at stirring speed 450rpm, stirring time 15min, 10% wt.% of SiC particles and 2% wt.% of MoS2, maximum tensile strength = 194.43 MPa has been obtained at stirring speed 550rpm, stirring time 10min, 10% wt.% of SiC particles and 2% wt.% of MoS2, maximum tensile toughness = 26J/mm^3 has been obtained at stirring speed 550rpm, stirring time 10min, 10 wt .% of SiC particles and 2 wt .% of MoS2 and the lowest wear rate = 1 x10^{-9}Kg/m has been obtained at stirring speed 350rpm, stirring time 15min, 10wt.% of SiC particles and 4wt.% of MoS2.
- The optimum prediction condition for the S/L ratio in which, the higher hardness, tensile strength, tensile toughness, and lowest wear rate has been obtained at A2B3C3D2, A3B2C3D2, A3B2C3D2, and A1B3C3D3 respectively. From the Grey Relational Analysis for multi-response characteristics, the optimum prediction condition for the S/L ratio has been obtained at stirring speed 550rpm, stirring time 10min, 10% weight fraction of SiC particles, and 2% weight fraction of MoS2 (i.e. A3B2C3D2). Al-SiC-MoS2 hybrid composite shows better enhancements in hardness, tensile strength, toughness, and wear resistance than the Al-SiC composite. Therefore, the enhancement of wettability has been achieved due to the addition of MoS2 in the Al-SiC composite.

From the ANOVA and S/N ration analysis, the machining performance for the optimum composites shows that:

- Surface roughness decreases with increasing the spindle speed and increasing feed rate and depth of cut lead to an increase in the surface roughness. The minimum surface roughness is achieved at a spindle speed of 1000rpm, feed rate of 0.1mm/rev, and a depth of cut of 0.4mm. Feed rate is the most significant factor affecting surface roughness of machined sample and followed by spindle speed and depth of cut.
- Material removal rate increases with increasing feed rate, depth of cut and spindle speed increases, and vice versa. Feed rate is the most significant factor affecting MRR of machined samples and followed by the depth of cut and spindle speed. The maximum MRR is achieved at a spindle speed of 1000rpm, feed rate of 0.3mm/rev, and a depth of cut of 0.4mm. The optimum prediction condition for the S/L ratio in which, the lower surface roughness and higher material removal rate have been obtained are at N3f1d1 and N3f3d3 respectively. From the Grey Relational Analysis of multi-response (lower surface roughness and higher MRR), the optimum prediction condition has been obtained at N1f3d3, and feed rate is the highly influential parameter.

5.2. Recommendation

Based on the results and conclusions found from this study, the following recommendations were made:

- Since Al-SiC-MoS2 hybrid composite shows higher enhancements in hardness, tensile strength, tensile toughness, and wear rate than Al-SiC composite, it can be recommended as a good replacement for materials used in the automotive and aerospace industry.
- Stir casting is suggested as the most feasible process due to the low cost, simplicity, and design of advanced stir casting set up using speed controller motor and temperature control unit has to be developed in the country.
- It will be good if the department follows the progress of individual students doing their thesis work and their advisor presents their progress at least once per month.
- It will be good if there is a good relationship and collaboration between departments to the department to facilitate fairly usage of different testing machines for the student.

5.3. Scope of Future Work

- The study can be further extended to different fabrication techniques and study its parametric effect on mechanical and tribological behavior of developed AMMCs.
- The study can be extended for developed a composite on creep, fatigue, stiffness, etc.
- The study can be extended to study the effect of SiC particle size and a small amount of MoS2 because the particle size and percentage volume fraction of the reinforcement play a significant role in mechanical and tribological behavior.
- The machinability of the optimum hybrid composite can be extended to study the comparison of effect cutting parameters on dry and wet machining.
- The study can be conducted to study the effect of the cutting parameter of optimum hybrid composite on cutting forces, power consumption, and machining time.
- The study can be extended to study the effect of other factors like cutting tool geometry, type of coolant, and type of cutting tool material on surface roughness and material removal rate.

SPECIAL AKCKOWLEDGEMENT

This research work is funded by Adama Science and Technology University under the grant number ASTU/SM-R/587/22, Adama, Ethiopia.

REFERENCES

Aatthisugan, I., Razal Rose, A., & Selwyn Jebadurai, D. (2017). Mechanical and wear behavior of AZ91D magnesium matrix hybrid composite reinforced with boron carbide and graphite. Journal of Magnesium and Alloys, 5, pp 20–25.

Ajagol, P., Anjan, B. N., Marigoudar, R. N., & Preetham Kumar, G. V. (2018). Effect of SiC Reinforcement on Microstructure and Mechanical Properties of Aluminum Metal Matrix Composite. IOP Conference Series: Materials Science and Engineering, 376, 012057. https://doi.org/10.1088/1757-899x/376/1/012057

Ajith, A. D. S., Dhanasekeran, C., Sivaganesan, S., & Sridhar, R. (2020). Investigation on the Mechanical Properties of Silicon Carbide Particulates in Al/SiC/MoS_2. Materials-Science-Forum. https://doi.org/10.4028/www.scientific.net/msf.979.89

Al Hawari, A., et al. (2014). A Life Cycle Assessment (LCA) of Aluminum Production Process. World Academy of Science, Engineering and Technology. International Journal of Mechanical, Aerospace, Industrial, Mechatronic, and Manufacturing Engineering. 8(4), 704-710.

Bharath., V., Madev Nagaral, V Auradi & S. A. Kori (2014). Preparation of 6061Al-Al2O3 MMCs by Stir Casting and Evaluation of Mechanical and Wear Properties. 3rd International Conference on Materials Processing and Characterization (ICMPC 2014). Procedia Materials Science, 6, pp1658 –1667.

Campbell, J. (2015). Complete Casting Handbook: Metal Casting Processes, Metallurgy, Techniques and Design. Elsevier Science.

D. K. Suker, M. S. Alsoufi, M. M. Alhusaini, S. A. Azam, (2016). Studying the Effect of Cutting Conditions in Turning Process on Surface Roughness for Different Materials. World Journal of Research and Review (WJRR) 2:16-21.

Das, S., Madheshiya, A., Gautam,S.S., Gautam, C.R., (2020). Mechanical, Surface morphological and multi-objective optimization of tribological properties of V2O5 doped lead calcium titanate borosilicate glass ceramics, Ceram. Int. 46, 19170–19180.

Duong, X., Mayer, J., & Balazinski, M. (2016). Initial tool wear behavior during machinin of titanium metal matrix composite (TiMMCs). International Journal of Refractory Metals-and-Hard-Materials-60-169.https://doi.org/10.1016/j.ijrmhm.2016.07.021

Dwivedi, S. P., Sharma, S., & Mishra, R. K. (2014). Comparison of Microstructure and Mechanical Properties of A356/SiC Metal Matrix Composites Produced by Two Different Melting Routes. International Journal of Manufacturing Engineering, 2014, 1–13. https://doi.org/10.1155/2014/747865

Elango, M., & Annamalai, K. (2020). Machining parameter optimization of Al/SiC/Gr hybrid metal matrix composites using ANOVA and grey Relational analysis. FME Transactions, 48(2), 173–179. https://doi.org/10.5937/fmet2001173m

Elango, M., & Annamalai, K. (2020). Machining parameter optimization of Al/SiC/Gr hybrid metal matrix composites using ANOVA and grey Relational analysis. FME Transactions, 48(2), 173–179. https://doi.org/10.5937/fmet2001173m

Fabrication Techniques of Metal Matrix Composites for Engineering Applications. (2019). International Journal of Engineering and Advanced Technology, 9(1S4), 918–922. https://doi.org/10.35940/ijeat.a1069.1291s419

Gowri Shankar, M., Shettar, M., Sharma, S., Kini, A., & Jayashree. (2018). Enhancement in Hardness and Influence of Artificial Aging on Stir Cast Al6061-B4C and Al6061-SiC Composites. Materials Today: Proceedings, 5(1), 2435–2443. https://doi.org/10.1016/j.matpr.2017.11.023

Gowri, M. C., Manjunath Shettar, Sharma SS, Achutha Kini, & Jayashree, (2018) Enhancement in Hardness and Influence of Artificial Aging on Stir Cast Al6061-B4C and Al6061-SiC Composites. Materials Today: Proceedings 5, pp2435–2443.

Halil, K., ˙Ismail Ovalı, Sibel Dündar, & Ramazan¸ (2019) Wear and mechanical properties of Al6061/SiC/B4C hybrid composites produced with powder metallurgy. J mater res technol.; 2019; 8(6):5348–5361.

Hashim, J. (2012). The Production of Cast Metal Matrix Composite by a Modified Stir Casting Method. Jurnal Teknologi. https://doi.org/10.11113/jt.v35.588

Hocheng, H., Yen, S., Ishihara, T., & Yen, B. (2007). Fundamental turning characteristics of a tribology-favored graphite/aluminum alloy composite material. Composites Part A: Applied Science and Manufacturing, 28(9–10), 883–890. https://doi.org/10.1016/s1359-835x(97)00055-9

Imayev, V.M., R.A. Gaisin, & R.M. Imayev, (2018). Microstructure and mechanical properties of near a titanium alloy-based composites prepared in situ by casting and subjected to multiple hot forging. Journal of Alloys and Compounds 762, pp555-564.

Jain, P., Soni, S., & Baredar, P. (2014). Review on Machining of Aluminium Metal Matrix Composites. Material Science Research India, 11(2), 114–120. https://doi.org/10.13005/msri/110204.

Jegan, T. C., Ravindran, D., & Anand, M. D. (2014). Material Characterization Study on Aluminium Metal Matrix Composites by Enhanced Stir Casting Method. Advanced Materials-Research-984–985. https://doi.org/10.4028/www.scientific.net/amr.984-985.3266

Kala, H., Mer, K. K. S., & Kumar, S. (2014). A Review on Mechanical and Tribological Behaviors of Stir Cast Aluminum Matrix Composites. Procedia Materials Science, 6, 1951-1960.

Kala, H., Mer, K., & Kumar, S. (2014). A Review on Mechanical and Tribological Behaviors of Stir Cast Aluminum Matrix Composites. Procedia Materials Science, 6, 1951–1960. https://doi.org/10.1016/j.mspro.2014.07.229

Kalaiselvan, N. Murugan, Siva Parameswaran. (2011). Production and characterization of AA6061–B4C stir cast composite, Materials and Design 32, 4004–4009.

Karthick, E., Joel Mathai, Michael Tony J, & Senthil Kumar Marikkannana, (2017) Processing, Microstructure, and Mechanical Properties of Al2O3 and SiC Reinforced Magnesium Metal Matrix Hybrid Composites. Materials Today: Proceedings 4, pp6750–6756.

Karvanis, K., Fasnakis, D., Maropoulos, A., & Papanikolaou, S. (2016). Production and mechanical properties of Al-SiC metal matrix composites. IOP Conference Series: Materials Science and Engineering, 161, 012070. https://doi.org/10.1088/1757-899x/161/1/012070

Kumar A., Shyam Lal, Sudhir Kumar, (2013). Fabrication and characterization of A359/Al2O3 metal matrix composite using electromagnetic stir casting method, J. Mater. Res. Technol.; 2(3):250–254.

Kumar Sharma, A., Bhandari, R., Aherwar, A., Rimašauskienė, R., & Pinca-Bretotean, C. (2020). A study of advancement in application opportunities of aluminum metal matrix composites. Materials Today: Proceedings, 26, 2419–2424. https://doi.org/10.1016/j.matpr.2020.02.516

Kuo, Y., Yang, T., & Huang, G. W. (2008). The use of a grey-based Taguchi method for optimizing multi-response simulation problems. Engineering Optimization, 40(6), 517–528. https://doi.org/10.1080/03052150701857645

Madeva, N, Shivananda B. K., V. Auradi, K. I. Parashivamurthy, & S A Kori, (2017) Mechanical behavior of Al6061-Al2O3 and Al6061-Graphite Composites. Materials Today: Proceedings 4, pp10978–10986.

Meena, K., A. Manna, D., S.S. Banwait, D., & Jaswanti, D. (2013). An Analysis of Mechanical Properties of the Developed Al/SiC-MMCs. American Journal of Mechanical Engineering, 1(1), 14–19. https://doi.org/10.12691/ajme-1-1-3

Miss. Laxmi1, Mr. Sunil Kumar2 (June 2017). Fabrication and Testing of Aluminium 6061 Alloy & Silicon Carbide Metal Matrix Composites" International Research Journal of Engineering and Technology (IRJET) Volume: 04 Issue: 06 http://www.irjet.net

Mohamadigangaraj, J., Nourouzi, S., & Jamshidi Aval, H. (2020). Statistical modeling and optimization of friction stir processing of A390-10 wt% SiC compo-cast composites.-Measurement-165.https://doi.org/10.1016/j.measurement.2020.108166

Navaneethakrishnan, S., & Athijayamani, A. (2015). Taguchi method for optimization of fabrication parameters with mechanical properties in fiber and particulate reinforced composites. https://doi.org/10.1007/s12588-015-9128-x

Palanikumar, K., & Karthikeyan, R. (2014). Assessment of factors influencing surface roughness on the machining of Al/SiC particulate composites. Materials & Design, 28(5), 1584–1591. https://doi.org/10.1016/j.matdes.2006.02.010

Parswajinan, C., Vijaya Ramnath, B., Abishek, S., Niharishsagar, B., & Sridhar, G. (2018). Hardness and impact behavior of aluminum metal matrix composite. IOP Conference Series: Materials Science and Engineering, 390, 012075. https://doi.org/10.1088/1757-899x/390/1/012075

Poovazhagan, L., Kalaichelvan, K., & Shanmugasundaram, D. (2012). Tensile Properties, Hardness and Micro Structural Analysis of Al 6061 – SiCP Metal Matrix Composites Fabricated by Ultrasonic Cavitation Approach. Advanced Materials Research,-622-1275.https://doi.org/10.4028/www.scientific.net/amr.622.623.1275

Poovazhagan, L., Kalaichelvan, K., Rajadurai, A., & Senthilvelan, V. (2013). Characterization of Hybrid Silicon Carbide and Boron Carbide Nanoparticles-Reinforced Aluminum Alloy Composites. Procedia Engineering, 64, 681–689. https://doi.org/10.1016/j.proeng.2013.09.143

Prabu, S. B., Karunamoorthy, L., Kathiresan, S., & Mohan, B. (2016). Influence of stirring speed and stirring time on distribution of particles in cast metal matrix composite. Journal-of-Materials-Processing-Technology,-171(2),-268–273. https://doi.org/10.1016/j.jmatprotec.2005.06.071

R. Karthigeyan, G. Ranganath, S. Sankaranarayanan.(2012). Mechanical Properties and Microstructure Studies of Aluminium (7075) Alloy Matrix Composite Reinforced with Short Basalt Fibre. European Journal of Scientific Research.ISSN 1450-216X Vol.68 No.4), pp. 606- 615.

R. N. Muni et al. (2016), “Aluminium matrix hybrid composites: a review of different reinforcements on mechanical and tribological characteristics”, International Journal of Exploring Emerging Trends in Engineering (IJEETE) Vol. 03, Issue 06, NOV-DEC, 2016 Pg. 367 – 376.

Radha, A., & Vijaya Kumar, K. (2015). An Investigation of Mechanical Properties on Aluminium 6061 Reinforced with SiC - Metal Matrix Composites. Applied-Mechanics-and-Materials. https://doi.org/10.4028/www.scientific.net/amm.787.568

Rahman, M. H., & Rashed, H. M. M. A. (2014). Characterization of Silicon Carbide Reinforced Aluminum Matrix Composites. Procedia Engineering, 90, 103–109. https://doi.org/10.1016/j.proeng.2014.11.821

Rajasekar Thiyagarajan, Vignesh Ganesan, Milon Selvam Dennison, & Nelson A.J.R (2018). Preparation and characterization of aluminium metal matrix composite by using stir casting technique. International Research Journal of Engineering and Technology (IRJET) Volume: 05 pp62-66.

Rajeswari, B., Amirthagadeswaran, K., & Ramya, K. (2014). Microstructural Studies of Aluminium 7075-Silicon Carbide-Alumina Metal Matrix Composite. Advanced Materials-Research-984–985,-194–199. https://doi.org/10.4028/www.scientific.net/amr.984-985.1944

Ramanathan, A., Krishnan P.K., and Muraliraja R., (2019). A review on the production of metal matrix composites through stir casting-Furnace design, properties, challenges, and research opportunities J. Manuf. Process. 42, 213–45.

Reddy, P. S., Kesavan, R., & Vijaya Ramnath, B. (2017). Investigation of Mechanical Properties of Aluminium 6061-Silicon Carbide, Boron Carbide Metal Matrix Composite. Silicon, 10(2), 495–502. https://doi.org/10.1007/s12633-016-9479-8

S, B. M., M, V., P, A. V., G, V. P., & P, S. (2021). Multi-objective optimization of process parameters in dry sliding wear characteristics of Al/sic composites using Taguchi grey relation analysis. Materials Today: Proceedings, 45, 1882–1886. https://doi.org/10.1016/j.matpr.2020.09.1333

S. B. Rayjadhav Dr. V. R. Naik. (February 2016). Development of Aluminum 6061-Sic Composite and It's use in Manufacturing of Dovetail by Single Response Optimization of Hardness and Surface Roughness by Taguchi Method in Stir Casting. IJIRST –International Journal for Innovative Research in Science & Technology| Volume 2 | Issue 09. www.ijirst.org

S. B. Rayjadhav, V. R. Naik. (2016).Multi-Objective Optimization of Hardness and Surface Roughness in Manufacturing of Developed Aluminum Metal Matrix Composite by Stir Casting using Grey Relational Analysis. Journal of Mechanical and Mechanics Engineering Volume 2 Issue 2

Şahin, Y. (2015). Analysis of abrasive wear behavior of PTFE composite using Taguchi ' s technique. l, 1–15. https://doi.org/10.1080/23311916.2014.1000510

Sasimurugan, T., & Palanikumar, K. (2011). Analysis of the Machining Characteristics on Surface Roughness of a Hybrid Aluminium Metal Matrix Composite (Al6061-SiC-Al.Journal of Minerals and Materials Characterization and Engineering, 10(13), 1213–1224. https://doi.org/10.4236/jmmce.2011.1013094

Sesharao, Y., Sathish, T., Palani, K., Merneedi, A., L, N., de Poures, M. V., & Maridurai, T. (2021). Optimization on Operation Parameters in Reinforced Metal Matrix of AA6066 Composite with HSS and Cu. Advances in Materials Science and Engineering, 2021, 1–12. https://doi.org/10.1155/2021/1609769

Shukla, M., Dhakad, S., Agarwal, P., & Pradhan, M. (2018). Characteristic behaviour of aluminium metal matrix composites: A review. Materials Today: Proceedings, 5(2), 5830–5836. https://doi.org/10.1016/j.matpr.2017.12.180

Siddharthan, B., Rajiev, R., Saravanan, S., & Naveen, T. K. (2020). Effect of Silicon Carbide in Mechanical Properties of Aluminium Alloy Based Metal Matrix Composites. IOP Conference Series: Materials Science and Engineering, 764, 012040. https://doi.org/10.1088/1757-899x/764/1/0120400

Sidhu, S. S., Batish, A., & Kumar, S. (2013). Fabrication and electrical discharge machining of metal–matrix composites: A review. Journal of Reinforced Plastics and Composites, 32(17), 1310–1320. https://doi.org/10.1177/0731684413489366

Singh, G., & Kumar, A. (2019). A Review Paper on Stir Casting of Reinforced Aluminium Metal MatrixComposite (MMC). International Journal of Current Engineering and Technology, 9(03). https://doi.org/10.14741/ijcet/v.9.3.14

Soltani, S., Azari Khosroshahi, R., Taherzadeh Mousavian, R., Jiang, Z. Y., Fadavi Boostani, A., & Brabazon, D. (2015). Stir casting process for manufacture of Al–SiC composites. Rare Metals, 36(7). https://doi.org/10.1007/s12598-015-0565-7

Subramanya Reddy, P., Kesavan, R., & Vijaya Ramnath, B. (2017). Evaluation of Mechanical Properties of Aluminum Alloy (Al2024) Reinforced with Silicon Carbide (SiC) Metal Matrix Composites. Solid State Phenomena, 263, 184–188. https://doi.org/10.4028/www.scientific.net/ssp.263.184

Suresha, S., & Sridhara, B. K. (2012). Friction characteristics of aluminium silicon carbide graphite hybrid composites. Materials & Design, 34, 576-583.

Sylajakumari, P. A., & Ramakrishnasamy, R. (2018). Taguchi Grey Relational Analysis for Multi-Response. 1–17. https://doi.org/10.3390/ma11091743

T. K. Durga Bhavani, G. S. V. Seshu Kumar, Prof. K. Satyanarayana, & I. Ajit Kumar. (2017). Optimization of Material Removal Rate and Surface Roughness in Turning of Aluminum, Copper and Gunmetal Materials using RSM. International Journal of Engineering Research And, V6(02). https://doi.org/10.17577/ijertv6is020359.

Toptan, F., Kerti, I., Rocha, LA. (2012). Reciprocal dry sliding wear behavior of B4C reinforced aluminum alloy matrix composites. Wear 290–291:74–85.

Tripathi, P., & Yadav, K. (2017). Hybrid Bamboo and Glass Fiber Polymer Composite – A Review. 4(04), 2014–2018.

Umamaheswarrao, P., Ravi Sankar, B., & Nancharaiah, T. (2020). Multi objective optimization of process parameters of Al 6061-SiCp metal matrix composite in end milling-Hybrid GRA-PCA approach. Materials Today: Proceedings, 26, 696–700. https://doi.org/10.1016/j.matpr.2019.12.407

Upinder Kumar Yadav, Deepak Narang and Pankaj Sharma Attri. (2012). Experimental investigation and optimization of machining parameters for surface roughness in CNC turning by taguchi method. International Journal of Engineering Research and Applications, 10:2060-2065

Velavan, K., & Palanikumar, K. (2015). Effect of Silicon Carbide (SiC) on Stir Cast Aluminium Metal Matrix Hybrid Composites – A Review. Applied Mechanics and Materials, 766–767, 293–300. https://doi.org/10.4028/www.scientific.net/amm.766-767.293

Vijay K.Patel, Bhupesh Goyal, Chinmay Shah. (2016). Optimization of Process Parameters of CNC Milling for Aluminium Metal Matrix Composite. International Conference on Multidisciplinary Research & Practice

Vijaya Ramnath, B., Elanchezhian, C., Jaivignesh, M., Rajesh, S., Parswajinan, C., & Siddique Ahmed Ghias, A. (2014). Evaluation of mechanical properties of aluminium alloy–alumina–boron carbide metal matrix composites. Materials & Design, 58, 332–338. https://doi.org/10.1016/j.matdes.2014.01.068

Yadav, K. K., and Dr. Dalbir Singh Lohchab (2016) Influence of Aviation Fuel on Mechanical properties of Glass Fiber-Reinforced Plastic Composite. International Advanced Research Journal Science, Engineering and Technology, Vol.3, pp 1-10

Ying, Yu., Hitoshi Ishii, Keiichiro Tohgo, Young Tae Cho, Dongfeng Diao, (1997). Temperature dependence of slidingwear behavior in SiC whisker or SiC particulate reinforced 6061 aluminum alloy composite. Wear, 213, 21-28.

APPENDICES

Appendix 1: Micro-Hardness Result for S-1 and S-2 (From Vickers Hardness)

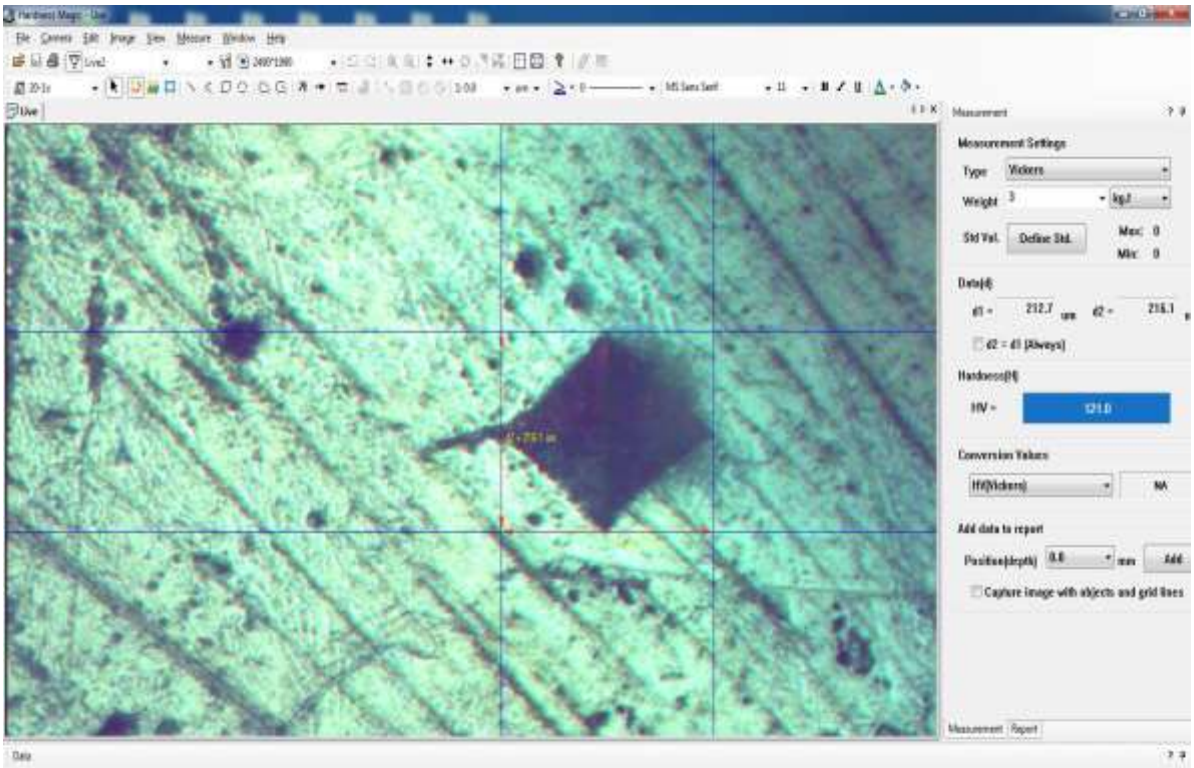

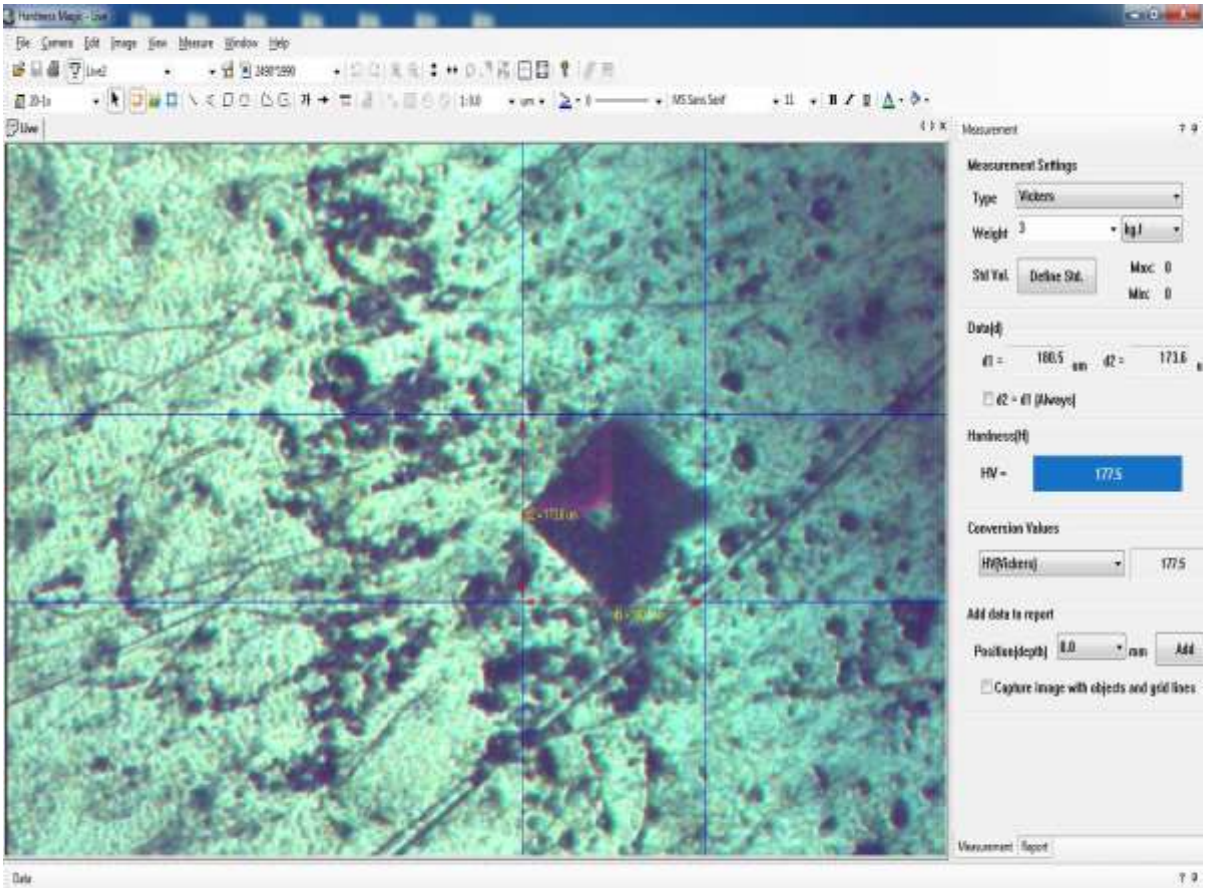

Appendix 2: Micro-Structural Analysis for S-1 and S-2 (From Optical Microscope)

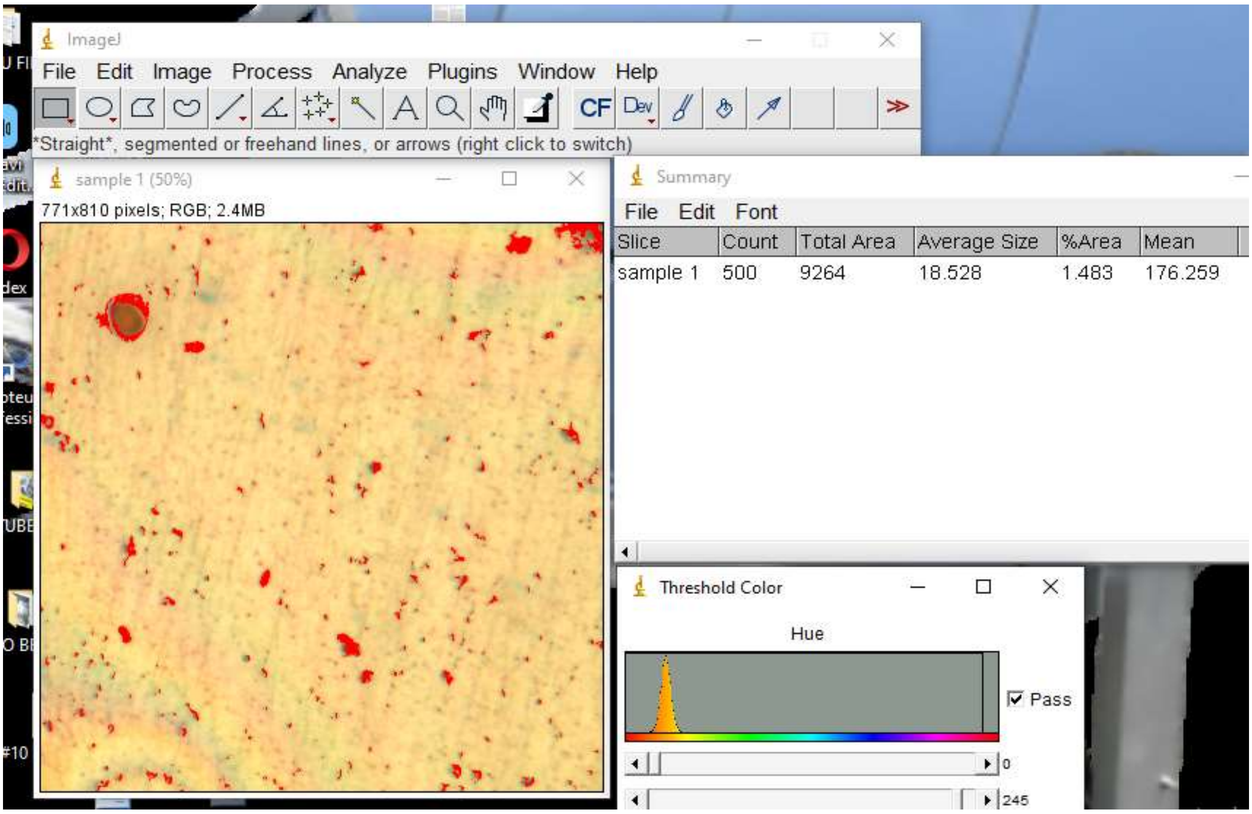

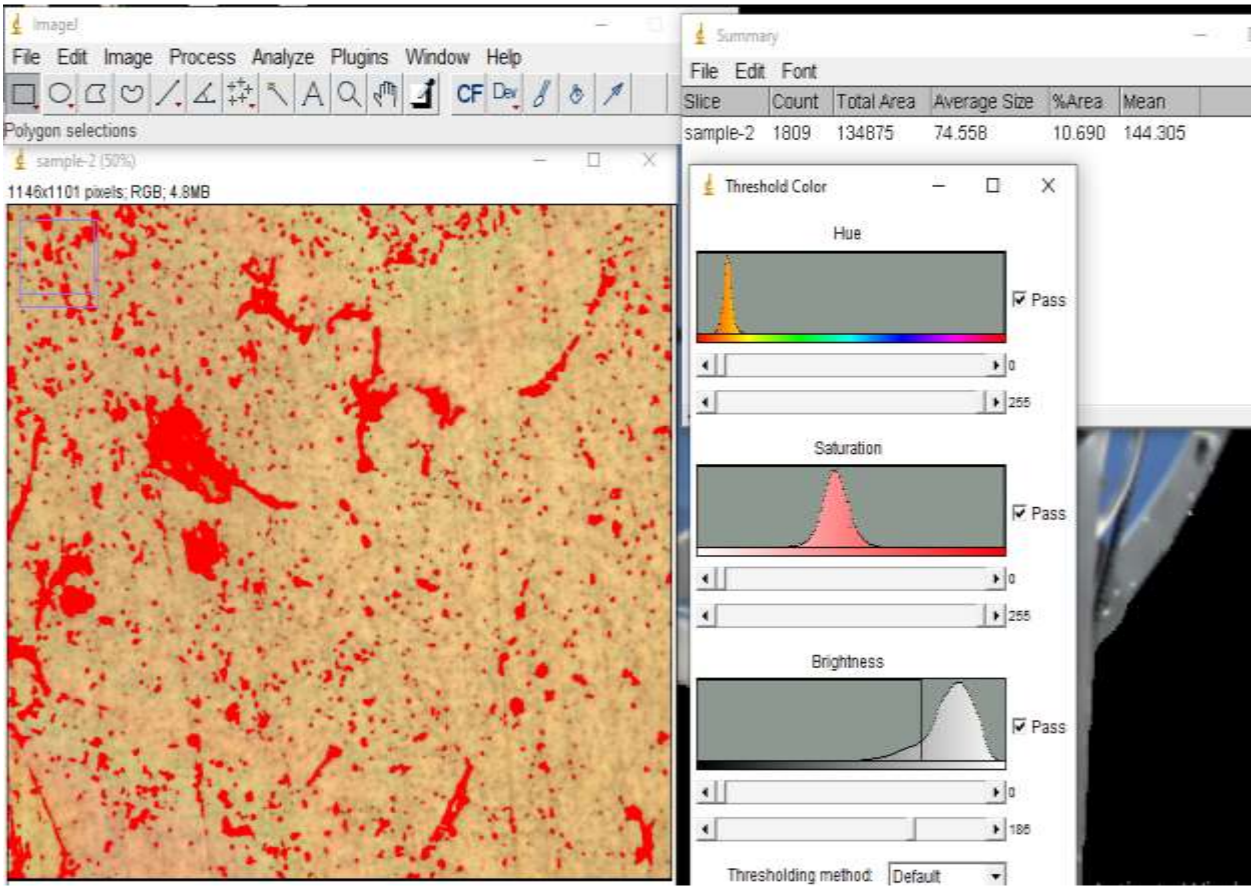

Appendix 3: Tensile Strength and Tensile Toughness Result for Sample-1 and Sample-2 (From UTM)

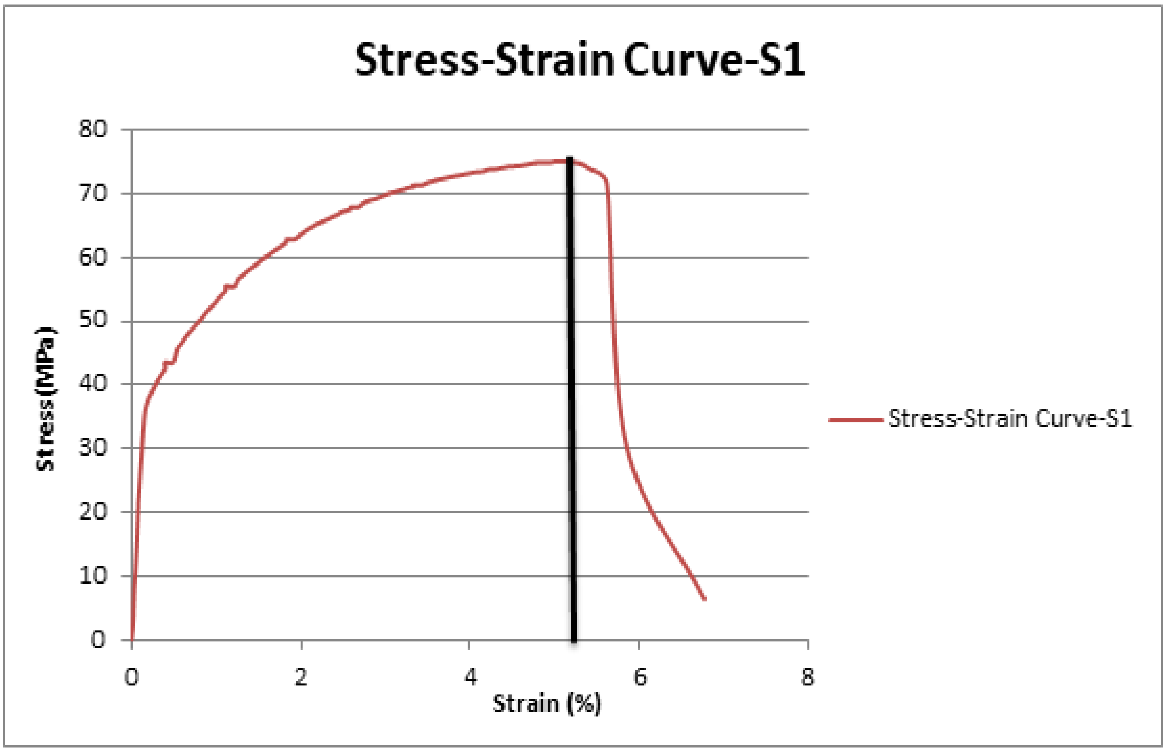

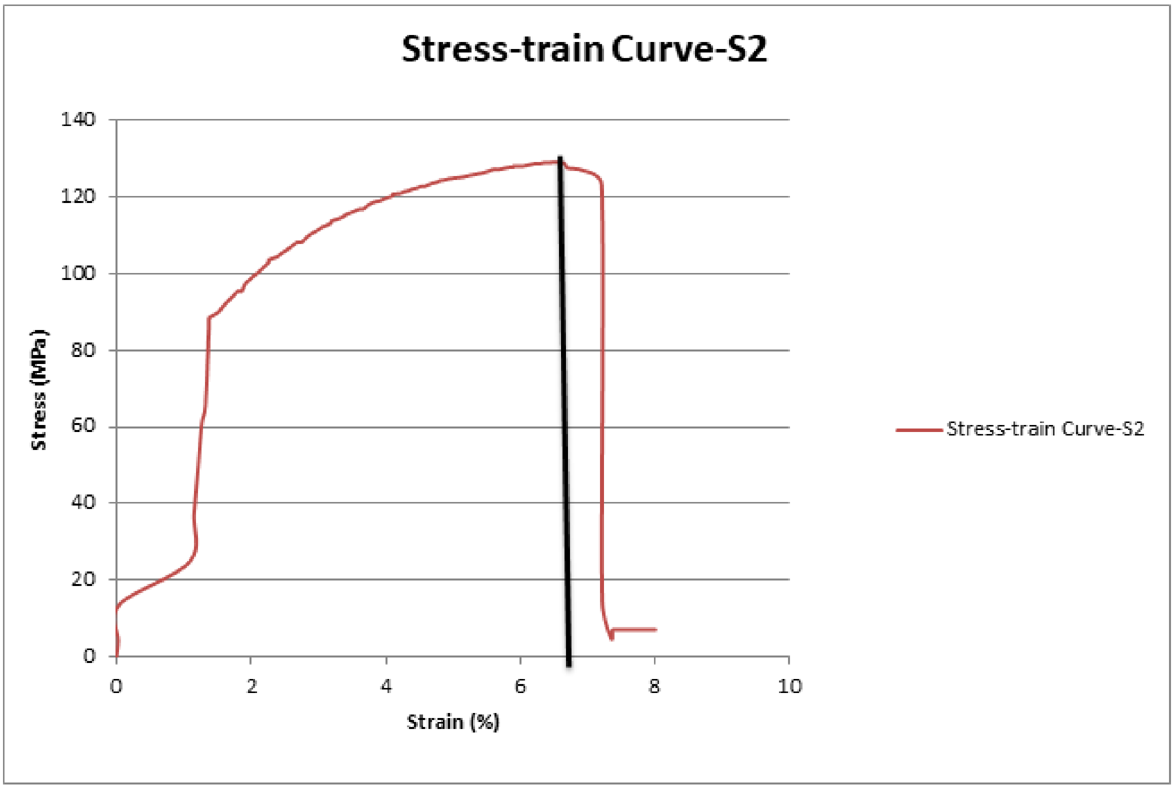

Appendix 4: Wear Rate Vs Time Result for Sample-1 and Sample-2 (From Pin On Disc Apparatus)

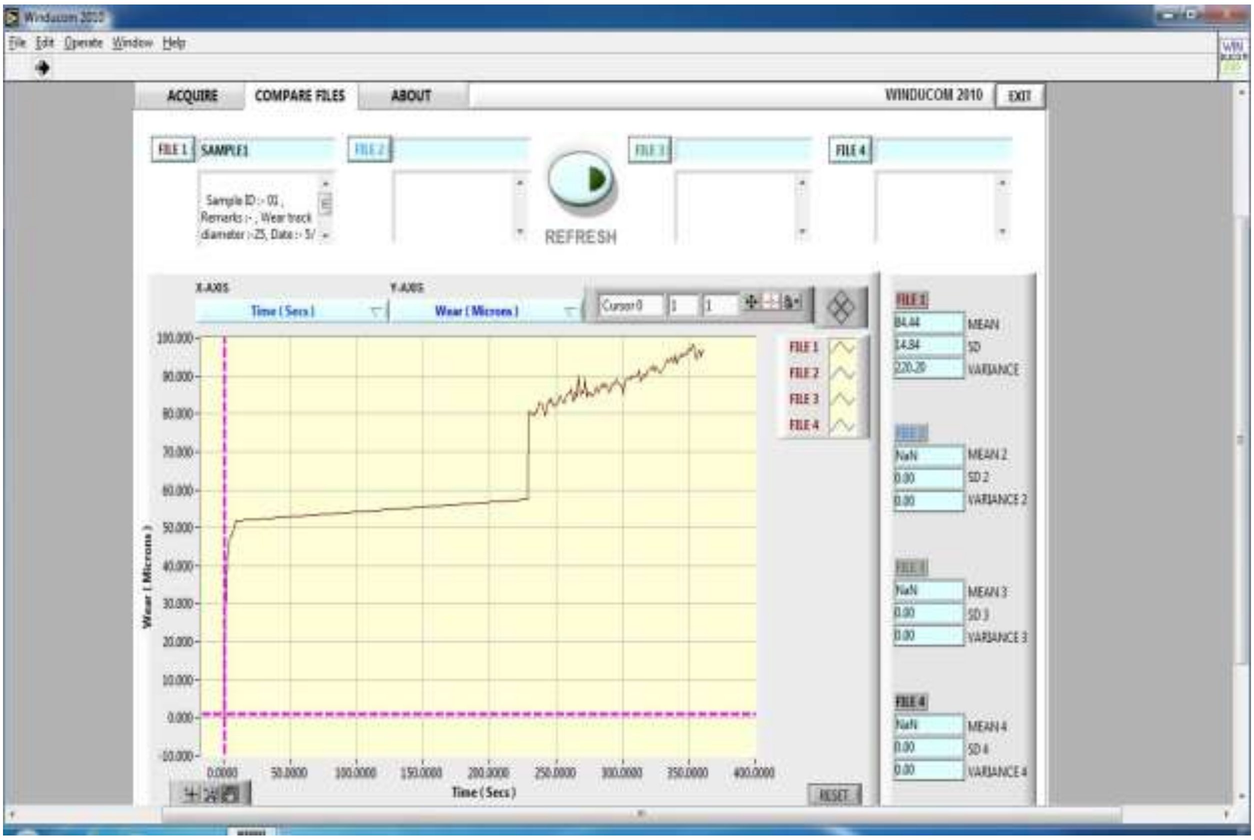

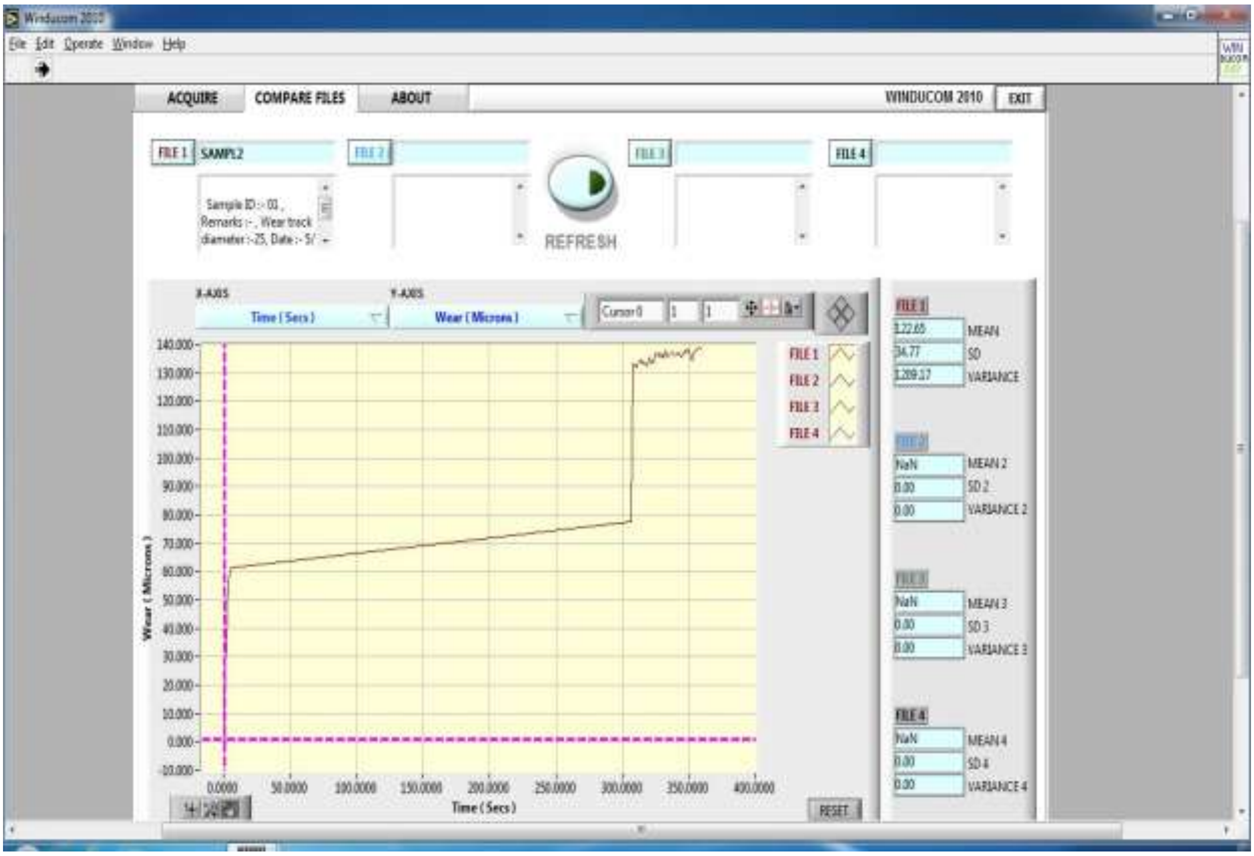

Appendix 5: Design of Experiment and Designation of Composite Name

Designation	Composition	Experimental Result			
		Hardness (HV)	Tensile Strength (MPa)	Tensile Toughness (J/mm^3)	Wear Rate ($x10^{-9}$Kg/m)
S_1	Pure Al 6061	123.30	75	14	10
S_2	Al 6061 + 5wt.% SiC + 2 wt.% MoS2	182.90	129.13	20	7
S_3	Al 6061 + 10 wt.% SiC + 4 wt.% MoS2	204.40	171.24	25	1
S_4	Al 6061 + 5wt.% SiC + 4 wt.% MoS2	173.80	104.6	19	6
S_5	Al 6061 + 10 wt.% SiC	199.50	180.85	23	4
S_6	Al 6061 + 2 wt.% MoS2	180.17	89.76	16	9.002
S_7	Al 6061 + 10 wt.% SiC + 2 wt.% MoS2	208.30	194.43	26	3
S_8	Al 6061 + 4 wt.% MoS2	162.60	82.41	15	9
S_9	Al 6061 + 5wt.% SiC	180.30	118.9	17	8

Appendix 6: Percentage of the F Distribution: F*0.05, V1, V2* (F0.05, 1, 8=5.32)

(v1 = numerator of DoF *and v2* = denominator of DoF)

$\nu_1 \backslash \nu_2$	*1*	*2*	*3*	*4*	*5*	*6*	*7*	*8*	*9*	*10*
1	161.5	199.5	215.7	224.6	230.2	234.0	236.8	238.9	240.5	241.9
2	18.51	19.00	19.16	19.25	19.30	19.33	19.35	19.37	19.38	19.40
3	10.13	9.55	9.28	9.12	9.01	8.94	8.89	8.85	8.81	8.79
4	7.71	6.94	6.59	6.39	6.26	6.16	6.09	6.04	6.00	5.96
5	6.61	5.79	5.41	5.19	5.05	4.95	4.88	4.82	4.77	4.74
6	5.99	5.14	4.76	4.53	4.39	4.28	4.21	4.15	4.10	4.06
7	5.59	4.74	4.35	4.12	3.97	3.87	3.79	3.73	3.68	3.64
8	5.32	4.46	4.07	3.84	3.69	3.58	3.50	3.44	3.39	3.35
9	5.12	4.26	3.86	3.63	3.48	3.37	3.29	3.23	3.18	3.14
10	4.96	4.10	3.71	3.48	3.33	3.22	3.14	3.07	3.02	2.98
11	4.84	3.98	3.59	3.36	3.20	3.09	3.01	2.95	2.90	2.85
12	4.75	3.89	3.49	3.26	3.11	3.00	2.91	2.85	2.80	2.75
13	4.67	3.81	3.41	3.18	3.03	2.92	2.83	2.77	2.71	2.67
14	4.60	3.74	3.34	3.11	2.96	2.85	2.76	2.70	2.65	2.60
15	4.54	3.68	3.29	3.06	2.90	2.79	2.71	2.64	2.59	2.54
16	4.49	3.63	3.24	3.01	2.85	2.74	2.66	2.59	2.54	2.49
17	4.45	3.59	3.20	2.96	2.81	2.70	2.61	2.55	2.49	2.45
18	4.41	3.55	3.16	2.93	2.77	2.66	2.58	2.51	2.46	2.41
19	4.38	3.52	3.13	2.90	2.74	2.63	2.54	2.48	2.42	2.38
20	4.35	3.49	3.10	2.87	2.71	2.60	2.51	2.45	2.39	2.35
21	4.32	3.47	3.07	2.84	2.68	2.57	2.49	2.42	2.37	2.32
22	4.30	3.44	3.05	2.82	2.66	2.55	2.46	2.40	2.34	2.30
23	4.28	3.42	3.03	2.80	2.64	2.53	2.44	2.37	2.32	2.27
24	4.26	3.40	3.01	2.78	2.62	2.51	2.42	2.36	2.30	2.25
25	4.24	3.39	2.99	2.76	2.60	2.49	2.40	2.34	2.28	2.24
30	4.17	3.32	2.92	2.69	2.53	2.42	2.33	2.27	2.21	2.16
40	4.08	3.23	2.84	2.61	2.45	2.34	2.25	2.18	2.12	2.08
50	4.03	3.18	2.79	2.56	2.40	2.29	2.20	2.13	2.07	2.03
100	3.94	3.09	2.70	2.46	2.31	2.19	2.10	2.03	1.97	1.93